Optimization of ship hull form for moderate sea state

Soe Thi Ha

Master Thesis

presented in partial fulfillment
of the requirements for the double degree:
“Advanced Master in Naval Architecture” conferred by University of Liege
"Master of Sciences in Applied Mechanics, specialization in Hydrodynamics, Energetics and Propulsion” conferred by Ecole Centrale de Nantes

developed at University of Rostock, Germany
in the framework of the

“EMSHIP”
Erasmus Mundus Master Course
in “Integrated Advanced Ship Design”

Ref. 159652-1-2009-1-BE-ERA MUNDUS-EMMC

Supervisor: Univ. Prof. Dr.-Ing. Robert Bronsart, University of Rostock

Reviewer: Prof. Pierre FERRANT, Ecole Centrale de Nantes

Rostock, February 2015

ABSTRACT

The challenge of international market and the search of increasing performances lead the process of ship design to a continuous enhancement in merchant field where the dedicated time for a thorough design is ever decreasing. While improving the performance of hull form, seakeeping is a crucial part for a cruise liner in order to serve the customers with maximum comfort onboard and considering the wave added resistance in calculating the total resistance of hull form for selecting the appropriate engine power.

Therefore, this work is motivated by the challenge to understand and clarify which approach is particularly suited for the performance of seakeeping behavior of the hull form design and select the optimum hull form design considering a couple of scenarios of different sea-states of operating routes and different speeds.

In this thesis, parametric modeling of the hull form is modified from the original geometry model of the ship hull which is provided from Meyer Shipyard by using Friendship Framework/CAESES. After getting parametric model, it is simulated by GL Rankine and validated with experimental results from HSVA. GL Rankine is coupled with CAESES and then, with different optimization approaches, optimal ship hull form is obtained in calm water condition.

The optimized model is checked for wave added resistance and analyzed for seakeeping behavior in moderate sea-state under different scenarios. In the another approach, the hull form is directly optimized for the total resistance of the ship, comprising the calm water resistance and the added resistance in seaway, followed by the analysis of seakeeping behaviors. Optimization is to be done especially on the fore body of the hull (e.g. bulbous bow). Finally, the results are analyzed to compare the optimal hull form with original design.

ACKNOWLEDGEMENTS

First of all, a special gratitude I give to my supervisor, Prof. Dr.-Ing. Robert Bronsart, whose contribution in stimulating suggestions and encouragement, helped me to coordinate my project especially in writing this thesis. I would also like to take this opportunity to thank Mr. Jonas Conradin Wagner and Ms. Eva Binkowski for giving valuable advice with technical problems and guiding me to the success of the master thesis.

Words cannot express how grateful I am to Dr.-Ing. Stefan Harries for being a tremendous mentor for me. His advice and help on both research as well as on this thesis have been priceless.

I would also like to acknowledge with much appreciation the crucial role of FRIENDSHIP SYSTEMS team that made my work possible and pleasant, receiving me with open arms and answering all my questions with delight.

It is inevitably that the development of this thesis won't be possible without the support from DNV-GL team, especially Mr. Vladimir Shigunov, Mr. Andreas Brehm and Mr. Alexander Von-graefe.

Furthermore, I also want to thank to Erasmus Mundus Organisation for their financial support granted through this whole program.

Last but not least, many thanks go to the coordinator of this EMSHIP program, Prof. Philippe Rigo whose have invested his full effort in organizing and managing this program. He continually and persuasively conveyed a spirit of adventure in regard to program arrangement and scholarship, and an excitement in regard to teaching. Without his supervision and constant help this great pleasure and challenging study period in Europe would not have been possible.

This thesis was developed in the frame of the European Master Course in "Integrated Advanced Ship Design" named "EMSHIP" for "European Education in Advanced Ship Design", Ref.: 159652-1-2009-1-BE-ERA MUNDUS-EMMC.

Soe Thi Ha – Rostock, January, 2015

TABLE OF CONTENT

LIST OF FIGURES

LIST OF TABLES

Declaration of Authorship

I declare that this thesis and the work presented in it are my own and have been generated by me as the result of my own original research.

Where I have consulted the published work of others, this is always clearly attributed.

Where I have quoted from the work of others, the source is always given. With the exception of such quotations, this thesis is entirely my own work.

I have acknowledged all main sources of help.

Where the thesis is based on work done by myself jointly with others, I have made clear exactly what was done by others and what I have contributed myself.

This thesis contains no material that has been submitted previously, in whole or in part, for the award of any other academic degree or diploma.

I cede copyright of the thesis in favour of the University of Rostock.

Date: 15-01-2015 *Signature: SOE THI HA*

1. INTRODUCTION

1.1. General

One of the main considerations in early design stage of ship is the prediction of ship performances in calm water and seaways. Last many decades, ships are usually designed based on power prediction in calm water without care considerations of actual operating conditions in seaways. Then, experienced based power allowance called sea margins are considered for the effect of seaways which can lead to optimistic or pessimistic estimations of actual required power. The reliable prediction of increment of power in waves is important for both ship designers and operators.

Generally, the prediction of ship hydrodynamic performances can be divided into resistance and propulsion, seakeeping and manoeuvring, but in this thesis, it will be more emphasized into resistance estimation in calm water and analysis of seakeeping behaviours. In order to understand the hydrodynamic performances, there are different kinds of approaches which are the empirical approach that is in the form of constants, formulae and curves developed from the parent ship or similar shapes, the experimental approach that is the testing of scaled model of original hull form and analysing the performances, expanding to full scale results and the numerical approach that has become increasingly important for ship resistance and powering.

Therefore, ship optimization based on CFD simulation becomes the major factor of developing new economically efficient and environmentally friendly ship hull forms. The reason is that diverging from the regular hull forms which are derived from parents' ships in empirical approach, CFD based optimization can generate thousands of different hull forms from which the best hull form with least calm water resistance and added resistance in waves can be selected. Reducing the resistance leads to less consumable power which pays off economically for ship owners and operators by saving operating costs. As for environmental aspects, it is directed to less emissions and noises, less wastage of fuels and prevention of corrosion of shore lines as a result of reduction of wave resistance emitted from the optimized hull form.

1.2. Objectives and Scope of Thesis

The main objective of the thesis is to study about the optimization of fore body of the hull form for cruise ship based on the technical specification provided by the PerSee project. The study of Rankine solver provided from DNV-GL has to be done and it is coupled to interface with the Friendship-Framework to check the resistances in both steady flow and seaway, as well as the seakeeping performances of the geometric hull form.

The challenge of international market and the search of increasing performances lead the process of ship design to a continuous enhancement in merchant field where the dedicated time for a thorough design is ever decreasing. While improving the performance of hull form, seakeeping is a crucial part for a cruise liner in order to serve the customers with maximum comfort onboard. So far, some projects related to optimization of hull forms for seakeeping have been found, but non of the completed works is related to optimization of hull forms regarding in sea states by using the newly in-house developed solver, GL Rankine because it is not expandingly used to simulate the resistance in calm water and also in sea states as well. Coupling of this new solver with Friendship Framework to optimize the hull form in resistance, considering added resistance in wave, is the challenge for the author to compromise the slover to run precisely for all the hull forms produced from algorithms. Therefore, this work is motivated to understand and clarify which approach is particularly suited for understanding the performance of seakeeping behavior of the hull form design and select the optimum hull form design considering a couple of scenarios of different sea-states of operating routes and different speeds.

In this thesis, the hull form for cruise vessel is optimized with fully-automated process, but it is allowed to operate manually as well. The fore body of hull form is modelled as fully parametric model in Friendship Framework and it is simulated with GL Rankine CFD code for obtaining the resultant resistances in calm water and in seaways, followed by validating the results from experiments which are performed in model basin at HSVA. The optimization process is done with CAESES to get the optimized hull form that can be checked later for seakeeping behaviours with moderate sea states which are 30% occurrences of operational profile calculated by the University of Rostock. The set-up optimization process permits to get the best hull form which is not only the resistance in calm water but also for added resistance in seaways as well.

1.3. Methodology and Approach

The original hull form model is given by Meyer Werft shipyard in IGES format to describe the detailed hull body of the cruise ship. By visualising the original hull form, a fully parametric model, which is generated from Techanical University Berlin, is modified in the frame work of CAESES using the selected design parameters which control effectively the hull form of the vessel.

After getting parametric model, the newly developed GL Rankine solver is set up to be able to run precisely with the resulting parametric model. There are a few parameters in set up file to control the panels created before running the simulation. Once the set up is developed, the simulation is started in order to get the results such as calm water resistance, trim and sinkage, added wave resistance and 6DOF motions.

Moreover, the validation of the results from CFD solver is performed by comparing the results from experiment which are done in HSVA towing tanks. In order to optimize the hull form with different speeds effectively, the common set up for all the speeds is necessary to generate. After that, the solver is coupled with CAESES which will perform different optimization processes.

Before starting opimization process, the design variables are chosen wisely by doing the sensistivity analysis of each variable on the resistance of the ship. With different optimization approaches including the exploration of the design space and single objective optimiation, the relevant optimal ship hull form is obtained in accordance with different speeds. The optimized hull form is again run for seakeeping simulation to obtain the added resistances in the relevant sea state which is provided from University of Rostock by calculating the 30% occurence of regular ship operation routines.

In addition to calculating the calm water resistance and checking seakeeping behaviours, the direct optimization of calm water resistance together with added resistance in waves can be done by coupling the CFD solver and CAESES.

Optimization will be done especially on the fore body of the hull, (e.g. bulbous bow) because GL Rankine solver utilizes the potential flow code which is mainly effective for fore body flow of the ship and less effective for viscous flow occured at the aft body. Finally, the results are analyzed to get the optimal hull form for early design stage. The flow chart mentioning the outline of approach is described in Fig. 1.1.

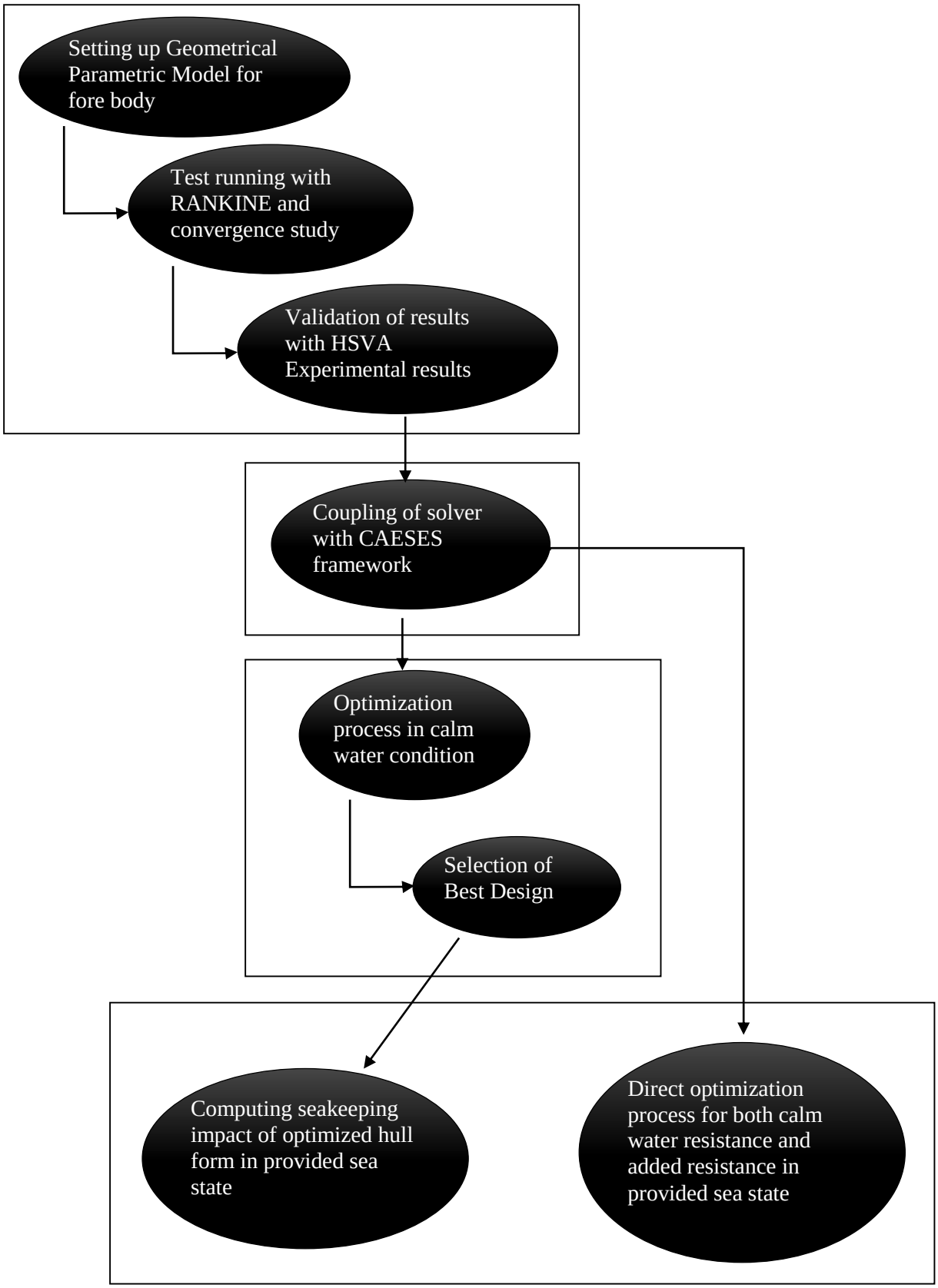

Figure 1.1. Flow Chart of Methodology

1.4. Literature Review

In fact, this thesis involves a wide range of engineering studies concerning the optimization processes, study of CFD solvers, knowledge and designing the sea-states of operating routes, creating parametric model of ship hull and so on. There are some papers available for the study of optimization of different hull forms for resistance, seakeeping and hydrodynamic loads in calm water and sea-state, wave making characteristics of ship hulls and parametric study on vessel body lines for seakeeping performance.

Grigoropoulos and Chalkias (2009) [1] wrote a paper about "Hull-form optimization in calm and rough water". Their work presents a formal methodology for the hull form optimization in calm and rough water using wash waves and selected dynamic responses, respectively. Parametric hull form modeling is used to generate the variant hull forms with some of the form parameters modified, which are evaluated in the optimization scheme based on evolutionary strategies. Rankine-source panel method and strip theories are used for the hydrodynamic evaluation. The methodology is implemented in the optimization of a double-chine, planning hull form. Furthermore, a dual-stage optimization strategy is applied on a modern fast displacement ferry.

Kim (2009) [2] made a thesis about "Multi-objective optimization for ship hull form design". His thesis covers the development of geometry modeling methods using NURBS representation and parametric representation for a complex geometry and to satisfy different design requirements, the development of various optimization algorithms. Both single- and multi-objective optimization algorithms are implemented. Several optimization algorithms are employed and compared with one another in various hull form optimization applications. Finally, a CFD module is developed to compute the flow field and evaluate the hydrodynamic performance of the new hull forms obtained during optimization cycles.

In 11th International Conference on Fast Sea Transportation from American Society of Naval Engineers, there is a topic about the automatic optimization of the fore hull form of a fast frigate. The fully automatic optimization chain has been implemented adopting the ModeFrontier optimization environment to interface the Friendship-Framework (parametric definition of the hull shape), the CFD codes developed by CETENA S.p.A. (to predict the steady wave resistance and unsteady seakeeping performances of each design candidate), and a MOGA genetic algorithm. Numerical results are validated by means of calm water model tests performed at the

Towing Tank. (Biliotti, Brizzolara, Viviani, Vernengo, Ruscelli, Galliussi, Guadalupi and Manfredini (2011) [3])

From Technical University Berlin, Heimann (2005) [4] wrote a thesis about 'CFD based Optimization of the wave-making characteristics of ship hulls' that covers a noble hull form optimization approach based on CFD evaluation of non-linear ship wave pattern and on wave cut analysis. It is a highly integrated and fully automated optimization scheme that performs the direct driven hull form adaptation by hydrodynamics, the objective function of optimization in terms of free wave spectrum and wave pattern resistance by wave cut analysis, optimization of wetted hull portion with dynamic trim and sinkage and wave formation along the hull and iterative marching scheme of optimization looping process with much freedom of hull variation.

Moreover, in International Journal on Marine Navigation and Safety of Sea Transportation, there is an article about "Optimizing the seakeeping performance of ship hull forms using Genetic Algorithm". It presents a study about the computational method to estimate the ship seakeeping in regular head waves. Optimizing is performed by linking the genetic algorithm with the computational method together with the displacement as the constraint for varying the hull shapes. Starting from the well-known S60 hull and classical Wigley hull form, new hull forms are obtained by running with two speeds of Fn=0.2 and Fn=0.3. With variable parameters as the combination of ship hull offsets and main dimensions, the peak values for vertical absolute motion at a point 0.15LBP behind the forward perpendicular, in regular head waves are utilized as the objective function of the optimization process. (Bagheri, Ghassemi and Dehghanian (2014) [5])

Percival, Hendrix and Noblesse (2001) [6] have mentioned about the topic "Hydrodynamic optimization of ship hull forms" in Elsevier Journal, 2001. The article focused on optimization of hull forms developed from Wigley hull using the simple CFD tool that estimates the friction drag by using ITTC formula and the wave drag using the zeroth-ordered slender ship approximation. This theoretical prediction is validated by comparing the experimental measurments for a series of eight hull forms. Then the hull forms are optimized with the same displacement and waterplane transverse moment of inertia of original one for different ranges of speeds.

There are a couple of reference works for optimization of hull forms for resistance and seakeeping behaviors, but there is no specific work for cruises liners considering the different operating routes and scenarios. So, this thesis will be more emphasized on this area and coupled the new CFD solver with the Friendship Frame works.

1.5. Outline of Thesis

In this thesis, the sections are organised in accordance with the method approach and in sequential order. In Chapter one, there is a short explanation of background and overview of the problem, motivation and challenge of this work, scopes of thesis, some available literatures and methods and approaches used for optimization. Chapter two introduces about the cruised ship that is going to be optimized and the operational profile and sea states that the vessel will be experienced during her life span. In order to obtain the large amounts of variant hull designs with less input data, CAESES use the parametric model of the original hull form and the modelling of this parametric form and its controlling design parameters are mentioned in Chapter three, including the sensitivity analysis for each design parameter upon changing the hull shape. As GL Rankine is the newly developed CFD solver for predicting the calm water resistance and hydrodynamic behaviours of ship in waves, the setting for this solver and validating of its results with experimental results from HSVA are described in Chapter four. In Chapter five, the coupling of CAESES and RANKINE solver is mentioned to get the results for calm water resistance and visualization of wave patterns generated.

Regarding for the main objective of this thesis, different approaches of optimization processes including DOE exploration with SOBOL and single objective optimization using Tsearch algorithm are explained in Chapter six. Chapter seven will describe the simulation of seakeeping behaviours and added resistance due to sea ways and also the direct optimization of calm water resistance and added resistance together. Finally in Chapter eight and nine, the achievements, the problems experienced, the summary of work done and outlooks to future research works are given.

2. CASE OF STUDY

As it comes to hydrodynamic optimization of ship, it does not only mean to power efficiency that needs to drive the ship, but it is important to study the performances of ship in moderate and heavy sea states. Therefore, the specialist engineers from Friendship Systems becomes a part of the project called PerSee, which studies the optimization of ships in sea states. The research and development project, PerSee, which stands for "Performance von Schiffen im Seegang" (performance of ships in sea states), targets for outcoming of new processes for optimization under operating conditions, as well as for the safety of ship in different sea states. [17] In order to estimate the added resistance and required engine power of the ship, various numerical and experimental methods are developed. Operational scenarios as well as minimum speed and power requirements are considered. In the project, different types of ships are optimized by integrating the developed numerical methods into the optimization software. Among different coordinated work packages, Friendship Systems has to perform parametrical optimization of the hull shape under operating conditions in seaways. [18] Herein this research, the new cruise ship that are going to be built in Meyer Werft is needed to optimized for calm water resistance and motion performances in moderate seaways by applying the in-house CFD solver called GL Rankine in Computer Aided Engineering platform CAESES / FRIENDSHIP-Framework, targetting for setting up complex processes that involve several simulation tools and improved usability in creating and understanding complex parametric models. [17]

2.1. Main Characteristics of Vessel

The design of the studied cruise vessel is provided from Meyer Werft as illustrated in Fig. 2.1 and the main characteristics of the vessel are mentioned in Table 2.1. The general arrangement plan, body plan and sheer plan of the ship are shown in Appendix A1.

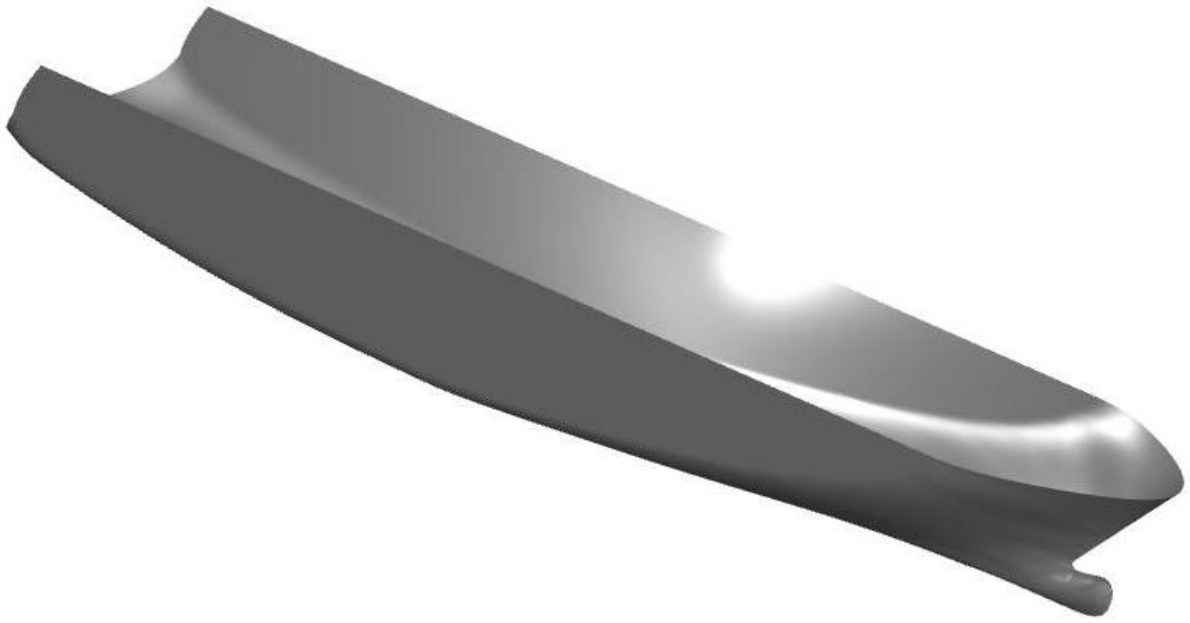

Figure 2.1. Original design of hull from provided from Meyer Werft

Main Characteristics			
Length between perpendiculars	L_{PP}	m	220.273
Breadth	B	m	32.200
Height	H	m	25.150
Draft	T	m	7.200
Block coefficient	C_B	m	0.651
Transverse metacentric height	GM_T	m	2.754
Vertical center of gravity	KG	m	15.054
Longitudinal center of gravity	LCG	m	99.601
Displacement volume	VOL	m^3	33229.000
Wetted surface area	WSA	m^2	7822.800

Table 2.1. Main characteristics of the vessel

2.2. Operating Conditions, Routes and Schedules

As this cruise vessel has not built yet and it is only in preliminary design state, the operating information of this vessel is not confirmed yet. Therefore, the realistic operating data of the similar vessel are considered as a sample. The typical routes of the ship are as follow; in summer, it will travel in European regions like Rome and the Eastern Mediterranean while in winter, it will sail in Caribbean Sea between Miami and Caribbean. Then it will cross the Atlantic Ocean twice per year in between summer and winter. The detailed operating routes of the ship for the whole year are mentioned in Table 2.2 and Fig. 2.2. (Walter (2014) [7])

	Operating Routes	**Duration**
Route 1	Rome – Santorini – Istanbul – Efes – Mykonos – Athens - Naples – Rome	10 days
Route 2	Rome – Messina – Athens – Efes – Rhodes – Santorini – Mykonos – Naples – Rome	10 days
Route 3	Rome – Funchal – Basseterre – Philipsburg – Labadee – Miami	15 days
Route 4	Miami – San Juan – Philipsburg – Basseterre – Miami	7 days
Route 5	Miami – Tenerife – Malaga – Cartagena – Barcelona – Nice – Florence – Rome	15 days

Table 2.2. Detailed operating routes of the cruise vessel

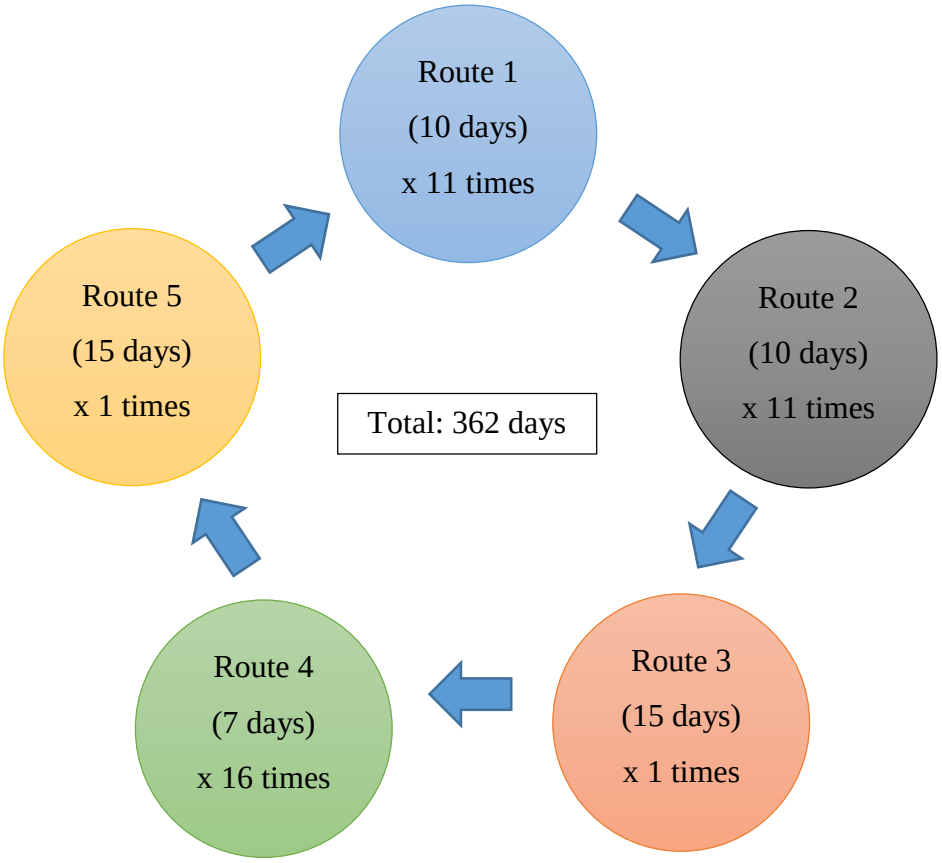

Figure 2.2. Ship operating schedule per year (Walter (2014) [7])

After considering the ship operating routes, the cruise liner will mainly operate in North Atlantic Ocean and Caribbean Sea from which the critical wave data have to be examined. Moreover, the ship is designed based on the following conditions at the draft of 7.2 m with zero trim;

- 22.0 knots at 100% MCR (2 x 17,500 kW) in calm water condition and
- 21.2 knots at 100% MCR (2 x 17,500 kW) at 15% sea margin.

Nevertheless, in this thesis the author will study at two different speeds of 15 knots and 21 knots which are the speeds used in experimental analysis in order to compare easily the numerical data with experiment results.

3. GEOMETRICAL MODELLING

3.1. Parametric Modelling of Fore Body

In traditional CAD-based geometric modelling, shapes are generated in terms of mathematically defined curves and surfaces by means of graphical user interface (GUI). By requiring the knowledge about ships topology appearance and mathematical representation, the initial set-up of the model which contains large amount of free variables is generated. After the initial set-up, global changes (e.g. length, width, and height) or local changes (e.g. entrance angle, shape of bulbous bow) cannot be done easily or very time consuming task. (Abt, Bade, Birk and Harries (2001) [8]) Therefore, instead of generating a lot of information about the hull form, 3D shape of the model is accomplished by using form parameters and a set of longitudinal curves in parametric modelling and automated optimization of bare hull which is developed by (Harries (1998) [9]) is processed. The vertices of B-spline longitudinal curves are computed from the original hull geometry and the form parameters, introducing fairness criteria as measures of merit for capturing global shape characteristics. (Abt, Bade, Birk and Harries (2001) [8]) The longitudinal positions of the curves are often matched between one and others to make sure that by varying the global parameters, a coherent shifting of the curves is obtained depending on those parameters, providing more feasible resulting hull geometry. Then, hull cross sections are defined on the basis of these curves. (Biliotti, Brizzolara, Viviani, Vernengo, Ruscelli, Galliussi, Guadalupi and Manfredini (2011) [3]) As mentioned in Chapter 1, only the fore body of the hull will be optimized and therefore, the aft part of the ship is directly taken from the original hull form definition.

Ping, De-xiang and Wen-hao (2008) [10] described about the parametric modelling of hull form by different consecutive steps;

Defining forms parameters
- principle dimensions and coefficients such as xPeak, xStern, xMainFrame, HalfBeam, deckHeight
- shape parameters for fore body such as AngleDWL, AngleStemMax, fullnessDWL, xFOB, u0Fillet, tanFOS
- shape parameters for bulbous bow such as length, zPeak, fullnessKeel01, fullnessTop01, fullnessSecKeel

Designing curve description
- longitudinal basis curves such as CPC, FOS, FOB, Deck, DWL, xPos

- supporting curves such as tanDWL, tanKeel, tanDeck, AngleStem, fullnessBilge, coonBulbHull
- bulbous bow curves such as keelElevation, topElevation, beamElevation, maxBeam, fullnessSeckeel, tanSecTop, xPos

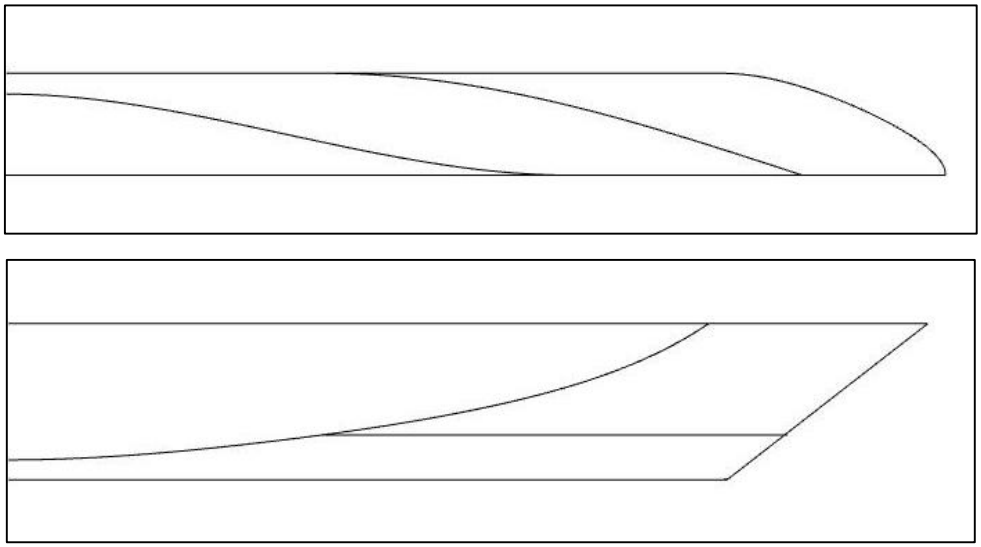

Figure 3.1. Control curves of Fore Body

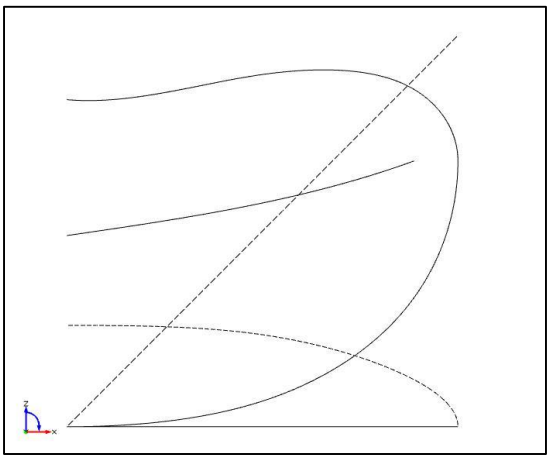

Figure 3.2. Control curves of Bulbous Bow

Creating the sections and curved engines -Section 1 with three segments using the curves CPC, FOB, FOS, xPos and fullnessBilge

- Section 2 with four segments using the curves CPC, FOB, DWL, tanDWL, FOS, xPos and fullnessBilge

- Section 3 with three segments using the curves CPC, DWL, tanDWL, FOS, tanKeel, xPos and fullnessBilge
- Section 4 which is the bow section created by the curve engine “Smooth Joint to Stem” feature by using the curves stem, AngleStem and xPos

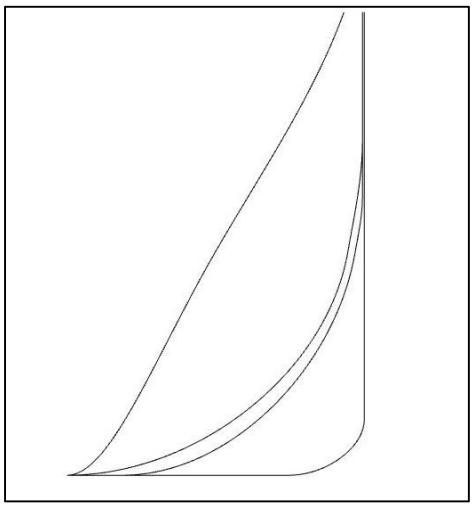

Figure 3.3 Different sections view of Fore Body

Generating hull form

- While generating the hull form, the special feature called ”Meta Surface” is used.
- Fore body 1 with curve engine ” Section 1” from midship to the start of DWL
- Fore body 2 with curve engine ”Section 2” from the start of DWL to the end of FOB
- Fore body 3 with curve engine ”Section 3” from the end of FOB to the end of FOS.
- Bow section with curve engine ”Section 4” from the end of FOS to the fore peak.
- Bulbous bow is also created using the same features as fore body.
- Fore body and bulbous bow is connected with two curve engines: CoonBulbHull and CoonsPatch surface.

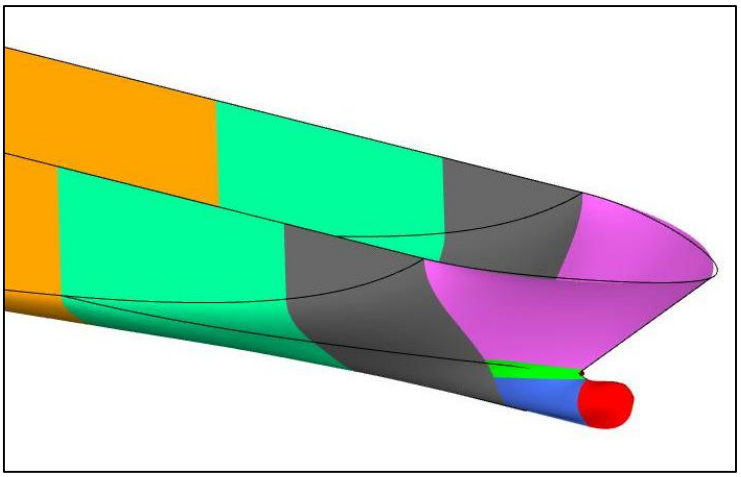

Figure 3.4. Different surfaces of Fore Body

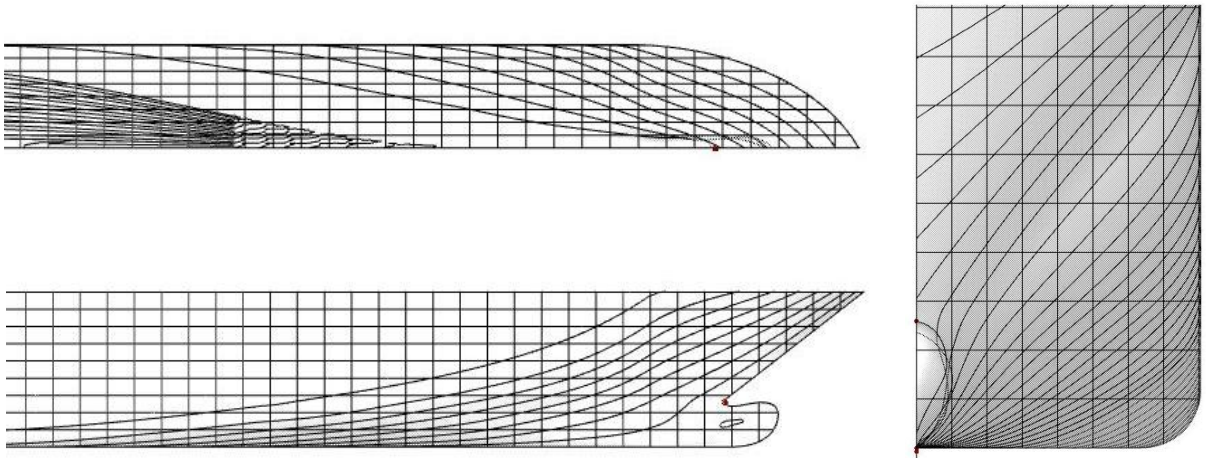

Figure 3.5. Lines plan of the model

3.2. Study on Design Parameters

After generating the parametric model, there are 14 parameters controlling the fore body of the ship and 12 parameters for bulbous bow shape. Some parameters have large effect on the changing of the geometry and some only have little influence. If all these parameters are selected to be optimized, there will be large amount of data that is needed and the design space will be huge to cover all possible combination of parameters. Therefore, it is necessary to define a few parameters as the critical ones. Obviously, the basic parameters that define the main dimension of the hull form (e.g. xStern, xPeak, xMainFrame, HalfBeam, deckHeight, draft) cannot be changed and the same for bulbous bow.

The following parameters can only imply on small changes of variation of the geometry and is omitted from selecting for design parameters:

No.	Parameters	Significance
Fore Body		
1.	AngleStemMax	Stem angle above waterline and unimportant for calculating the resistance of hull form.
2.	fullnessDeckFwd	Fullness of Deck curve and unimportant for calculating the resistance of hull form.
3.	tanFOS	Tangent of FOS curve at the deck and unimportant for calculating the resistance of hull form.
4.	xCPC	Middle position of CPC curve (position of keel forward that should kept unchanged not to get irrelevant shape).
5.	xFOS	End position of FOS curve (Sensitive and narrow ranges for variability).
Bulbous Bow		
6.	fullnessBeam	Fullness of beamElevation curve (very sensitive upon small changes and narrow ranges for variability).
7.	fullnessSecTop	Fullness of top section curve (Sensitive and narrow ranges for variability).
8.	fullnessTop01	Fullness of topElevation curve (very sensitive and can lead to formation of "pin head" bulb).
9.	yBeamStart	Start position of beamElevation curve (width of bow which is sensitive and can occur irregular shaped bow).
10.	zMaxBeamStart	Start position of max Beam curve (sensitive and can occur irregular shaped bow).
11.	zTop	End position of topElevation curve (sensitive and can appear snake shaped bow).

Table 3.1. List of parameters that have small effect on geometry

Therefore, only the following 9 parameters are left to study how are their behaviors on the geomerty and how they affect on the hydrodynamic aspects of the hull form.

AngleDWL - It changes the entrance angle of hull form upon moving the ship forward in water at designed waterline. By intialising the range from 10˚ to 25˚, the calculation for the resistance is done with GL Rankine CFD and it shows that the trend for the resistance is going down upon increasing the angle from 10˚ to 24˚ and it is up again from 24˚ to 25˚.

fullnessDWL - Same as angleDWL, it alters the shape of curve at designed waterline. Varying from 700 to 800 of its value, the resistances are calculated, but there is no trend upon changing its values because the results show in random manner. Therefore, it can be assumed that this parameter does not have influence on hydrodynamic aspects of hull form.

u0Fillet - It affects upon changing the shape of basic curve at the connection between the forebody and the bulbous bow. From calculating the resistance for the value of 0.1 to 0.22, the results show the upward direction from 0.1 to 0.13 and downward again from 0.13 to 0.22.

xFOB - It is the end position of flat of bottom curve (FOB) which controls the flat surface of hull bottom. Upon changing its position from 155 to 195, the resistance goes down from 155 to 185 and goes up again from 185 to 195.

fullnessKeel01 - For bulbous bow shape, the fullness of keelElevation curve which alters the shape of lower part in longitudinal direction is changed by using this parameter. Setting the values from 0.14 to 0.21, the resistance of hull from tends down upon on increasing the values.

fullnessSecKeel - Like fullnessKeel01, it changes the shape of bulbous bow in lowe part transversally. The trend of result increases from 0.8 to 0.87 of the value of this parameter and then decreases from 0.87 to 1.05.

zPeak - The height of the bulbous bow tip is controlled by this parameter and from the values of 0.65 to 0.73, the resistance is higher and from 0.73 to 0.78, the result is lower again.

tanSecKeel - This parameter also vary the transver sectional curve of bulbous bow. It is the start tangent value of keel sectional curve varying its values from 32˚ to 70˚. The decreasing trend of the result is shown on increasing its value.

tanTopEnd - It is the tangent value of end position of topElevation curve at the area of joining the upper part of bulbous bow and the fore body. It ranges from -25˚ to -95˚ and shows the upward trend from -25˚ to -55˚ and downward trend from -55˚ to -95˚.

In summary, there are 8 design parameters left for optimization process, excluding fullnessDWL. In Fig. 3.6 and Fig. 3.7, the examples of the effect of design parameters on changing the shape of hull form are illustrated. Annex A2 will show the study of each variable parameter affecting on the wave resistance and total resistance of the ship.

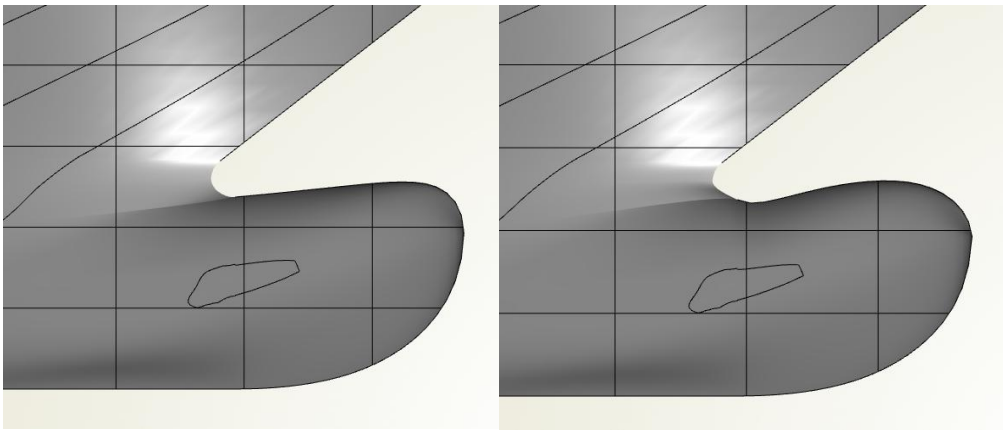

Figure 3.6. Varying of bulbous bow shape by controlling design parameter (longitudinal direction)

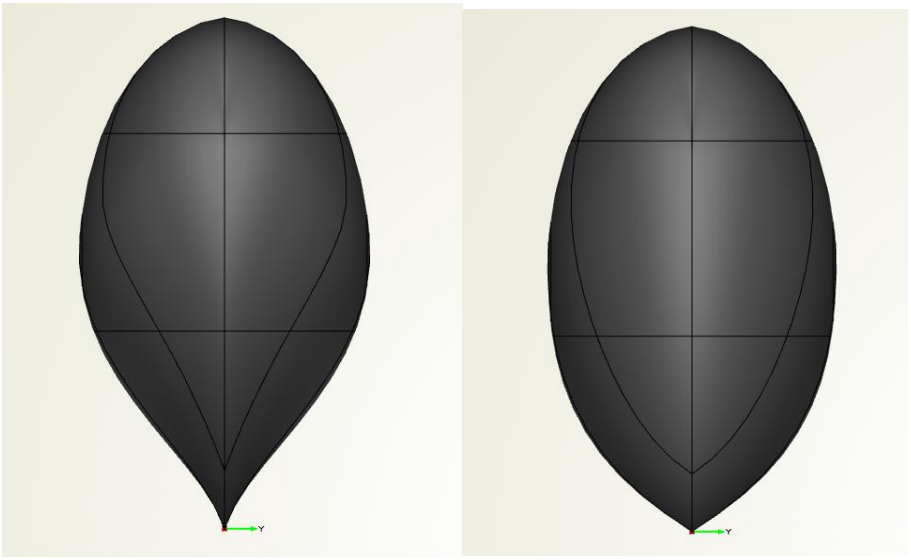

Figure 3.7. Varying of bulbous bow shape by controlling design parameter (transverse direction)

4. COMPUTATIONAL FLUID DYNAMIC (CFD) METHOD

Determination of the wave pattern and the resistance of the ship moving with a constant speed either in calm water or in sea states is the significant objective study of ship hydrodynamics. Therefore, the wave flow around the entire hull design is important. In assessment of ship hydrodynamics and optimization, CFD solvers play an important role to compute the flow fields for different operation conditions and to evaluate objective functions. It is necessary to be accurate, fast, reliable, automatic for their usage in optimizing process and also to communicate with the other components in the chain. At present, there are a lot of effective, reliable and fast CFD tools that are available to evaluate the numerical solution of wave flows. The solvers for invisid potential flow are using widely for different ship types and flow cases. (Heimann (2005) [4])

By means of accuracy and computational costs, various kinds of CFD solvers have their own advantages and disadvantages. Therefore, selection of relevant solvers for each case that can capture the necessary accurate results with minimum cost is crucial for every project. Fig. 4.1 shows relation of CFD methods with their accuracy and computational time. (Ferrant (2013) [12])

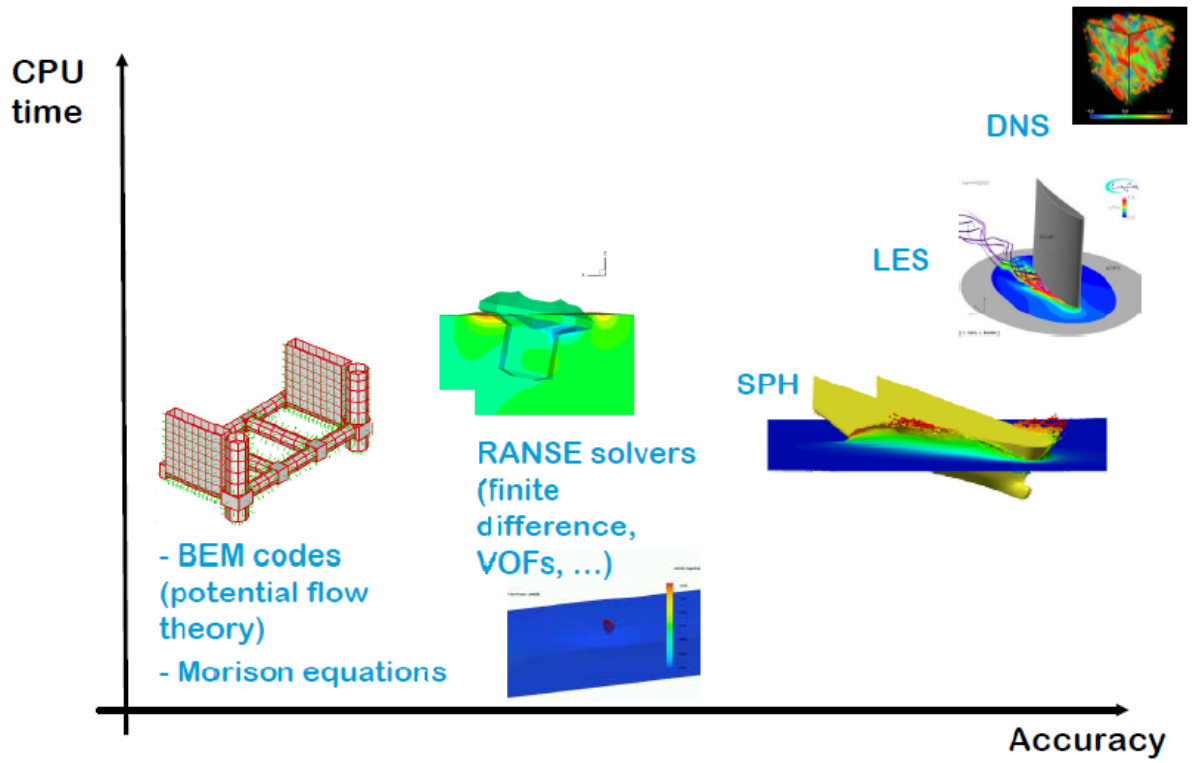

Figure 4.1. Available CFD methods with their accuracy and CPU time (Ferrant (2013) [12])

Although current CFD methods cannot obtain the same accuracy as in Experimental Fluid Dynamic (EFD) by testing in towing tank and cannot compete for power prediction, they are useful for comparing differnt hull forms and designs in term of hydrodynamic aspects. In comparison with EFD, they are fast, relatively inexpensive, not sensitve to uncertainities of measurement, reproducible and able to provide detailed flow information. (Heimann (2005) [4])

CFD solvers with Reynolds-averaged Navier-Stokes equations (RANSE) can obtain very accurate results for seakeeping predictions (transfer functions of ship motions and loads in regular waves). Nevertheless, for variety of loading conditions, various ship speeds and numerous wave periods and directions, these tools require too much computational time. Therefore, at early design stage, potential flow code solvers are utilized practically. (Söding, Graefe, Moctar and Shigunov (2012) [13]) In commercial industries, CFD solvers based on nonlinear free surface Rankine panel method are widespread for semi-automated or fully-automated hull shape improvement. These free surface Rankine methods are straightforward in handling, fast and generate reliable results in terms of detailed flow information for a variety of applications. (Heimann (2005) [4])

In this thesis, potential flow code GL Rankine is used to calculate the wave resistance and total resistance in steady flow computation and added resistance in waves for seakeeping analysis.

4.1. GL RANKINE solver

GL Rankine solver is developed as in-house solver by DNV GL. Söding, Graefe, Moctar and Shigunov (2012) [13] mentioned that it is based on Rankine source methods which satisfy the free surface condition numerically. Two flows are considered in these methods; the steady flow around the moving ship, including steady ship waves and the oscillatory flow due to waves and ship motions. As the frequency domain approaches are fast and accurate enough, these approaches are used in this method.

Especially at high forward speeds, GL Rankin can improve the accuracy of seakeeping computations because it is based on the linearization of flow due to ship motions and incoming waves with respect to wave amplitudes. Then, the interaction of steady non-linear flow around the ship in calm water, including ship waves and dynamic squat, with oscillatory flow due to incident waves are taken into account. Therefore, the steady flow field participates not only in

average forward motion of the ship, but also in the periodic ship motion, giving more accuracy at higher speeds.

Seakeeping computations are proceeded by the solutions of non-linear steady flow problem. While steady flow solution is fully non-linear with respect to free surface deformations, dynamic trim and sinkage and all boundary conditions, the seakeeping contribution only depends on wave amplitude linearly, considered up to first order. Moreover, quadratic transfer functions are computed to obtain added resistances and side drift forces in waves.

By using GL Rankine, the following computation can be done (as described in user manual);

- resistance in calm water, taking into account shallow water and channel walls
- dynamic squat in calm water, taking into account shallow water and channel walls
- linear transfer functions of ship motions in regular waves
- sectional loads, relative motions and accelerations in waves
- mapping of pressure distributions onto nodes of a finite-element mesh
- hydrodynamic interaction of ships with the same forward speed and course

4.1.1. Non-linear Steady Flow Computation

By assuming the inviscid, incompressible and irrotational fluid, GL Rankine computes the steady flow around the ship using non-linear free surface boundary conditions. The resultant velocity potential has to fulfil the Laplace equation (conservation of mass) in the fluid domain, Kinematic and Dynamic boundary conditions on the free surface, 'No flow through the surface' on the bottom wall, side channels (if applicable) and on the body surface and Atmospheric pressure at the free surface. In order to propagate the wave created by the ship only in downstream, the radiation condition has to be fulfilled on the free surface. In accordance with the boundary element approach, it is only necessary to discretize the boundaries of computational domain which are the submerged surface of the ship and the corresponding free surface. The underwater ship body is discretized by the unstructured triangular grid and the free surface, by the block-structured quadrilateral grid.

An iterative approach is required due to non-linear free surface boundary condition and a Newton-like iteration for the residuum is used. After each iteration step, Rankine source strengths are updated by using under-relaxation parameter which is set up manually. There is assumption of zero pressure at the lower edge of the transom in case of submerged transom and free surface is connected with transom lower edge which is not panelised. Sometimes, in order

to prevent wave breaking which cannot be modelled by this method, it is essential to initialize the additional wave damping factor which also has to be controlled manually.

After getting new source strengths, the forces and moments acting on the ship are calculated by integration and they are used to determine the dynamic trim and sinkage. The accurate dynamic attitude is obtained at convergence by small updating of ship attitude at each Newton iteration step and from the Dynamic free surface boundary condition, the new height of free surface at all grid points is achieved after adapting the ship attitude. And also the grid on the submerged ship surface is update to reach up to the corrected waterline.

It is needed to generated the unstructured grid on the body surface properly to resolve steady wave resistance and at slow speed, the amount of panels is typically about 4000 on one side of the submerged body. But, the structured quadrilateral grid for free surface can be generated automatically based on the ship size and speed. For Froude number smaller than 0.15, it is quite difficult to obtain the convergent solution by this method. (Söding, Graefe, Moctar and Shigunov (2012) [13])

4.1.2. Seakeeping Computation

For motion in waves, forces and moments acting on the ship surface depends linearly on the incoming wave amplitudes for this method in linear response computation. By superimposing the potential from the stationary problem and the potential of periodical flow which oscilates with the wave frequency, the total potential needed for seakeeping analysis is calculated. For all these potentials, it is necessary to fulfil the Laplace equation and boundary conditions on the free surface at z = zeta0, (not at z = 0), considering its deformation due to steady forward motion, boundary condition on the time-averaged wetted part of the ship hull, and radiation conditions at infinity. The steady free surface elevation zeta0 is obtained by interpolation from the steady solution grid onto the seakeeping grid. From Rankine source strengths of stationary problem, the steady potential is determined. ‘No flow through the surface’ condition is satisfied at body fixed referance frame.

As in steady computation, the same triangular grid is utalized for the ship submerged hull and the structured grid on the free surface. Seakeeping computation are determined in large series over various ship forward speeds and wave periods and directions. Therefore, applying empirical formulae based on extensive grid-dependency studies, the extension and fineness of the free surface grids are adapted automatically to the ship size, speed and the encounter

frequency and direction of incoming wave, doing independently from the free surface grids used in steady solution.

In Rankine methods for seakeeping computation, waves must not be reflected at the boundary of free surface panel grid and the flow field should not be disturbed far away from the ship. Therefore, the freesurface grid consists of an inner free surface grid with the same structure as the grid for nonlinear steady computation, and an outer free surface grid. The different boundary condition is fulfilled on the outer grid to prevent reflection from the artificial free surface grid boundary. As shown in Fig. 4.2, the free surface grid is divided into the inner and outer grids, consisting of forward and aft parts and two side grids. (Söding, Graefe, Moctar and Shigunov (2012) [13])

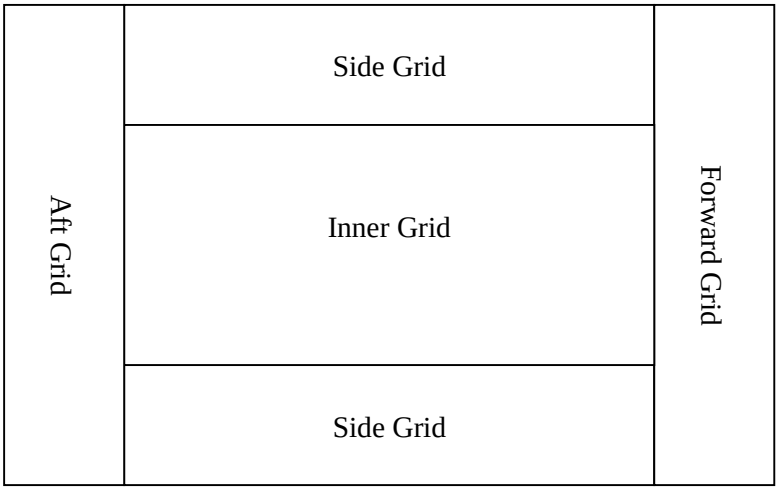

Figure 4.2. Divisions of free surface grid

4.1.3. Using GL Rankine Solver

Since GL Rankine solver does not have Graphical User Interface (GUI), it has to be run with executable xml file, which is called config.xml or other arbitrary name, in the command line. This file includes all the command for computation and input and output files such as geometry of hull form or result files. In the first section, some information about the project is mentioned. The second section is the computation section which contain all the pre-processing, simulation method and post-processing commands. The followings are the general constructions of computation section;

- In pre-processing step, generation of unstructured body panel mesh and block structured free surface mesh are included.

- The body part surface can be uploaded into the solver as legacy VTK files or STL files-ASCII or STL files-binary.
- It can be uploaded several bodies and body parts. For symmetric body, only the half of the body is needed to input and the algorithms generate the panels on the body surface and on the free surface, assuming that a body part is "topological similar" to a ship half.
- If the uploaded surface is in STL format, it must be a watertight grid of plane triangles that should be small enough to describe the ship hull geometry (recommended from 20,000 to 50,000 triangles). The surface should not have hanging nodes, gaps or overlapping triangles and also the normal vectors should be pointed into the fluid. The surface should not include transom stern and deck surface, or else they have to be removed by the command while computing with non-linear method.

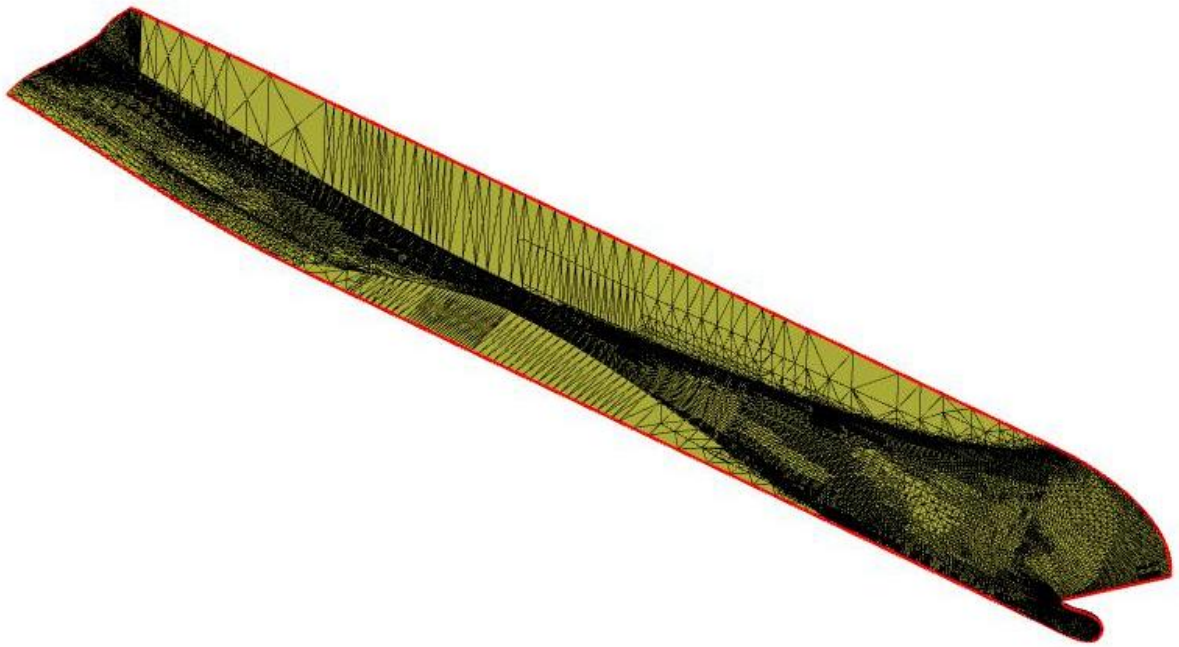

Figure 4.3. Imported ship body surface in STL format

- The body panel generation can be done by using the factors; '**lMid**', '**lBow**', '**lAft**', '**zAft**' and '**zBow**', while other parameters can be set to default values or set manually. For non-linear computation, '**zAft**' and '**zBow**' should be proportional to the stagnation height $\mathbf{z = u^2/2g}$ (recommended for **zAft** ~ min(0.3**z**, **lAf**t) and **zBow** ~ min(0.5**z** to 1.0**z**, **lBow**)). It is important to set these two parameters carefully because they are the initial position of wave height at the bow and aft of the ship surface.

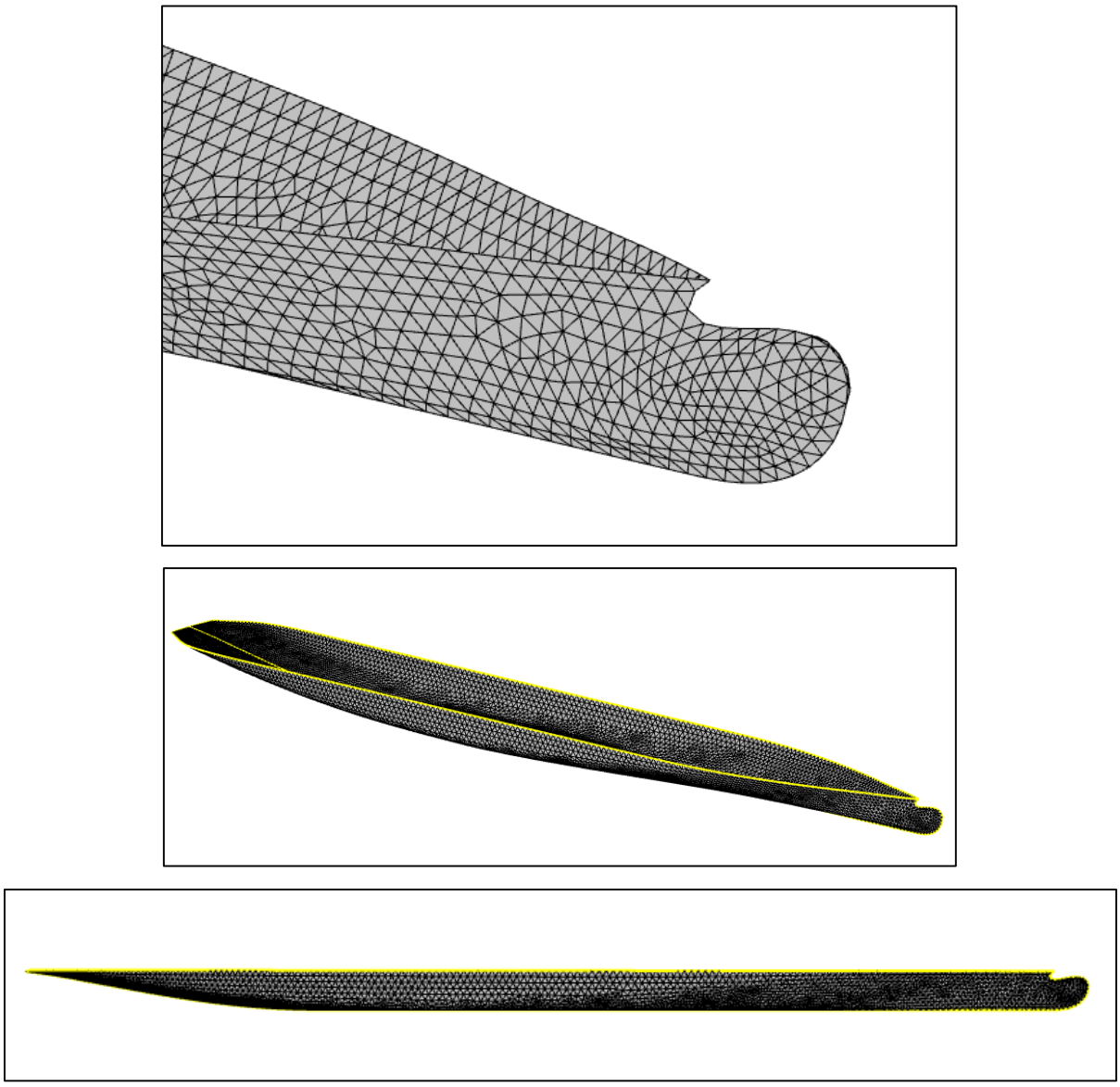

Figure 4.4. Manually created unstructured body mesh in GL Rankine

- If the origin of coordinate system of the input geometry is set at the aft base line of the ship, it should be transformed into the undisturbed water plane and the centre of gravity should be located above or below the origin in GL Rankine method. It is recommended to shift to LCB of ship in x-direction and draft of ship in z-direction. If applicable, translation, rotation and scaling action of the surface can be done.
- For generation of free surface, the quadrangular panel grids can be created automatically depending on the ship size and forward speed, or else it can be set manually by controlling the parameters.

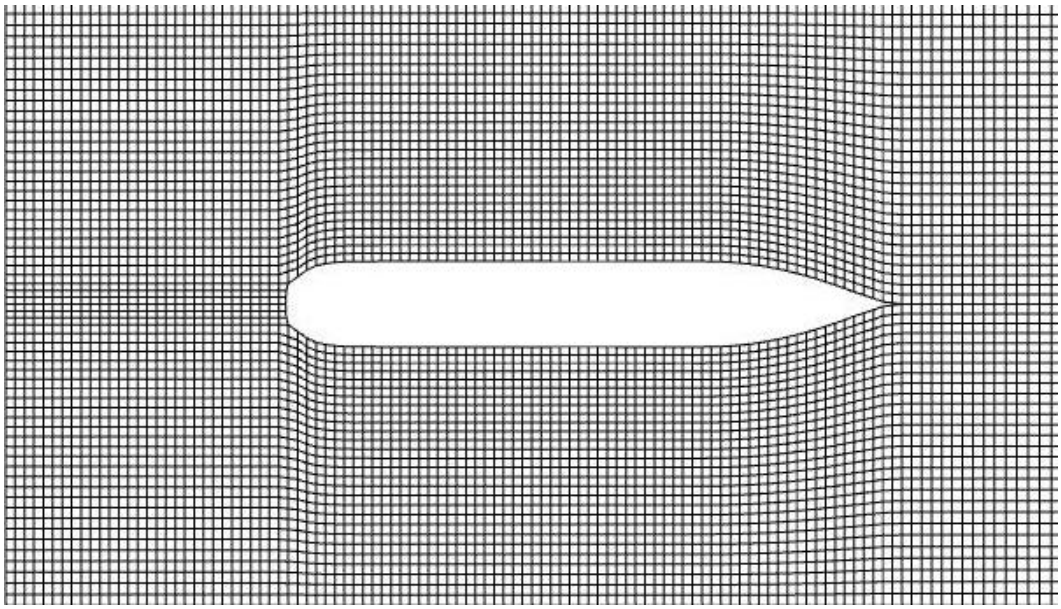

Figure 4.5. Automatically created structured free surface mesh in GL Rankine

- In simulation step, it can be done with Non-linear steady computation or Double body flow computation.
- It is necessary to define the position of centre of gravity of the ship from the origin of GL Rankine coordinate system (**cogX**, **cogY** and **cogZ**). **cogX** and **cogY** are automatically defined by the solver from hydrostatic calculation, but **cogZ** has to be set by calculating from the ship data.
- In order to avoid the wave breaking behaviour, it is sometimes needed to use the wave damping factor '**wdp**' and also to get effective convergence, the relaxation number '**relax**' and the initial relaxation number '**relax0**'. These factors are quite sensitive and needed to set carefully if it is not possible to use their default values.
- In post-processing step, all the results can be extracted by SHR2 file and ASCII file. In SHR2 file, only the results of the last iteration are kept, while the results of all iterations history are stored in ASCII file. In addition, VTK files of body panel and free surface for all the iterations can be extracted for visualization purpose.
- For seakeeping calculation, it is required the result file from steady flow computation. The SHR2 result file is loaded as input in seakeeping command.
- The information about the ship body has to be known before starting the seakeeping computation, such as metacentric height, roll damping and radii of gyration in X, Y and Z direction.

- For inputting wave data, it can be loaded in terms of wave frequencies or encountered wave frequencies that can be set as automatically or manually. Only regular waves can be imported with GL Rankine.
- This method can be set up the motion constraints of the ship in 6 degree of freedoms (6DOF).
- As mentioned above, free surface generation in linear seakeeping computation consists of inner grid and outer grid with different boundary conditions, whereas the outer grid is coarser than the inner grid. It can also be generated by default command or created manually.

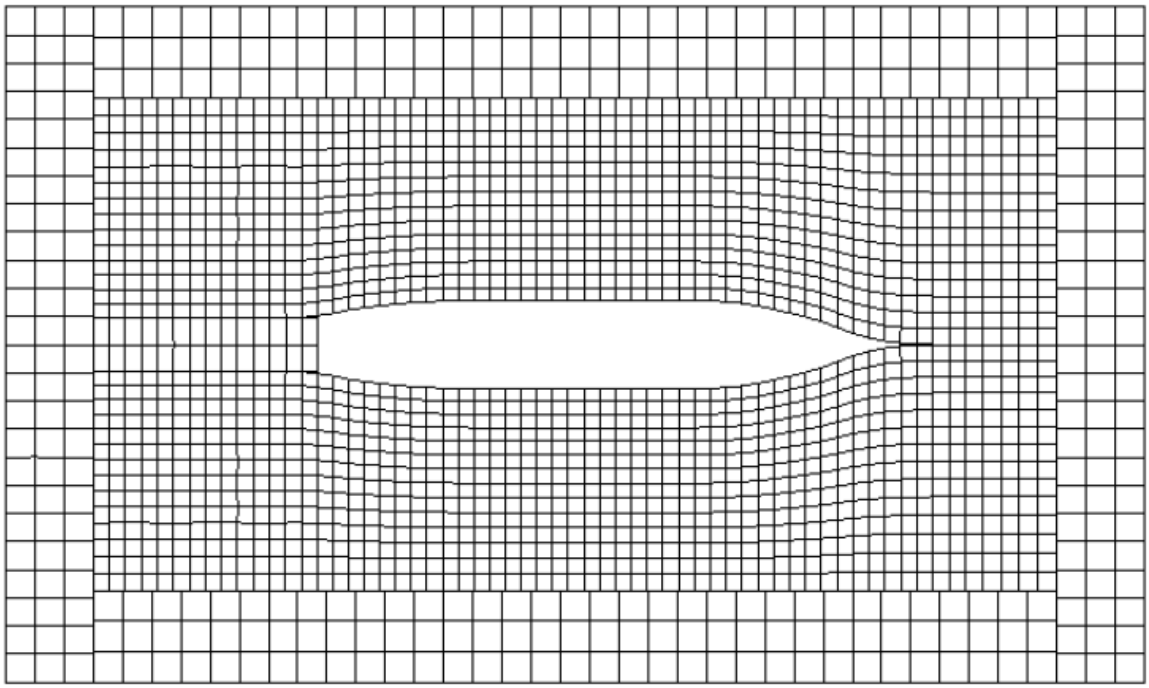

Figure 4.6. Free surface grid created from GL Rankine in seakeeping computation

- Same as in steady computation, the results files are extracted with two type of files; SHR2 file and ASCII file.
- The set up input XML file for steady flow computation and seakeeping computation are shown in Annex A3.

4.2. Validation of Numerical Results with Experiment

The set-up file is done after trying and adjusting the parameters for different situations and finally, the simulations for different speeds for both steady flow computation and seakeeping analysis are finished with the resonable results. But in order to explore to accuracy of the results that come out from GL Rankine solver, they are validated with the experimental results that are done in HSVA model basin in August, 2013.

4.2.1. Description of Experiment

The model test was performed with a cruise liner model in regular waves at the draught of 7.2m (full scale) with zero trim value in the framework of Persee project. The test was executed at two different speeds, which are 15 knots and 21 knots. The main investigation in the towing tank is to find out the wave added wave resistance and the motion behaviour of the vessel. Before testing in regular waves, towing tests in clam water were done in order to obtain the values of calm water resistance. By emphasizing mainly for the motion behaviours in short waves whose wavelengths are with the scale less than 1.0 of ship length, the wavelengths tested were selected in the range of scale from 0.17 to 2.5 of ship lengths for regular waves. The results of wave added resistance are calculated in terms of non-dimensional coefficients (C_{AW}) and the motion characteristics, in linear response amplitude operators (RAOs). For the purpose of allowing six degree of freedoms (6DOF) for the tested model, a special towing frame and two articulated force balances were designed and constructed. Instead of attaching a pair of propeller dummies, the test was performed without any propeller, but a pair of full spade type rudders according to the design given by Meyer Werft was assembled to the test model.

The length between perpendiculars of the full scale cruise ship is 220.273 m and twin propellers with a centre skeg and a pair of bilge keels are included in the design of cruise vessel. Therefore, in accordance of lines drawings given by Meyer Werft, the test model was created with the scale of 1:36. Based on the design provided for original vessel, a pair of tapered bilge keels was attached to the bilge of the model with an angle of 45°. For the simulation of turbulent flow around the model, two sand stripes were fitted at the stations 19.5 and 21.5. The detailed dimensions and particulars of model scale and full scale are mentioned in Table 4.1.

By adjusting the longitudinal distribution of ballast weights, the radii of gyrations for pitch of 26.3% of L_{PP} were obtained with respect to L_{CG}. With the same way, the ballast weights were

moved vertically to achieve the values of transverse metacentric height GM_T of 2.754 m for the model. The inclining test in calm water was done to ascertain these values. With ultra-sonic wave gauges, the wave elevation values were measured at six positions near the ship model for each test run. (Hong and Valanto (2014) [14])

	Symbol	Unit	Full scale	Model
Scale	λ		36	
Length on waterline	L_{WL}	m	220.273	6.1187
Length between perpendiculars	L_{PP}	m	220.273	6.1187
Breadth	B	m	32.200	0.8944
Breadth on waterline	B_{WL}	m	32.200	0.8944
Draft	T_{mean}	m	7.200	0.2000
Draft at aft perpendicular	T_{AP}	m	7.200	0.2000
Draft at forward perpendicular	T_{FP}	m	7.200	0.2000
Transverse metacentric height	GM_T	m	2.754	0.0765
Vertical center of gravity	KG	m	15.054	0.4182
Height of metacenter above BL	KM_T	m	17.804	0.4946
Longitudinal center of gravity	L_{CG}	m	99.601	2.7667
Longitudinal center of buoyancy	L_{CB}	m	99.601	2.7667
Vertical center of buoyancy	KB	m	4.027	0.1119
Block coefficient	C_B		0.6507	
Radius of gyration ixx	i_{xx}	m	14.470	0.4019
Radius of gyration iyy	i_{yy}	m	58.070	1.6131
Displacement volume	VOL	m^3	33229.0	0.7122
Depth, moulded	D	m	19.800	0.5500
Depth of the model	D_{model}	m	17.280	0.4800
Wetted surface area	WSA	m^2	7822.8	6.036
midship section coefficient	C_M	m	0.980	
waterline area WLA	WLA	m^2	5974.9	4.610
Height of roll center above BL		m	14.510	0.4031

Table 4.1. Particulars of model scale and full scale of cruise liner (Hong and Valanto (2014) [14])

Figure 4.7. Side view of test model (Hong and Valanto (2014) [14])

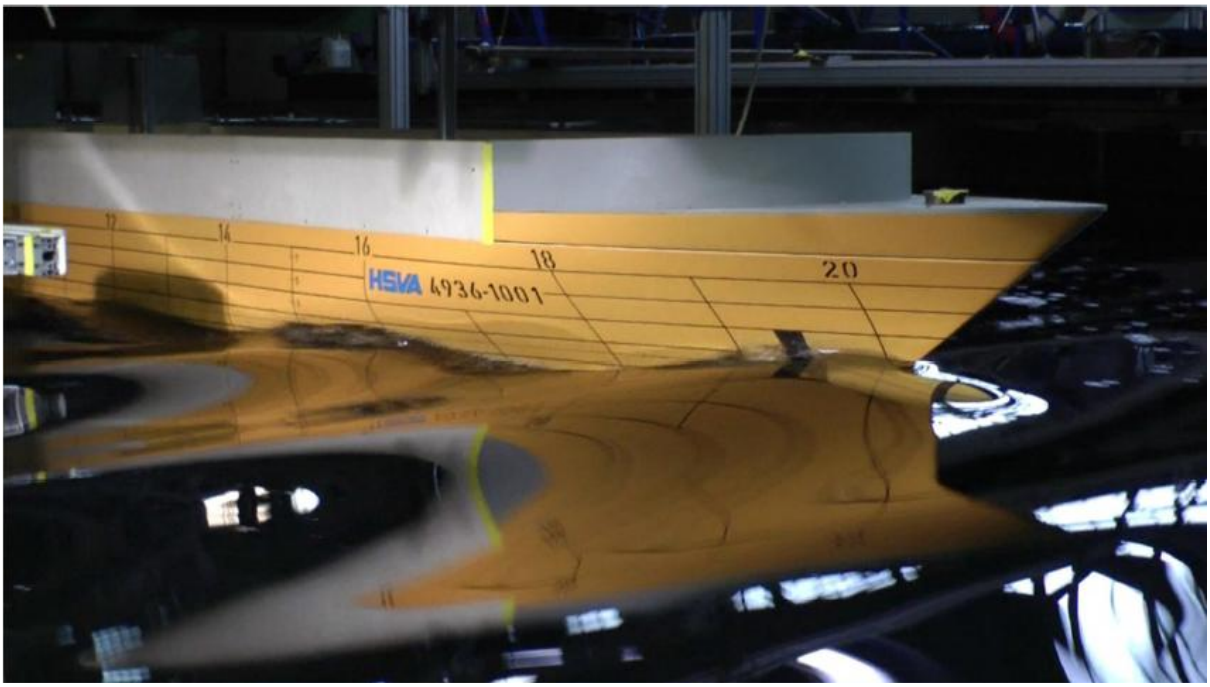

Figure 4.8. Testing process in towing tank (Hong and Valanto (2014) [14])

4.2.2. Calculations and Comparisons of Result values

Calm water resistance

After testing the model in calm water, the total resistances are measured for both speeds. As usual, non-dimensional coefficient of total resistance (C_{TM}) for the model is calculated by Eq. 1, while the friction resistance coefficient (C_{FM}) is obtained by ITTC 57 formula, Eq. 2. Here for this vessel, the form factor is not able to know exactly from information provided from the original ship designer and so, it is assumed as 0.2. Therefore, the residual resistance coefficient of the model (C_{RM}) is achieved by Eq. 3.

$$C_{TM} = \frac{R_{TM}}{\frac{1}{2}\,\rho_M\, S_M\, V_M^2} \tag{1}$$

$$C_{FM} = \frac{0.075}{(log_{10}(Rn_M) - 2)^2} \tag{2}$$

$$C_{RM} = C_{TM} - C_{FM}(1 + k) \tag{3}$$

where; $Rn = \frac{V\ L_{WL}}{\upsilon}$

By Froude number similitude, the coefficients of the residual resistances of the model scale and full scale are the same and therefore, C_{RS} for full scale is obtained. By following the same procedure as the model scale, the total resistance coefficient of the full scale ship (C_{TS}) is achieved and finally the total resistance of the full scale vessel is calculated. In Fig. 4.9, the comparison of the numerical results simulated by GL Rankine and the experimental results performed by HSVA are described accordingly. It can be seen that although the experiment was done for two speed and its curve shows the straight line, the curve for numerical results shows some curvature. At two extreme speeds, the total resistance at 15 knots has the increment of 6% in numerical results compared to that in experimental results, while the total resistance at 21 knots is reduced 5% in simulation. Nevertheless, these differences are in the range of acceptable limit and it can be said that GL Rankine has the relevent accuracy.

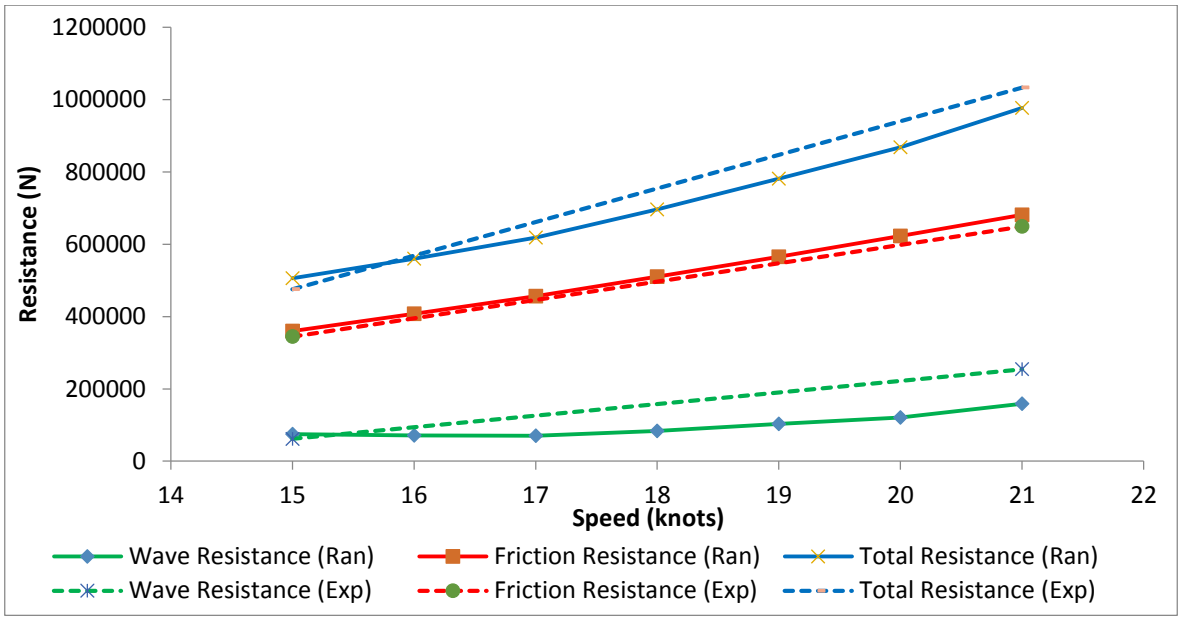

Figure 4.9. Comparison of total resistances between experiment and numerical analysis

Wave added resistance

As mentioned above, the towing tests in regular waves were performed at the draught of 7.2 m with a cruise liner model at the two speeds of 15 and 21 knots. The wave added resistance (R_{AW}) is achieved by extracting the calm water resistance from the total resistance of the model in waves. The transfer function and the non-dimensional coefficient of the wave added resistance are computed by using the Eqs. 4-5. Assuming the wave added resistance coefficients of both model and full scale ship are the same, the transfer function of wave added resistance of the cruise liner is obtained by using the same equations as in model scale. (Hong and Valanto (2014) [14])

$$Transfer\ function\ of\ R_{AW} = \frac{R_{AW}}{\zeta_a^2} \tag{4}$$

$$C_{AW} = \frac{R_{AW}}{\rho g\left(B^2/L_{WL}\right) \cdot \zeta_a^2} \tag{5}$$

For the numerical results, the simulation is done by GL Rankine solver with the same wave amplitudes as the experiment in head waves (180°). The comparison is shown in Fig. 4.10 and Fig. 4.11 for the speeds of 15 knots and 21 knots, describing the wave added resistance (C_{AW}) verses the ratio between ship length to wavelengths of incoming waves. It is observed that the

ship length to wavelength ratio of up to 1.5, both results are closed enough, but are differing more and more upon increasing the ratio. But, the trends for both results has a certain amount of similarity.

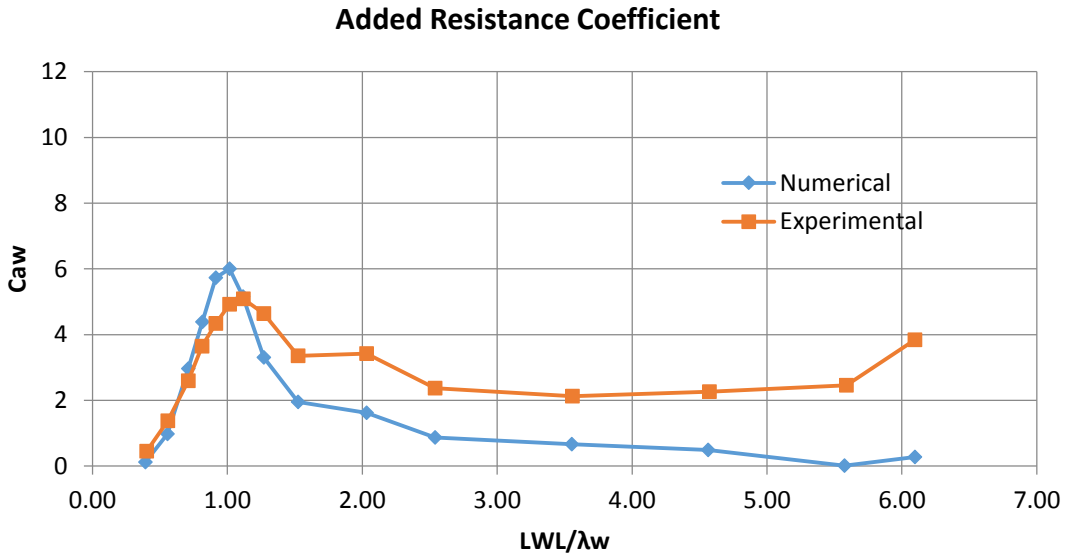

Figure 4.10. Comparison of C_{AW} between experiment and numerical analysis at 15 knots

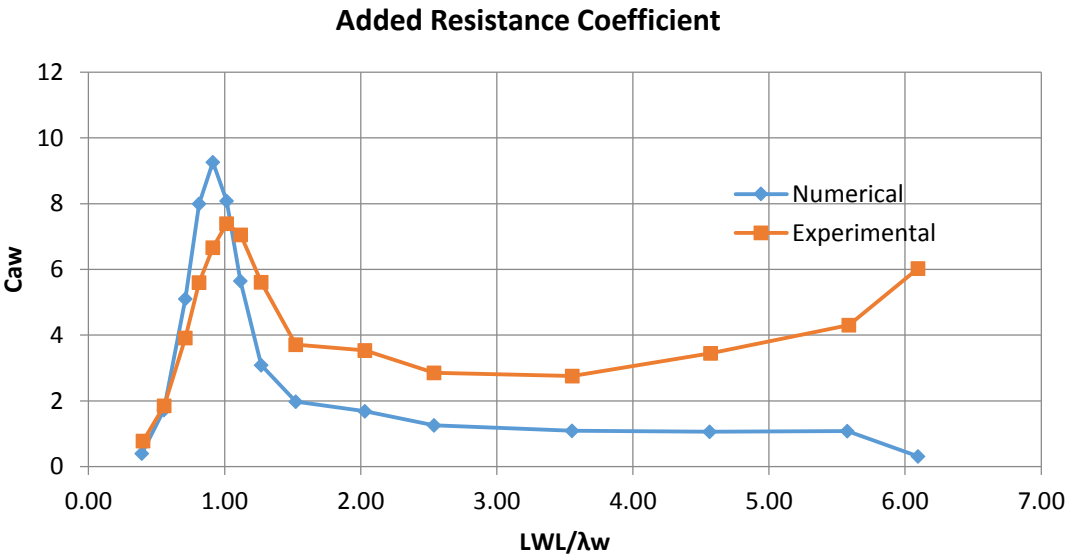

Figure 4.11. Comparison of C_{AW} between experiment and numerical analysis at 21 knots

Response Amplitude Operator (RAO) of motions

In the experiment, the RAOs of each motion for 6DOF were determined based on the 1st order amplitude and the relative phase of each response, which was calculated by the harmonic analysis. (Hong and Valanto (2014) [14])

$$RAO_X = \frac{X_a}{\zeta_a} \tag{6}$$

The results of the RAOs of the motions simulated by numerical analysis and performed by towing test are mentioned in Figs. 4.12-4.17. Among all the motions in 6DOF, surge motion, heave motion and pitch motion are dominant than the other motions. By comparing with the experimental results, these motions have the quite closed trend and results for all waves, except for heave motion which has some fluctuations in experimental results between the ship length to wave length ratio of 0.7 and 1.52.

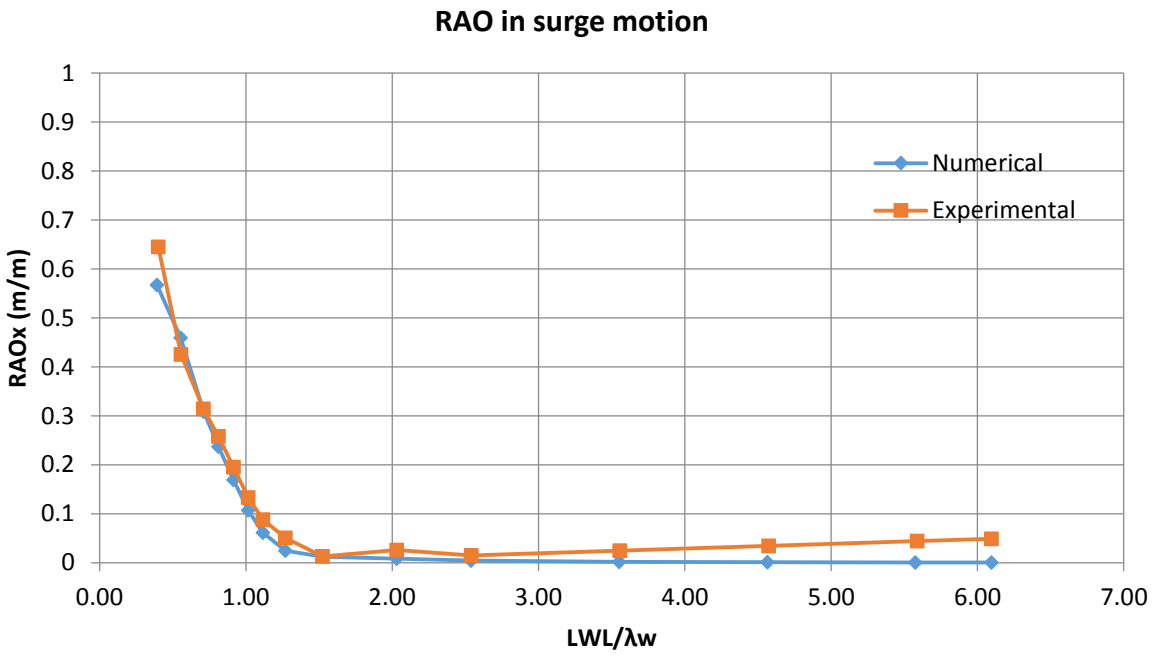

Figure 4.12. Comparison of RAO in surge motion at 15 knots

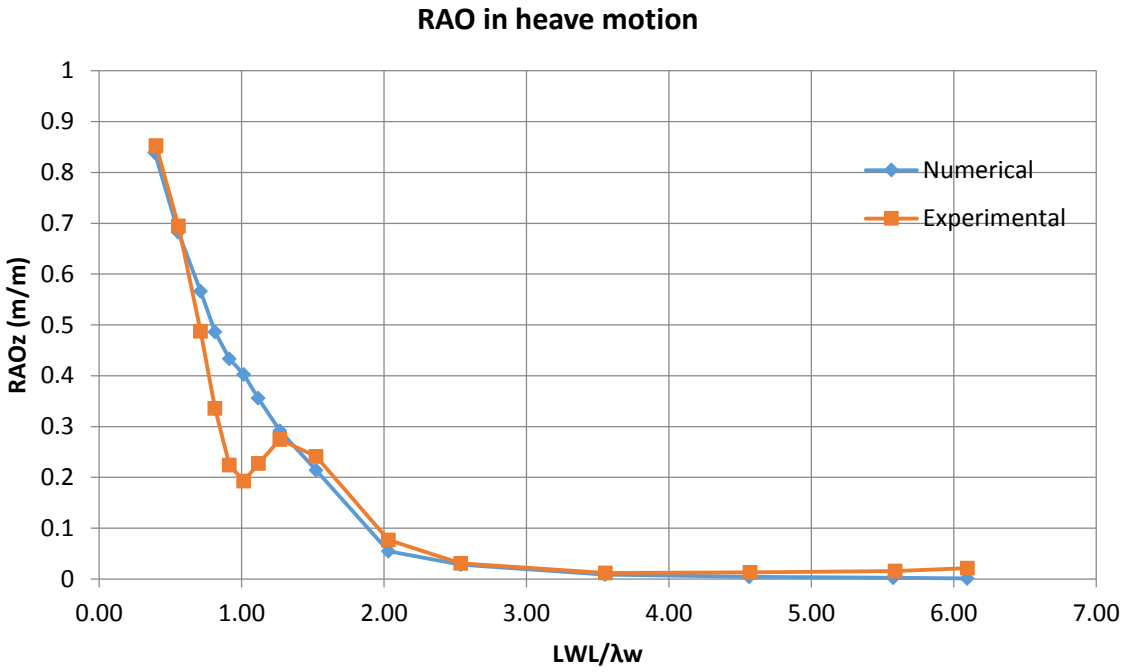

Figure 4.13. Comparison of RAO in heave motion at 15 knots

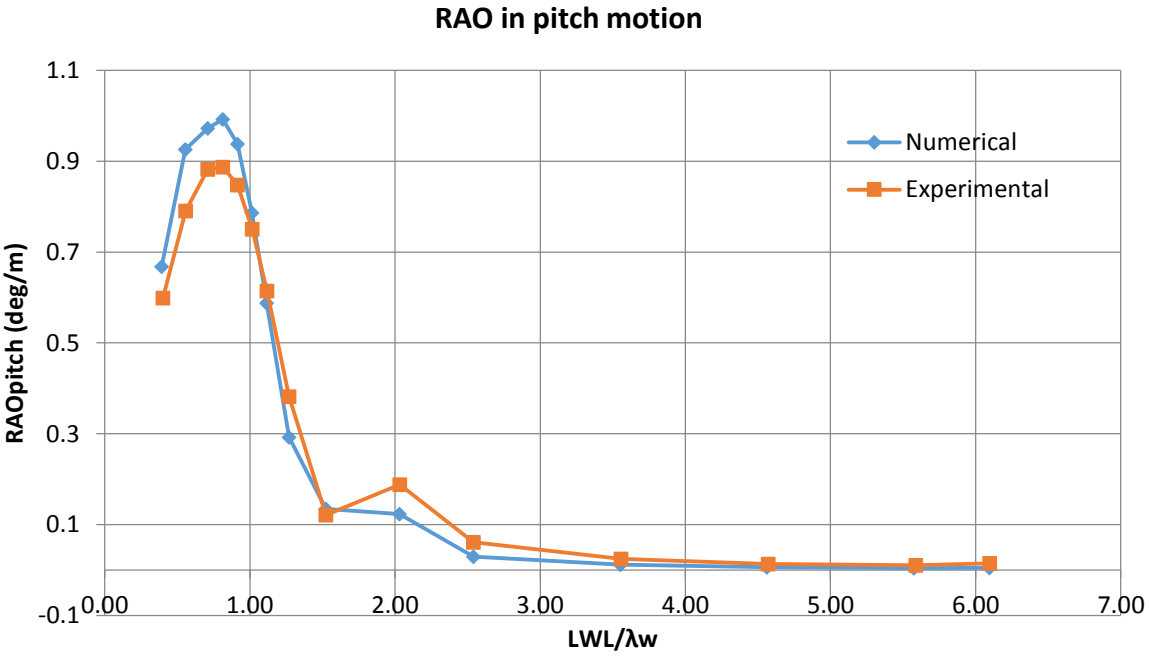

Figure 4.14. Comparison of RAO in pitch motion at 15 knots

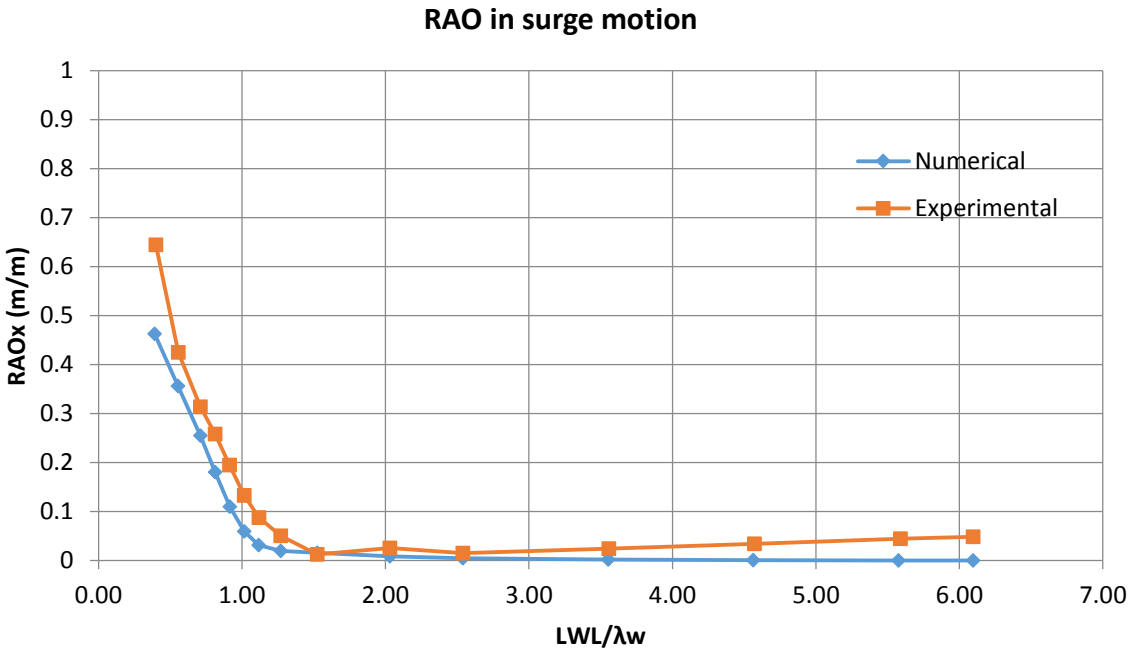

Figure 4.15. Comparison of RAO in surge motion at 21 knots

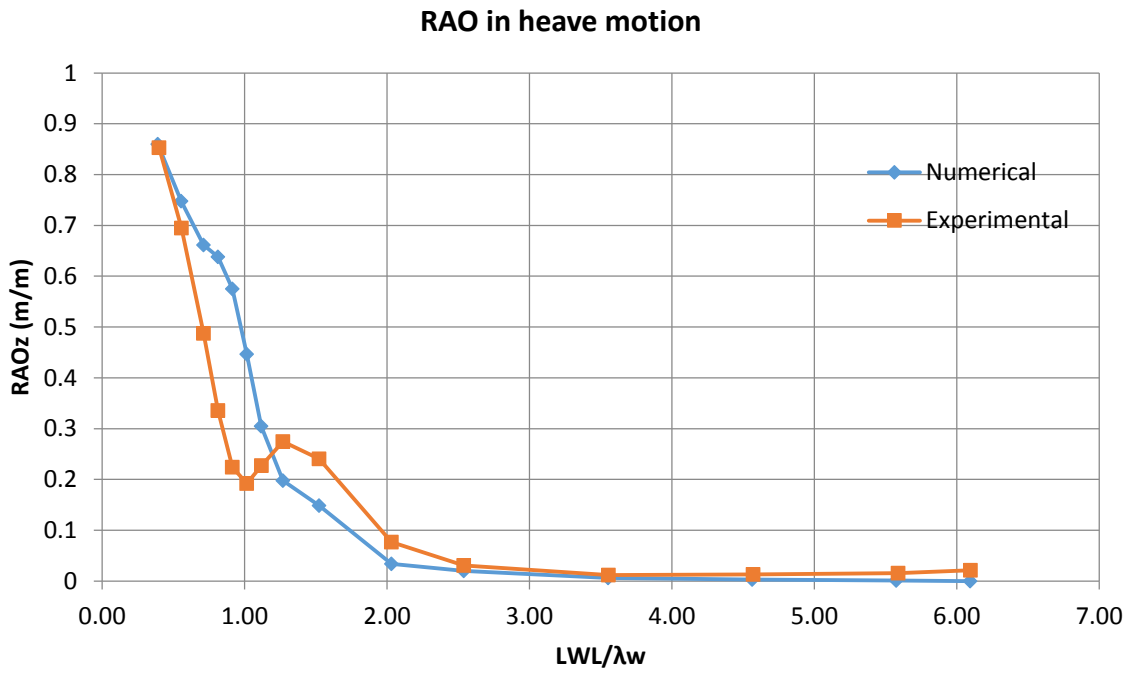

Figure 4.16. Comparison of RAO in heave motion at 21 knots

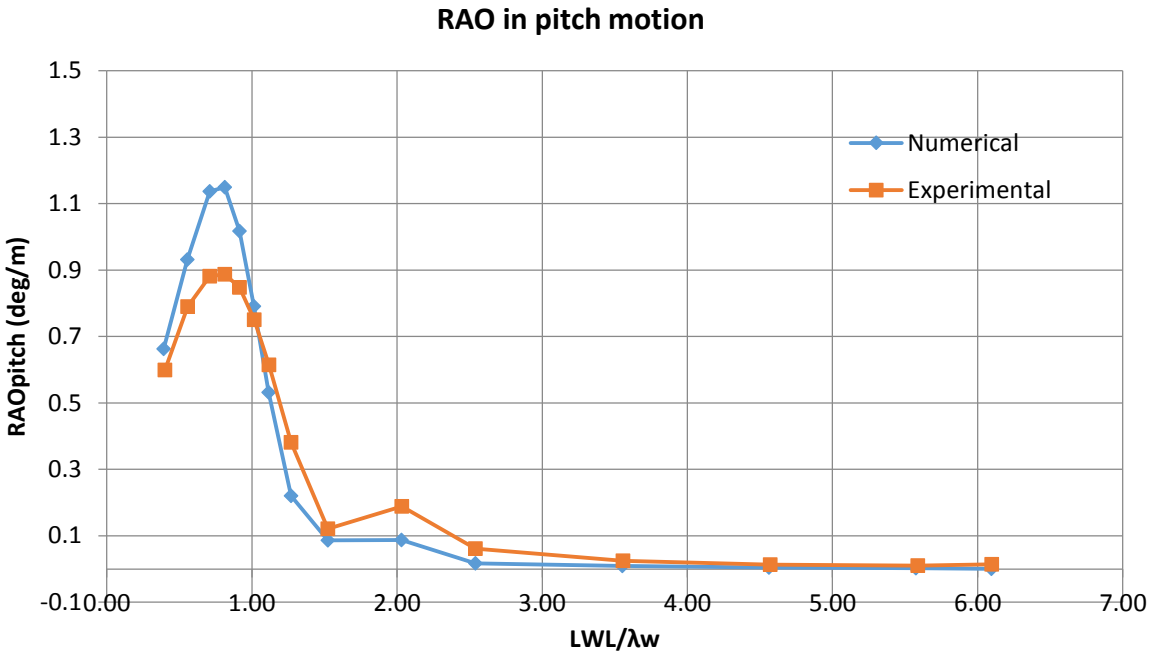

Figure 4.17. Comparison of RAO in pitch motion at 21 knots

5. COUPLING OF CFD CODE WITH CAESES

After getting the stable set-up for GL Rankine and validating its results with experimental data, it is necessary to joint this solver with CAESES frame work to get the automatic optimization process and hull form design updating process depending on the objective results come out from the solver. In addition, it is important to do the post processing process of the results to visualize clearly from the user for studying of its design changes and updated results such as panel creation, hull form design, wave pattern, calm water resistance and wave added resistance and so on.

CAESES/FFW is an integration platform that can launch and control the CFD (or other) simulation studies. Any CFD code that can be run in batch mode from a geometry file and input script can be coupled. Other than CFD simulations, other CAE tools can also be coupled. In particular, tools for flow simulation (CFD) or structural analysis (FEM) can be plugged-in and controlled from within CAESES/FFW.

Software connection tutorial in CAESES is mentioned in detail about how to couple the external software in the framework of CAESES/FFW to undertake design studies and shape optimization. Basically, the software should be merely able to run in batch mode. Geometry from CAESES/FFW is exported to the software and template input files that control the software can additionally be manipulated for each design. Finally, result data such as simulation results are then directly loaded into CAESES/FFW. They can be accessed and utilized by the user, for instance, in optimization loops – being the natural next step when the simulation is connected.

The basic setup to couple with external software is as follows:

- Simulation software that runs in batch mode (script, executable)
- Optional ASCII input files that control the external software
- ASCII output files, in particular containing key result values such as pressure loss, resistance etc. (csv, txt, etc.)
- Optional output screenshots that will be shown in the picture viewer of CAESES/FFW.
- Optional output files (vtk, tecplot) for interactive 3D post-processing such as plane cuts, streamlines, etc.

For the connection with GL Rankine code, there will be two software connectors; the former is for the simulation of CFD code and extraction of the results for clam water resistance and the

latter is for the visualization of free surface for the last iteration that is created from moving of ship in calm water.

5.1. Coupling for Simulation of Resistances

In Fig. 5.1, it will show the overview of this connector. The input files for the simulation are the ship geometry file in STL format which is modelled by using CAD system in CAESES, the set-up file for GL Rankine solver and new folder creating test file in order to store all the result VTK files of free surface generation and static pressure distribution on the body for all iterations upon running the simulation.

As the hull geometry is changed during the optimization process due to updating of the design parameters, the input data for the set up file are also varied depending on the input geometry. Therefore, there are four input variable data created for the set-up file. The simulation will run for the hydrostatic calculation first for each hull design and these four input variables will be updated.

After simulation, the result values will be extracted from the ASCII file in which the results for all the iterations history are stored. From this file, three result values will be extracted; the number of iteration, wave resistance and friction resistance. Total resistance will be computed after getting the form resistance by multiplying the friction resistance with the form factor 0.2. For the case of optimizing directly for sea state, wave added resistance value will be extracted additionally from another attached result file from seakeeping computation.

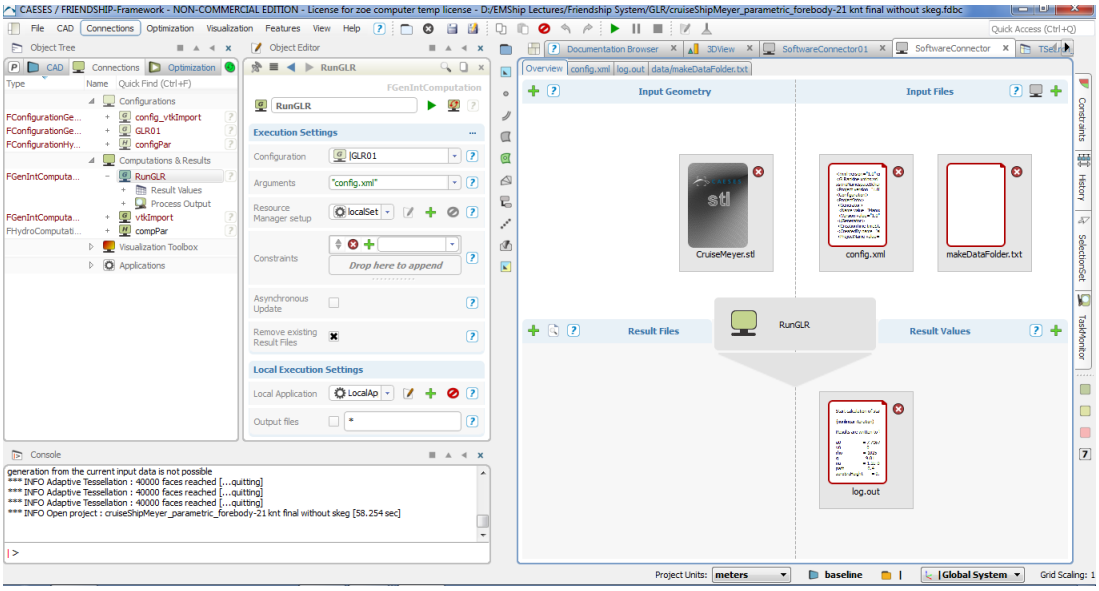

Figure 5.1. Overview of software connector for GL Rankine solver

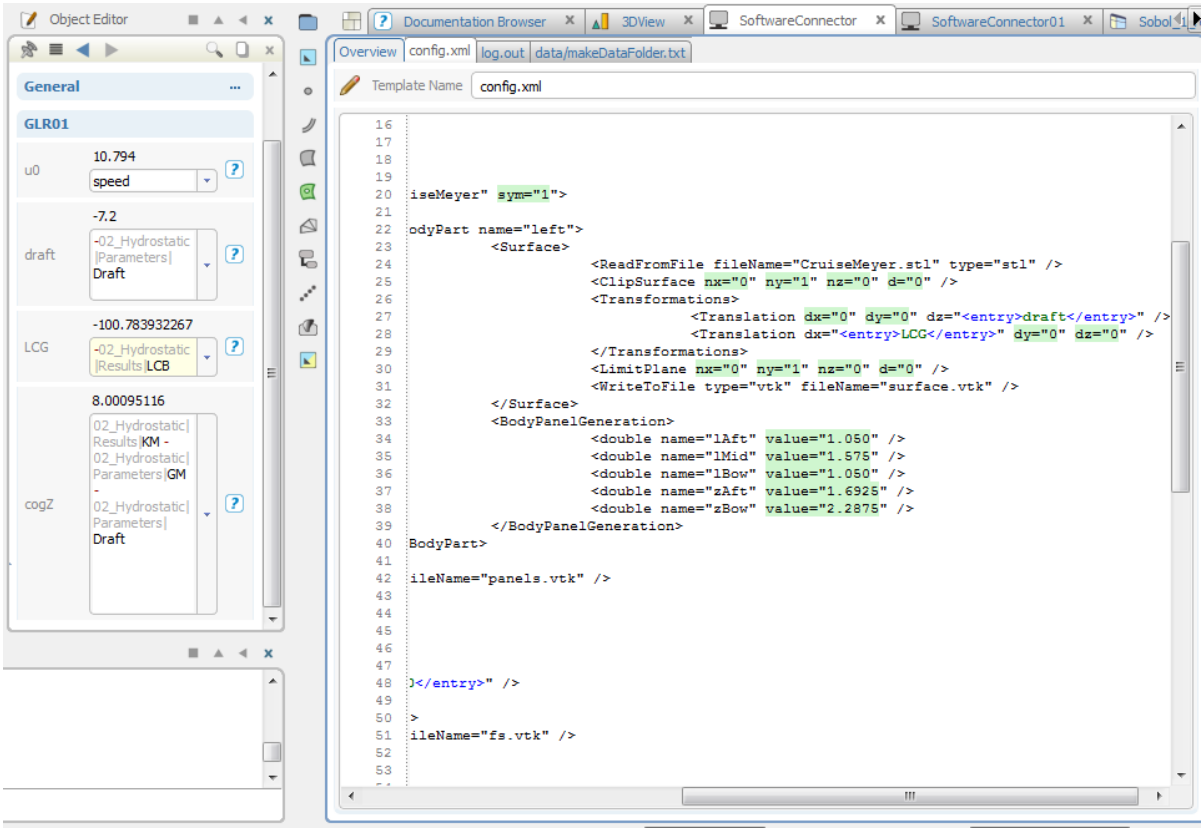

Figure 5.2. Input file set-up for the solver

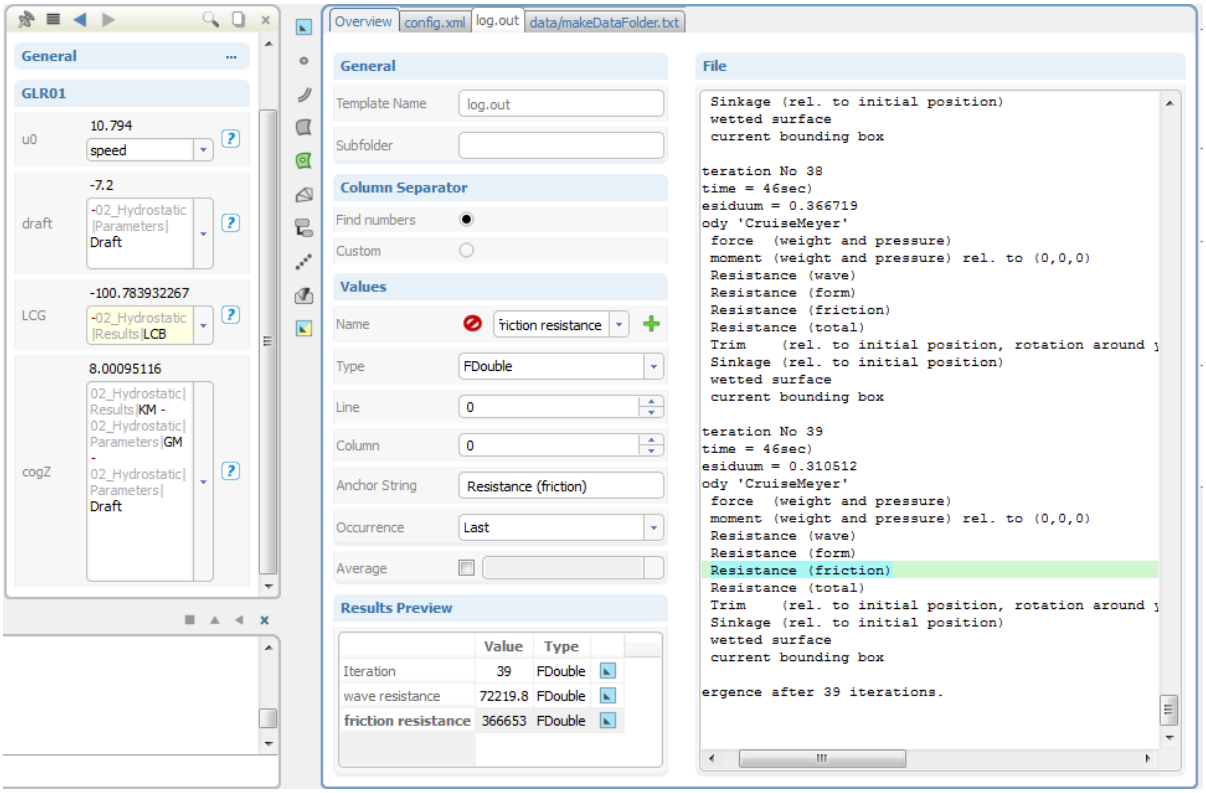

Figure 5.3. Result file set-up for the solver

5.2. Coupling for Visualization

For post processing, it is needed to do another software connector because the file used for extracting the results is the ASCII file that contains all the iteration history. Therefore, the results for the last iteration have to be extracted and visualized. From the previous software connector, the number of iteration is extracted and so, two string parameters are created for VTK files of free surface and static pressure distribution on the body for the last iteration. These two VTK files are copied to the folder by copy.bat text file and are used as the results files for visualization. In order to make sure that this software connector is run together with the previous one, one result parameter is created in the text file and is evaluated during the optimization process.

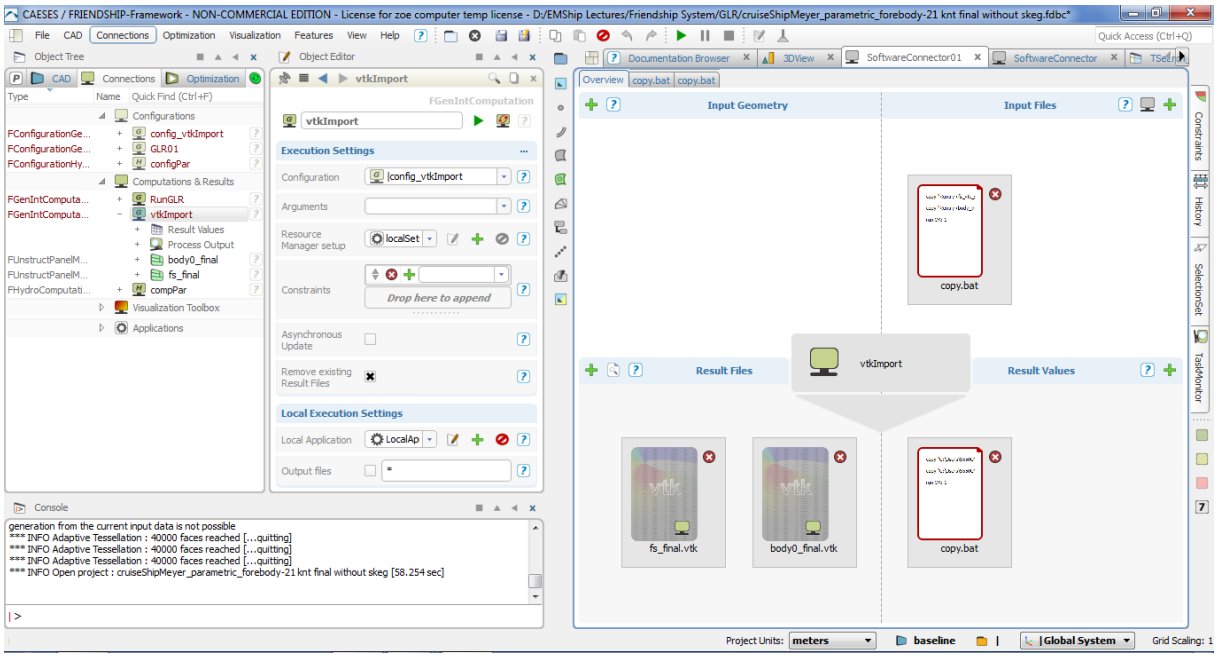

Figure 5.4. Overview of software connector for visualisation

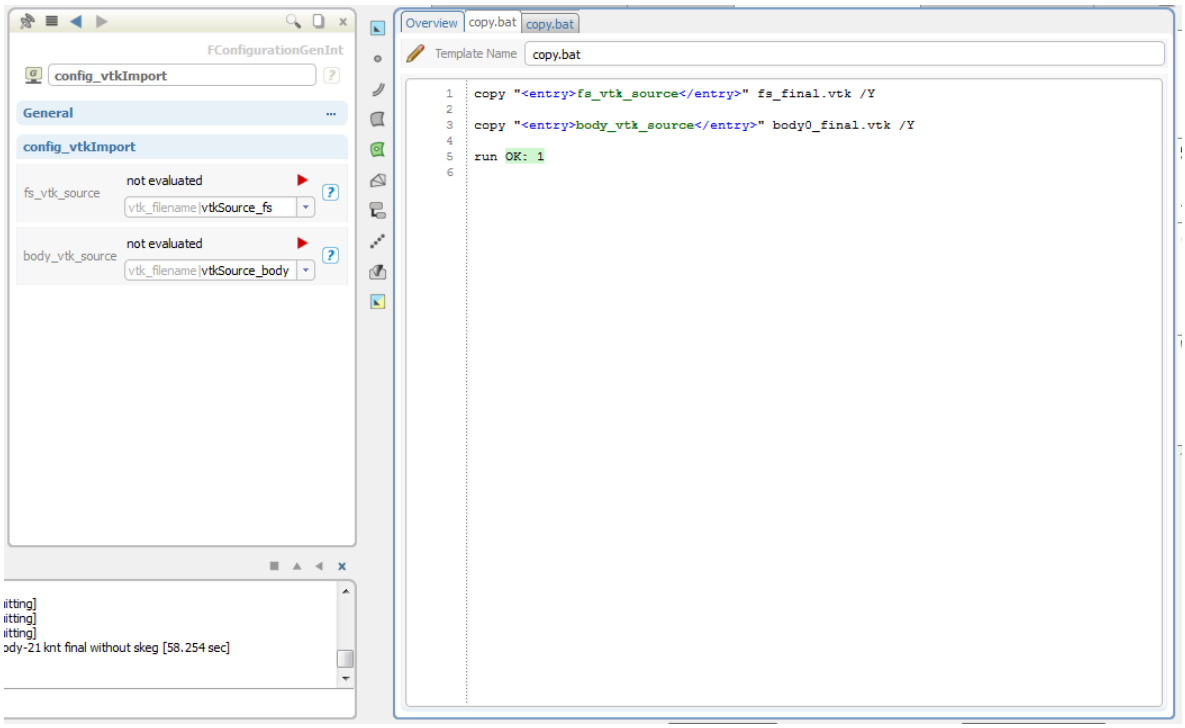

Figure 5.5. Input file set-up for visualisation

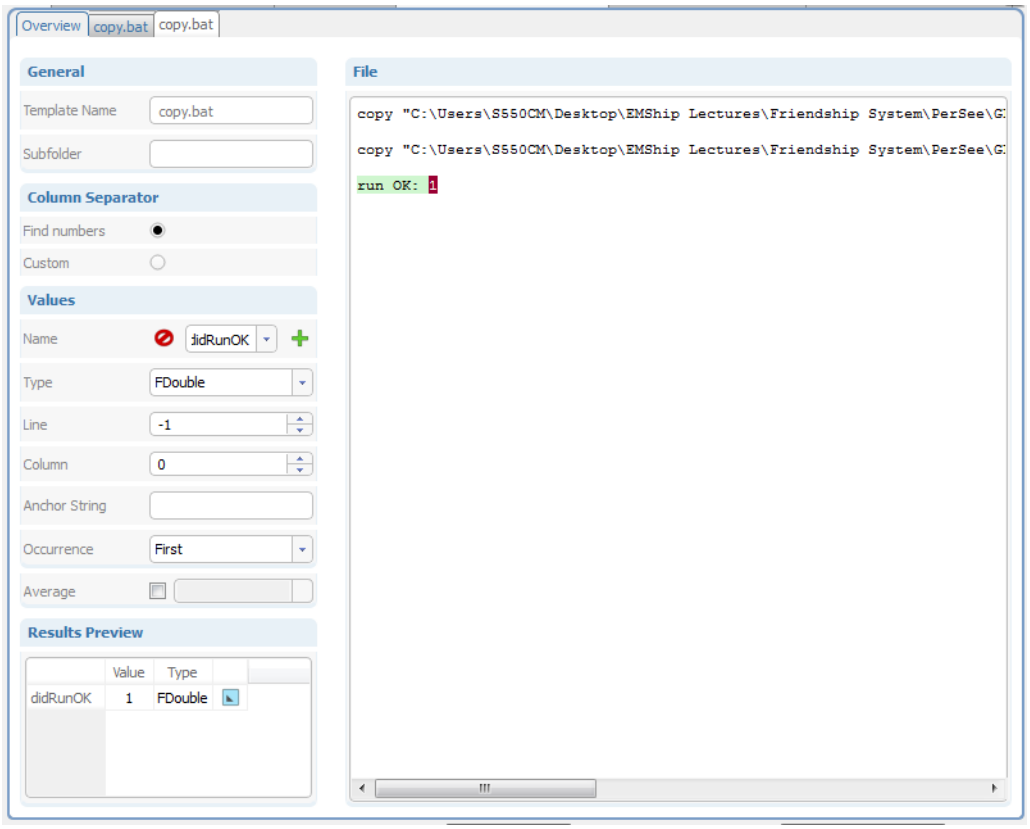

Figure 5.6. Result file set-up for visualisation

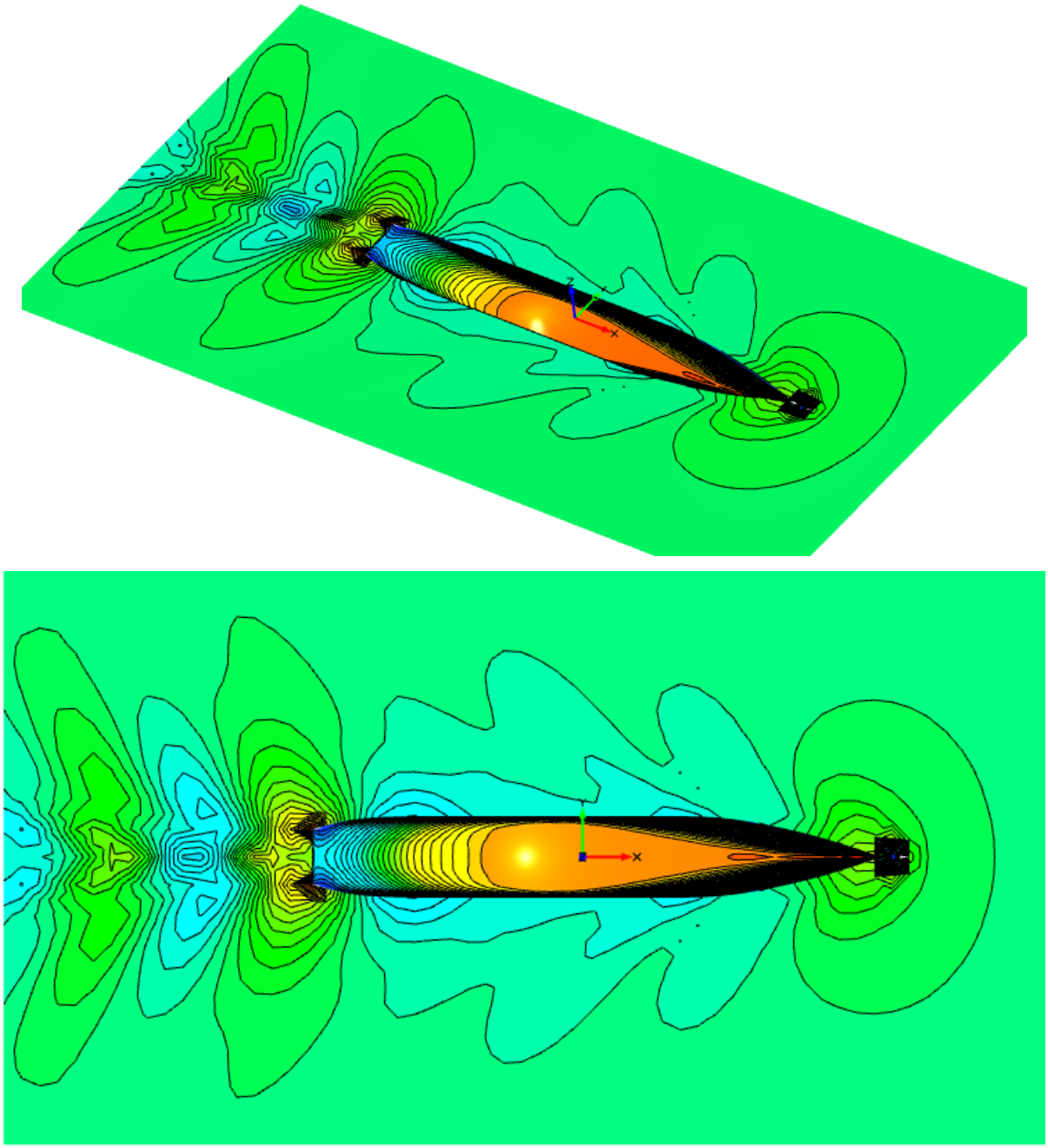

Figure 5.7. Visualisation of free surface generation and static pressure distribution on the body

6. OPTIMIZATION PROCESS IN CALM WATER CONDITION

In the past, optimization is a long and costly experiment test with limited number of designs. Nowadays, with the numerous optimization methods, thousands of designs can be simulated and optimized with effective algorithms in a short time without doing any experiments and it is cost effective. The efficiency of algorithm is depending on the types of constraints, number of objectives, function of the problem to solve, time required for the process and accuracy of the objectives. There are two different categories of optimization algorithms; Deterministic Algorithms and Stochastic Algorithms. In this section, optimization process will be performed for simulation in calm water condition, calculating the total resistance of the ship by applying some constraints.

6.1. Design of Experiment

The first step toward the optimization is the Design of Experiment (DOE) which is usually driven by a random or quasi-random process, aiming at exploring the design space and optimization potential given the defined design variables and constraints. By doing DOE, optimization process can be driven towards the global optimum, not to local optimum. Designers can determine simultaneously the individual and interactive effects of many factors that could affect the output results of the design with DOE as illustrated in Fig. 6.1. (Harries and Brenner (2014) [15])

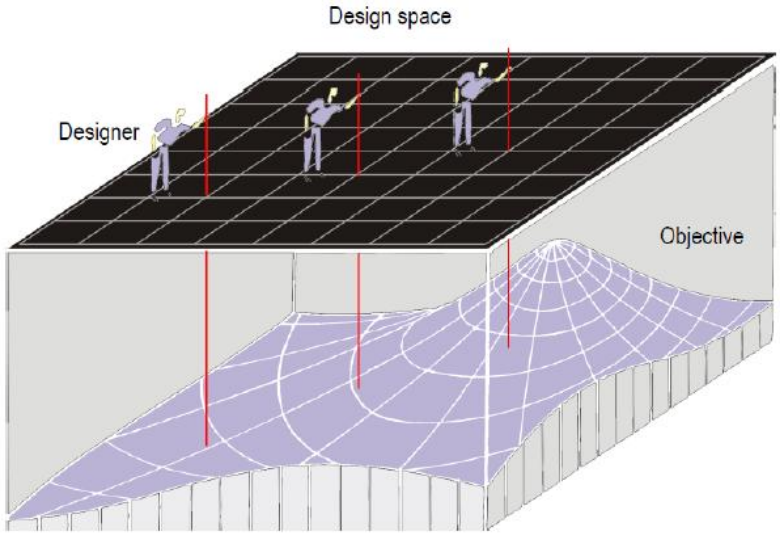

Figure 6.1. Exploration of design space (Harries and Brenner (2014) [15])

The design engine that is used for the simulation, in other words the algorithm responsible for the variation of the design variables, is the SOBOL algorithm which is a deterministic algorithm that imitates the behavior of a random sequence. The documentations in CAESES/FFW mention that this kind of algorithm is also known as quasi-random or low discrepancy sequence. The quasi-random feature is very beneficial in order to avoid local concentrations and that the variations are well spread within the range of the design variables. Similar to random number sequences the aim is a uniform sampling of the design space. Sobol type algorithms are known to have superior convergence than random sequences.

The design constraints are primarily stability constraints; location of the center of buoyance and metacenter, as well as boundaries/margins for the displacement for which very often in ship design, larger vessels are favored in terms of the Required Freight Rate due to the larger economies of scale. Therefore, the following constraints are applied to the optimization process;

- Displacement of new designs will not be reduced more than 1% of that of original design.
- Metacentric height of new designs will not be shifted more than +/- 1% of that of original design.
- Longitudinal center of buoyancy and vertical center of buoyancy of new designs will not be shifted more than +/- 1% of that of original design.

Table 6.1 will show the design variables and their boundaries while running SOBOL to explore the design space.

Design Variables	Lower Limit	Base Model Value	Upper Limit
AngleDWL	10	18	25
u0Fillet	0.1	0.19	0.22
xFOB	155	180	195
fullnessKeel01	0.14	0.14	0.21
fullnessSecKeel	0.8	0.87	1.05
tanSecKeel	32	53	70
tanTopEnd	-95	-85	-25
zPeak	0.65	0.765	0.78

Table 6.1. Design Variables and their boundaries for DOE

By using SOBOL, the study of DOE is done for 100 designs. Annex A4 will represent the distribution of design variables in the design space which are explored by SOBOL. The

designed space are well covered for all range for each design variable. Figs. 6.2-6.3 show the result of total resistance in calm water for 15 knots and 21 knots via the explored designs in design space.

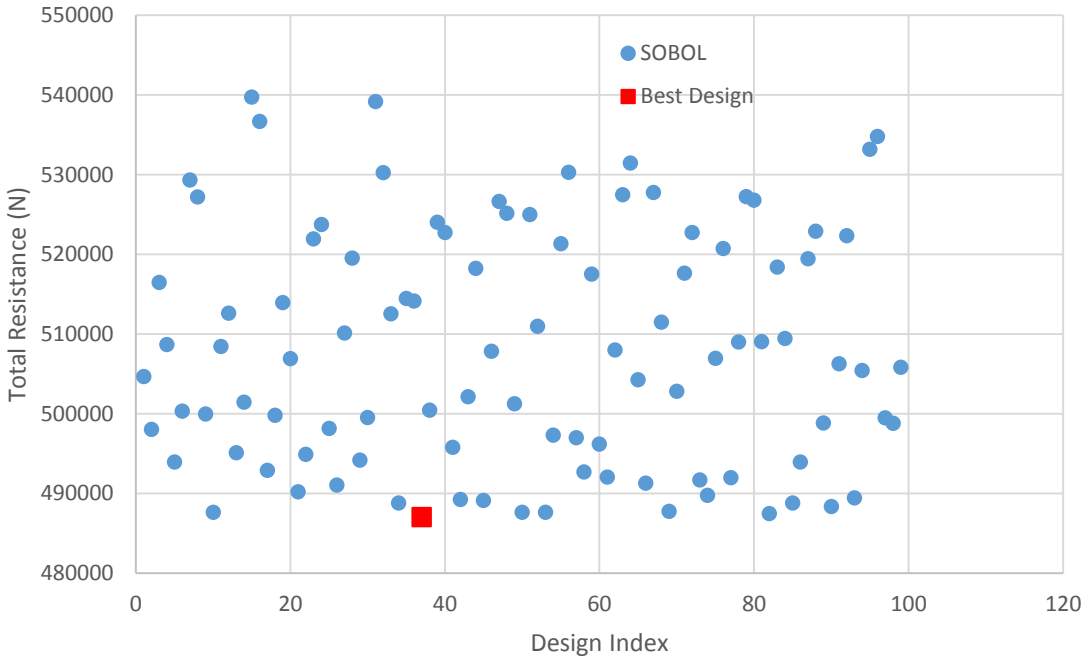

Figure 6.2. Exploration of designs in SOBOL for total calm water resistance at 15 knots

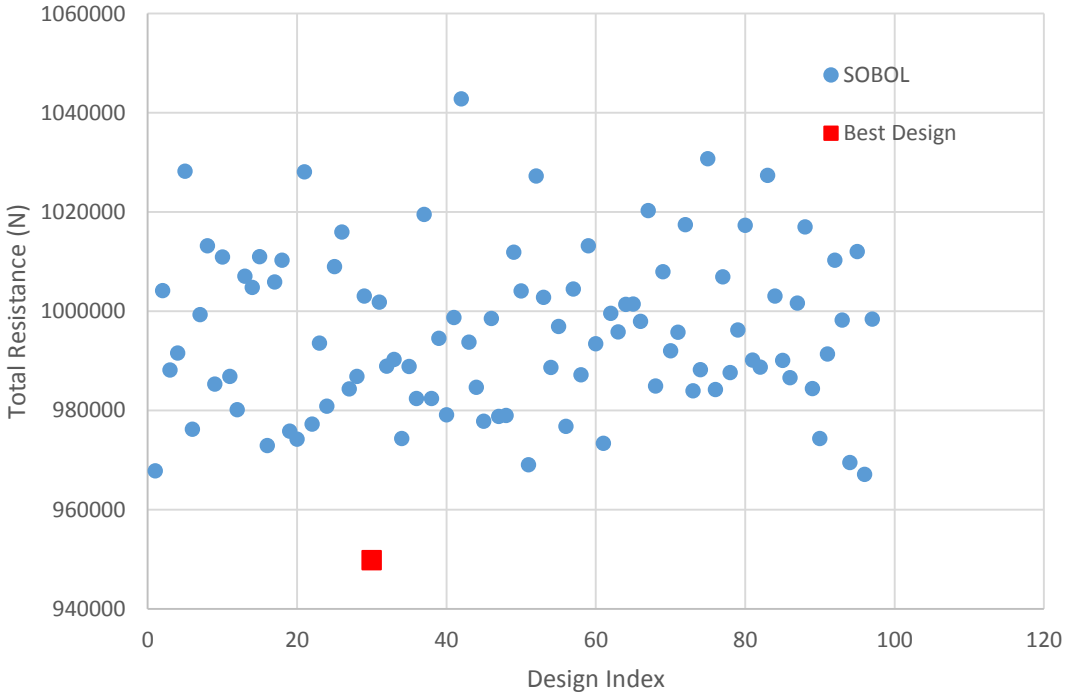

Figure 6.3. Exploration of designs in SOBOL for total calm water resistance at 21 knots

6.2. Single Objective Optimization

The main design engine that is used for optimization process is Tsearch method, after selecting best design in the design space that is explored earlier by SOBOL. As per mentioned in the documentations in CASESE/FFW, the Tangent Search (Tsearch) Method promises to be a reliable solver for small scaled, single-objective optimizations problems with inequality constraints. The major features of the Tsearch Method are to detect a descent search direction in the solution space, to ensure fast improvement in the promising search direction, and to keep the search in the feasible domain.

Within the permissible solution space the Direct Search Method is applied which consists of exploratory moves that start from a so-called base point along the variable axes followed by global moves in the descent search direction found in a successful exploratory moves. If a constraint bound is approached a tangent move in hyperspace is conducted tangential to the constraint either to keep the search in the feasible domain or to bring it back to the feasible domain.

The method is capable of detecting a local minimum of the solution space which is of dimension N*V according to the number of free variables. A descent search direction is determined by at most2*N*V function evaluations. Free variables are subject to explicit bounds, i.e. a lower and an upper bound. Satisfactory results are usually obtained by setting the initial step size to be 5% to 10% of the respective variable range. The minimum step size is about 5% to 10% of the initial step size. If more than just one objective is given, a weighted sum is taken into account.

Firstly, the model is optimized for the speed 15 knots and the results of the optimization process, including the designs obtained by DOE study are presented in Fig. 6.4 with the design index and total resistance of the model.

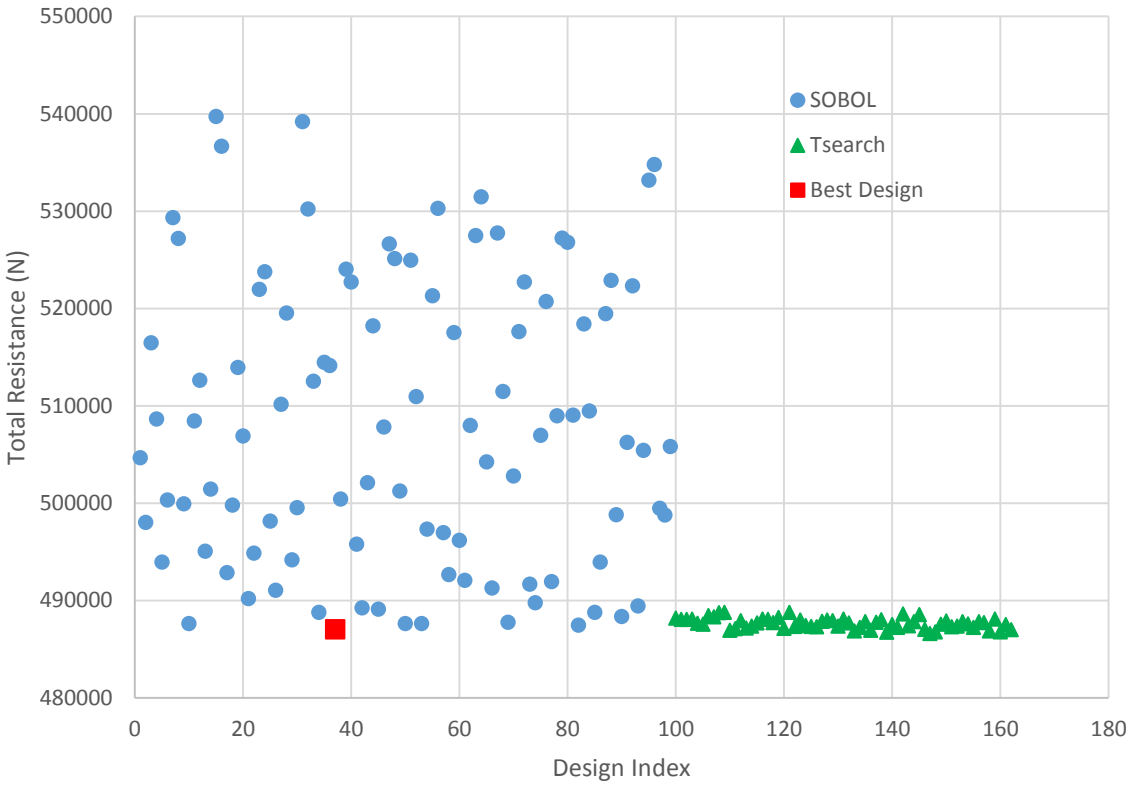

Figure 6.4. Single objective optimization at 15 knots

In comparison with based model, the optimized model has a reduction of 25.14% in wave resistance, 0.14% in friction resistance and 3.82% in total resistance of the ship. The lower region of the bulbous bow of optimized model is sharper transversally and the tip is a bit lower than the original design, while its fore body has the wider entrance angle (flare angle) at designed water line as shown in Fig. 6.5.

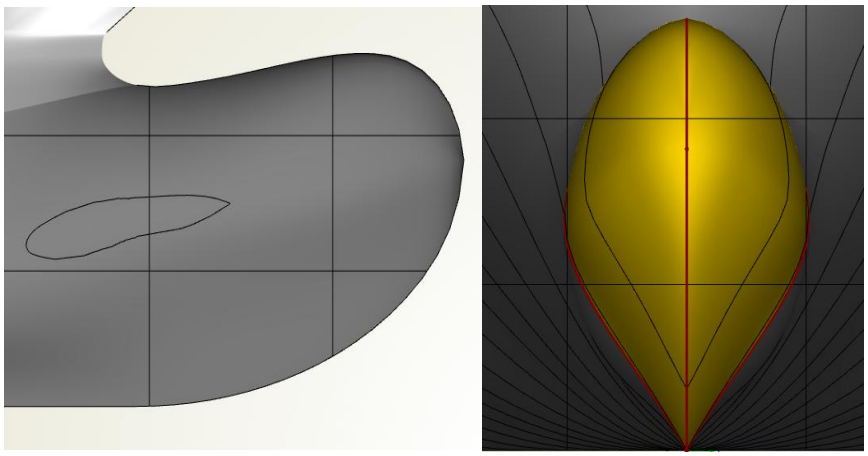

Figure 6.5. Optimized model with Tsearch at 15 knots

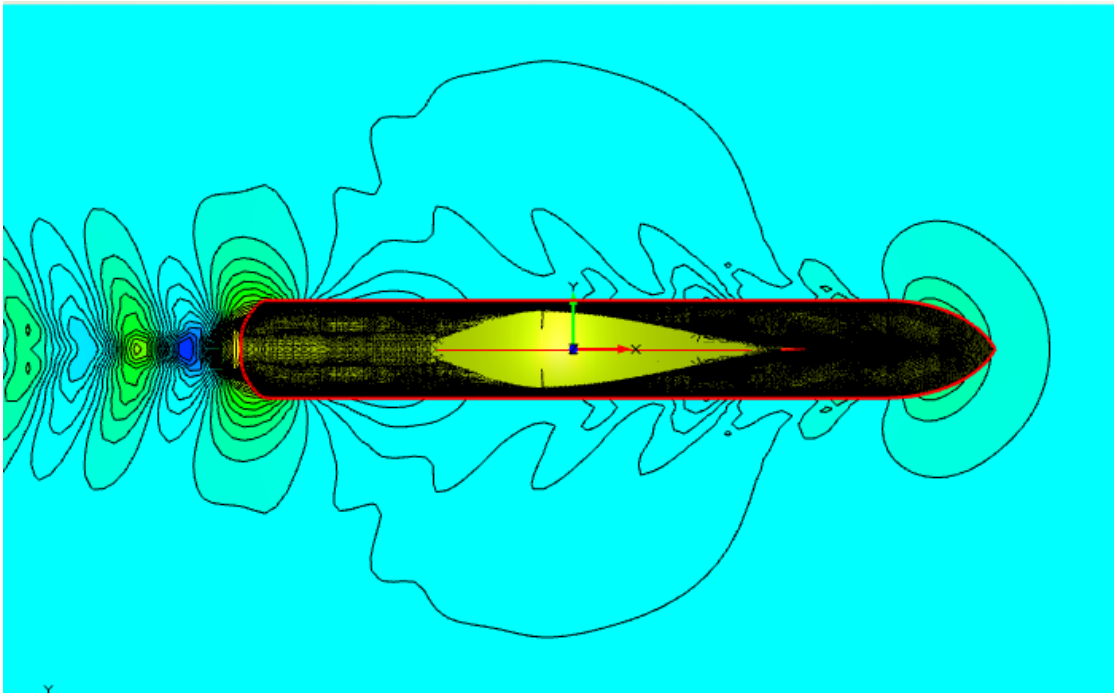

Figure 6.6. Wave patterns of optimized model at 15 knots

The same procedure is applied to optimize the model at 21 knots with Tsearch. Fig. 6.7 illustrates the results of the optimization process, including the designs obtained by DOE study with the design index and total resistance of the model. As seen in Fig. 6.7, it can be said that the optimization did not work properly because most of the designs created from Tsearch have higher total resistance than the best design selected from SOBOL search and only one design has the lower value.

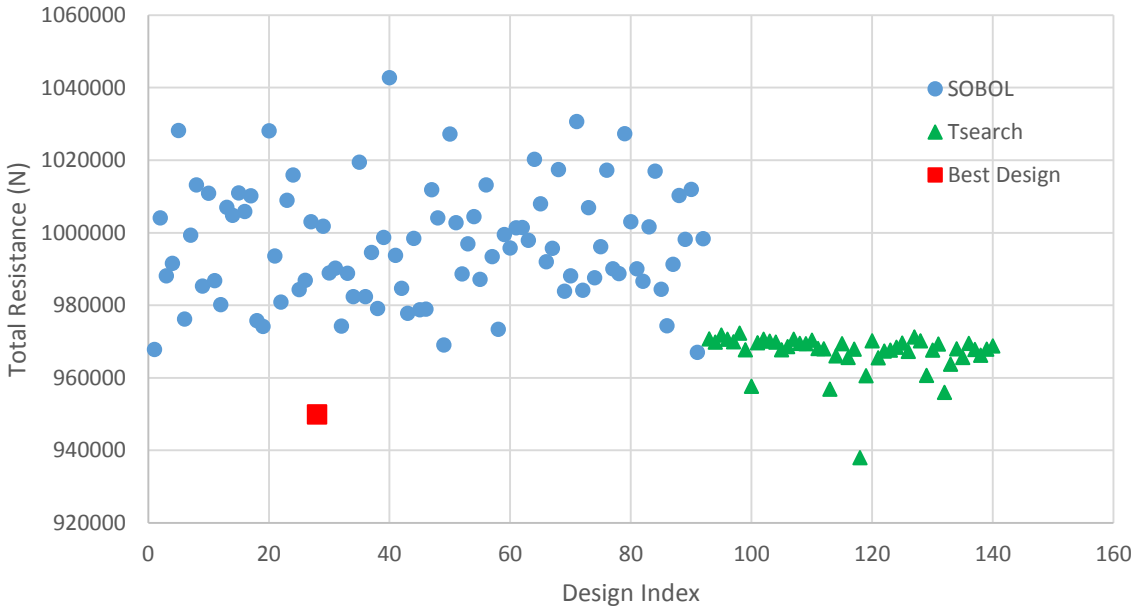

Figure 6.7. Single objective optimization at 21 knots

In comparison with based model, the optimized model has a reduction of 15.27% in wave resistance, 0.08% in friction resistance and 2.42% in total resistance of the ship. The lower region of the bulbous bow of optimized model is sharper transversally and the tip is a bit lower than the original design, while its fore body has the narrower entrance angle (flare angle) at designed water line as shown in Fig. 6.8.

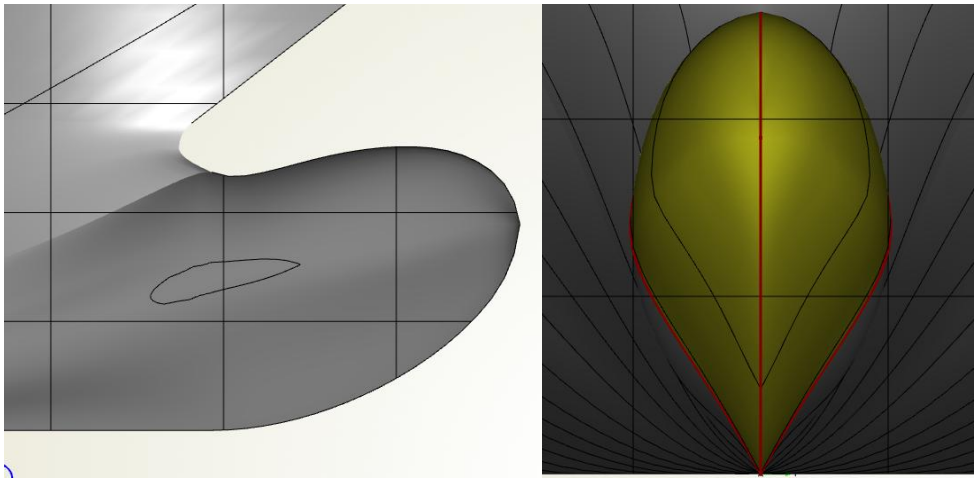

Figure 6.8. Optimized model with Tsearch at 21 knots

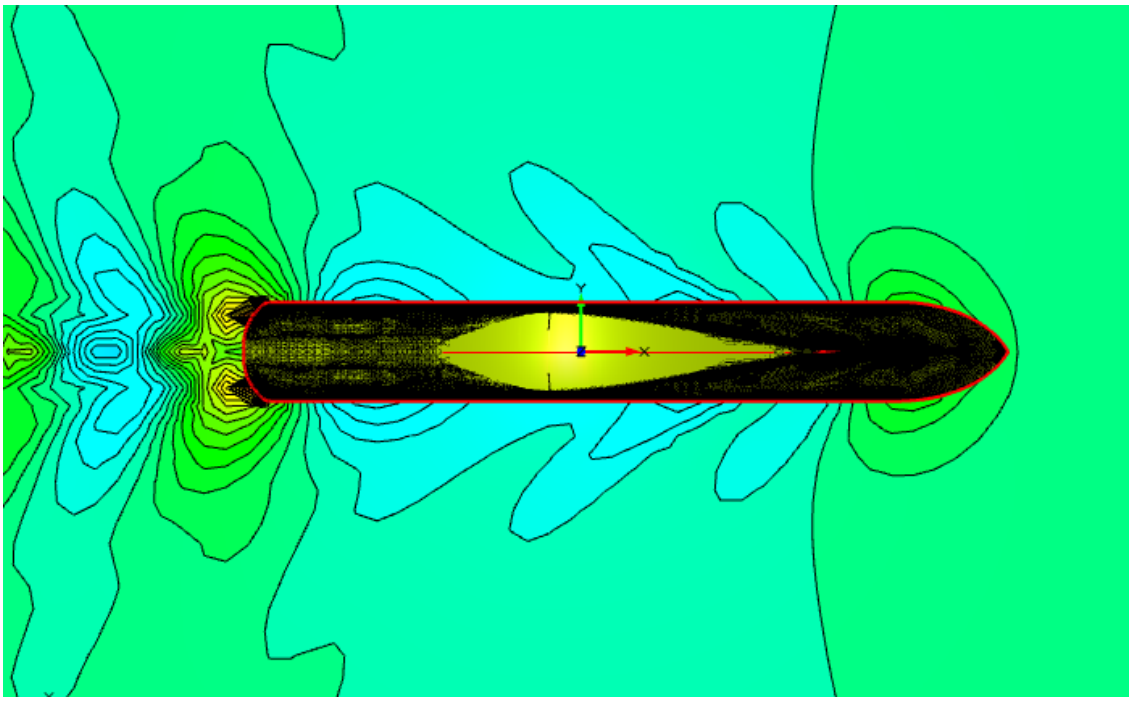

Figure 6.9. Wave patterns of optimized model at 21 knots

6.3. Optimum Models

After running the optimization process for both speeds, the models optimized from each speed have similar shape but a bit different values of design variable parameters. Therefore, it is necessary to compare these two optimized models and select the most feasible one for both speeds. Table 6.2 shows the performance of each model comparing to that of based model, together with the number of designs that are created from SOBOL and Tsearch for the optimization process. The number of designs mentioned in this table are only the feasible designs that can be run by the CFD solvers and those designs that have error in CFD run are omitted from the table. For 15 knots, all the designs are feasible with the CFD solvers, although 25 designs have error while running the simulation at 21 knots. As seen in the table, the optimum design, while performing the single objective optimization at 15 knots, has the reduction of 3.82% in total resistance with the speed 15 knots, but it has the increment of 5.25% in total resistance with 21 knots. Nevertheless, the best design in the single objective optimization at 21 knots, reduces the total resistances in both speeds, which are 2.42% at 15 knots and 1.13% at 21 knots.

Optimization Process	No. of Designs		Resistance Performance	
	DOE	Tsearch	15 knots	21 knots
Optimum for 15 knots	100	63	-3.82%	5.25%
Optimum for 21 knots	92	48	-2.42%	-1.13%

Table 6.2. Comparison of performances of optimum designs at two speeds

After comparing the resistance performance, the study on geometry changes from the base model for both optimum models is done furthermore. As seen in Table 6.3, the influences of all design parameters for both optimized models are not the same. It is true that the lower region of the bulbous bow has the great influence in total resistance at both speeds because both models tend to have the sharper sectional shape in lower region of the bow and the bow tips are a bit lower than the original shape as well. The flare angel at DWL for optimum model at 15 knots seems to be bigger (wider), the model at 21 knots has a bit narrower flare angel. The position of FOB for both optimums are shifted forward from that of based model.

Design Parameters	Based Model	Optimum Model at 15 knots	Variation	Optimum Model at 21 knots	Variation
AngleDWL	18	23.9071	32.82%	17.6656	-1.86%
u0Fillet	0.19	0.180313	-5.10%	0.10375	-45.39%
xFOB	180	183.225	1.79%	191.25	6.25%
fullnessKeel01	0.14	0.157219	12.30%	0.188312	34.51%
fullnessSecKeel	0.87	1.00576	15.60%	1.04219	19.79%
tanSecKeel	53	61.0938	15.27%	61.6875	16.39%
tanTopEnd	-85	-31.4062	-63.05%	-62.1875	-26.84%
zPeak	0.765	0.721094	-5.74%	0.751563	-1.76%

Table 6.3. Comparison of geometrical variations of optimum designs at two speeds

So far after the optimization process in calm water condition, it can be said that the optimized model at 21 knots has the greater performance than that at 15 knots because it has lower resistance for both speeds. Nevertheless, the further detailed study for both models should be done, considering the wave induced resistance in sea state. This will be performed in next chapter.

7. OPTIMIZATION PROCESS IN MODERATE SEA STATE

As one of the objective of this thesis, it is necessary to continue to do the optimization in sea state after studying in calm water condition. The cruise liner will be mainly operated in North Atlantic Ocean and Caribbean Sea as mentioned in Chapter (2). Therefore, the wave data and the study of sea states are done in these regions. This process is performed by those specialists in the University of Rostock. The wave scenario data that the vessel has to deal with are resulted for all specific wave height ($H_{1/3}$) and are chosen for five operating conditions, covering 33% of the total operating time by the vessel as mentioned in Table 7.1. The weighted values (w) and (wTotal) are represented in the percentage of the respective operating conditions with respect to the five chosen operating conditions (w) and with respect to the total operating time of the vessel (wTotal).

Speed [kn]	Draft [m]	$T_{1/3}$ [s]	Wave Frequency	w [%]	wTotal [%]
18	7	5.5	1.142545	0.28	0.09
18	7	6.5	0.966769	0.24	0.08
18	7	4.5	1.396444	0.18	0.06
18	7	7.5	0.837867	0.18	0.06
20	7	5.5	1.142545	0.12	0.04

Table 7.1. Wave scenario data and their weighted values

In order to select the most frequent wave that can happen during the vessel's operating time, the wave with highest weighted value and most common in both speeds whose specific period of 5.5 s is chosen. Therefore, this wave is used in calculating the added wave resistance of the vessel in the sea states. The added wave resistance in irregular waves is calculated by Eq. 7; (Shigunov, personal communication)

$$X_d = \sum_{\omega} \sum_{\mu} \frac{X_d(u_s, \mu, \omega)}{\zeta_a^2} w(\omega, \mu) \tag{7}$$

where;

$\frac{X_d(u_s,\mu,\omega)}{\zeta_a^2}$ is the transfer function of added wave resistance which is computed by GL Rankine.

$w(\omega, \mu)$ is the weight function and is calculated by Eq. 8;

$$w(\omega, \mu) = 2S_{PM}(\omega) \,.\, D(\mu) \,.\, \Delta\omega \,.\, \Delta\mu \tag{8}$$

where the spreading function $D(\mu)$ is calculated by assuming the function as $cos^2(\theta)$. Pierson-Moskowitz Seaway Spectrum $S_{PM}(\omega)$ can be computed by Eq. 9;

$$S_{PM}(\omega) = \frac{H_S^2 T_z}{8\pi^2}\left(\frac{2\pi}{\omega T_z}\right)^5 \exp\left[-\frac{1}{\pi}\left(\frac{2\pi}{\omega T_z}\right)^4\right] \tag{9}$$

As mentioned above, the most relevant seaway is chosen as the specific wave period T_z = 5.5 s and its corresponding wave height H_s = 1.5 m and so, $S_{PM}(\omega)$ becomes;

$$S_{PM}(\omega) = \frac{0.205}{\omega^2}\exp\left[-\frac{0.542}{\omega^4}\right] \tag{10}$$

Therefore, by using Eqs. 10 and 8, the weights for the relevant waves ranging from the frequency 0.4 rad/s to 1.2 rad/s are calculated as in Table 7.2.

ω[rad/s] / μ[°]	**weights not normed to 1**			**weights normed to 1**		
	180	**150**	**120**	**180**	**150**	**120**
0.4	0.000	0.000	0.000	0.000	0.000	0.000
0.5	0.000	0.000	0.000	0.000	0.000	0.000
0.6	0.017	0.013	0.004	0.007	0.005	0.002
0.7	0.088	0.066	0.022	0.037	0.028	0.009
0.8	0.171	0.128	0.043	0.072	0.054	0.018
0.9	0.222	0.166	0.055	0.093	0.070	0.023
1.0	0.238	0.179	0.060	0.100	0.075	0.025
1.1	0.234	0.176	0.059	0.098	0.074	0.025
1.2	0.219	0.164	0.055	0.092	0.069	0.023

Table 7.2. Calculation results of weights for the relevant waves

From this table, the wave whose frequency is 1.0 rad/s with the direction 180˚ and wavelength 61.638 m is selected as it has the most weight value.

7.1. Seakeeping Analysis of Optimum Designs in Calm Water Condition

Although the hull form has been optimized for two speeds in calm water condition, seakeeping performance of each optimum design is checked by simulating the design in the selected sea state with GL Rankine solver. The results of the added wave resistance values of both optimized designs are listed in Table 7.3, comparing with the results of based design. As seen in this table, the best design optimized at 21 knots has the more outweighed performance in power consumption as it reduces the total resistance in waves for both speeds and improves the stabilization as well other than in surge motion, while the optimum design at 15 knots proves greater performance in heave and pith motion with increasing total resistance.

		Calm-water Resistance	Added Resistance	Total Resistance	RAO in Surge Motion	RAO in Heave Motion	RAO in Pitch Motion
		(N)	(N)	(N)	(m/m)	(m/m)	(rad/m)
Based Model	15 knots	505953.6	31173.6	537127.2	0.00168	0.00826	0.00022
	21 knots	976833.2	55425.3	1032258.5	0.00197	0.00627	0.00017
Optimum Model at 15 knots	15 knots	486601.9	29361.9	515963.8	0.00236	0.00668	0.00019
	Difference	-3.82%	-5.81%	-3.94%	40.02%	-19.09%	-12.92%
	21 knots	1028075.8	51556.4	1079632.2	0.00267	0.00479	0.00014
	Difference	5.25%	-6.98%	4.59%	34.96%	-23.52%	-19.46%
Optimum Model at 21 knots	15 knots	500230.3	30174.1	530404.4	0.00195	0.00759	0.00020
	Difference	-1.13%	-3.21%	-1.25%	15.67%	-8.03%	-5.23%
	21 knots	953229.6	57642.2	1010871.8	0.00221	0.00587	0.00017
	Difference	-2.42%	4.00%	-2.07%	12.09%	-6.34%	-1.59%

Table 7.3. Comparison of resistance and seakeeping performances of optimum designs at two speeds

7.2. Direct Optimization in Sea State

In this process, the optimization is done directly for the total resistance in sea state, comprising the total calm water resistance and the added wave resistance induced be the specific incoming waves. As mentioned above, herein, the process will be done for only one wave scenario which is the frequency of 1.0 rad/s with the direction 180˚. The set-up file for the CFD solver is written for both computations directly which are steady flow computation and seakeeping computation.

By coupling the two result files from the computation with CAESES, the solutions extracted are wave resistance and friction resistance in calm water condition and added wave resistance in seaway and then the total calm water resistance and total resistance of the ship in sea states are calculated furthermore. The model is directly optimized for total resistance in seaway with two different speeds mentioned above.

7.2.1. Single Objective Optimization

Similar to the chapter 6, DOE of the design space is explored first for 50 design variants with SOBOL, followed by the single objective optimization in each speed with Tsearch algorithms. Figs. 7.1-7.2 represent the design variants explored by the optimizing process, together with the SOBOL design variants and the best design selected from the SOBOL to start the optimization in the frame of design index and the total resistance in selected sea state. The optimization process at 21 knots did not go well to get the optimized model as per Fig. 7.2 because all the designs except the first one have the higher and higher results and it can be said that the process is divergent. One possibility is that SOBOL can search the design with minimum resistance value and Tsearch cannot find minimized value anymore and goes for the designs with higher solutions. Therefore, the first design is selected as the optimum one in optimizing with Tsearch at 21 knots.

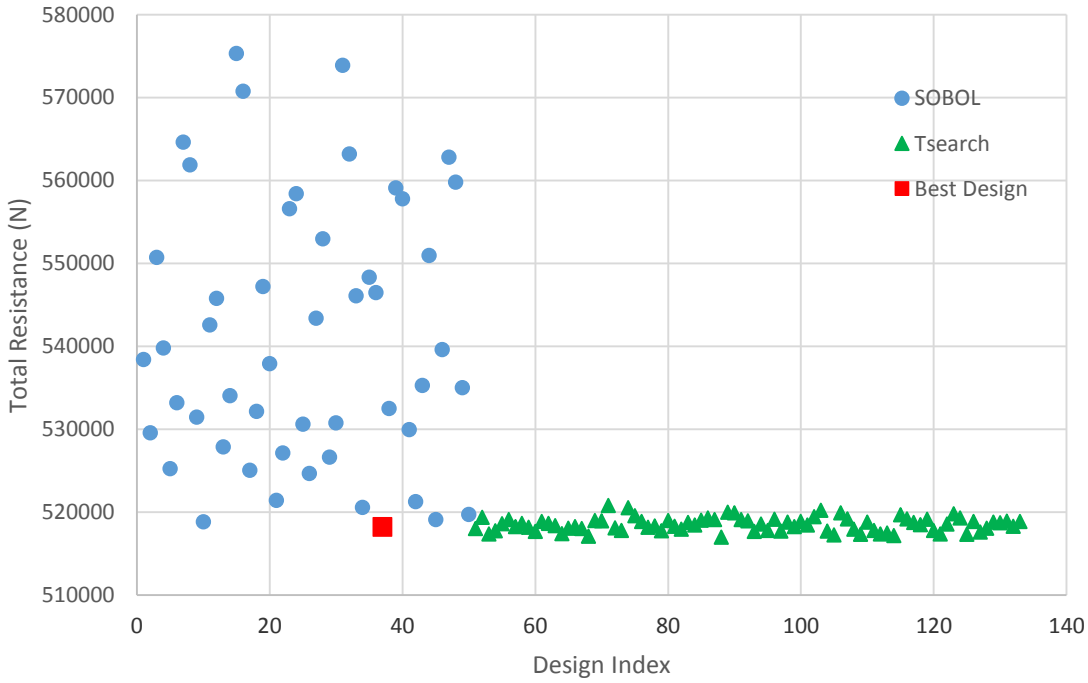

Figure 7.1. Single objective optimization at 15 knots

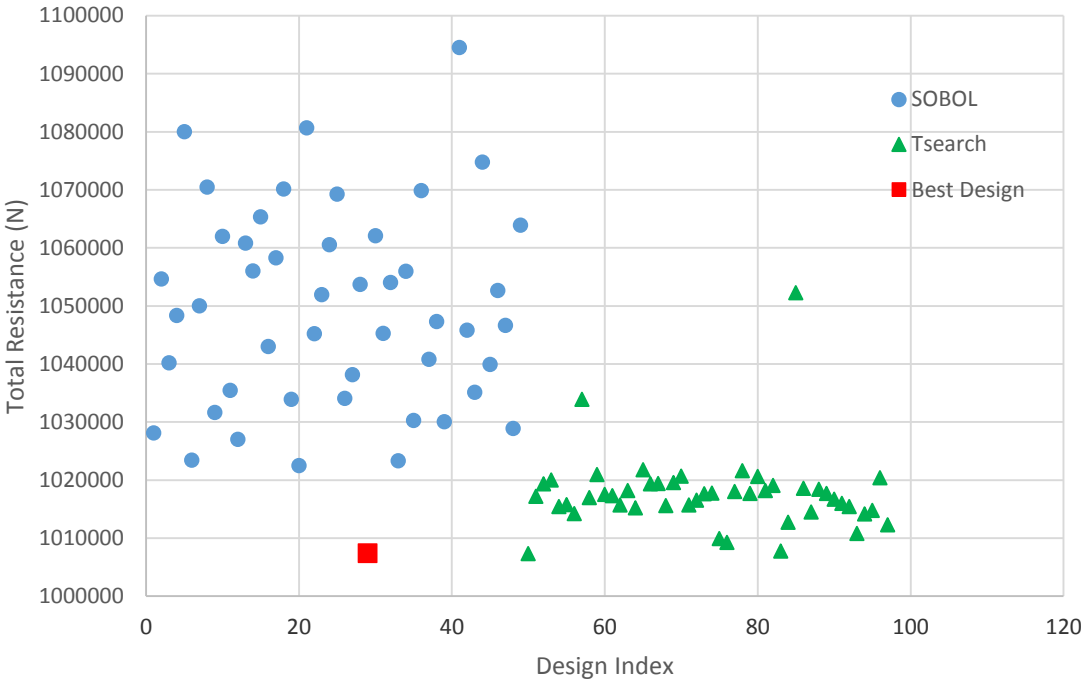

Figure 7.2. Single objective optimization at 21 knots

The optimum models obtained from optimization at each speed are illustrated in Figs. 7.3-7.4 and interestingly, the modification of the designs of each model from the original shape at the respective speeds is very similar to that of models optimized in calm water condition. The changes of geometry of all the optimized models at both speeds in two different approaches are shown in Table 7.4.

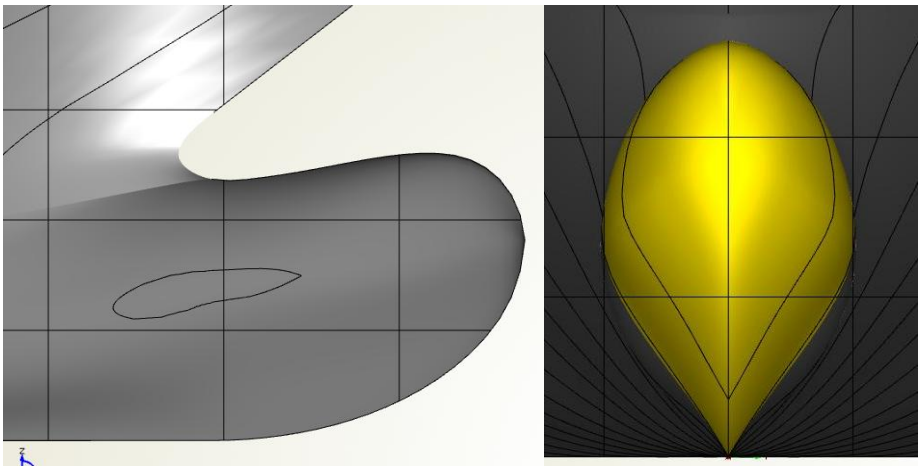

Figure 7.3. Optimized model with Tsearch at 15 knots

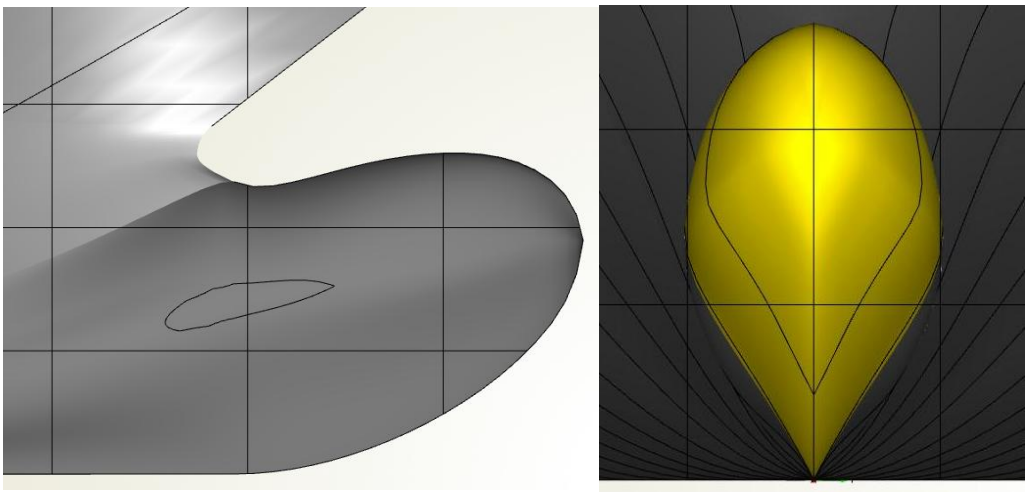

Figure 7.4. Optimized model with Tsearch at 21 knots

Design Parameters	Based Model	Optimization in calm water condition				Optimization in sea state			
		Optimum at 15 knots	Variation	Optimum at 21 knots	Variation	Optimum at 15 knots	Variation	Optimum at 21 knots	Variation
AngleDWL	18	23.9071	32.82%	17.6656	-1.86%	22.55	25.28%	17.4375	-3.13%
u0Fillet	0.19	0.180313	-5.10%	0.10375	-45.39%	0.1776484	-6.50%	0.10375	-45.39%
xFOB	180	183.225	1.79%	191.25	6.25%	184.375	2.43%	191.25	6.25%
fullnessKeel01	0.14	0.157219	12.30%	0.188312	34.51%	0.1542188	10.16%	0.1903125	35.94%
fullnessSecKeel	0.87	1.00576	15.60%	1.04219	19.79%	1.0070313	15.75%	1.0421875	19.79%
tanSecKeel	53	61.0938	15.27%	61.6875	16.39%	61.09375	15.27%	61.6875	16.39%
tanTopEnd	-85	-31.4062	-63.05%	-62.1875	-26.84%	-32.65625	-61.58%	-62.1875	-26.84%
zPeak	0.765	0.721094	-5.74%	0.751563	-1.76%	0.7210938	-5.74%	0.7515625	-1.76%

Table 7.4. Comparison of geometrical variations of optimum designs at two speeds

7.2.2. The Optimum Model

The optimum model is selected based on the Table 7.5 which shows the comparison of all the best designs obtained from both optimization approaches, in calm water condition and at sea state, at the different speeds. Similar to optimization process in calm water condition, there are still unfeasible designs which cannot be run by the CFD solver while optimizing in waves at 21 knots although all the designs can extract for the solution at 15 knots.

			Calm-water Resistance	Added Resistance	Total Resistance	RAO in Surge Motion	RAO in Heave Motion	RAO in Pitch Motion
			(N)	(N)	(N)	(m/m)	(m/m)	(rad/m)
Based Model		15 knots	505953.6	31173.6	537127.2	0.00168	0.00826	0.00022
		21 knots	976833.2	55425.3	1032258.5	0.00197	0.00627	0.00017
In calm water	Optimum Model at 15 knots	15 knots	486601.9	29361.9	515963.8	0.00236	0.00668	0.00019
		Difference	-3.82%	-5.81%	-3.94%	40.02%	-19.09%	-12.92%
		21 knots	1028075.8	51556.4	1079632.2	0.00267	0.00479	0.00014
		Difference	5.25%	-6.98%	4.59%	34.96%	-23.52%	-19.46%
	Optimum Model at 21 knots	15 knots	500230.3	30174.1	530404.4	0.00195	0.00759	0.00020
		Difference	-1.13%	-3.21%	-1.25%	15.67%	-8.03%	-5.23%
		21 knots	953229.6	57642.2	1010871.8	0.00221	0.00587	0.00017
		Difference	-2.42%	4.00%	-2.07%	12.09%	-6.34%	-1.59%
at sea state	Optimum Model at 15 knots	15 knots	487885.5	29114.1	516999.6	0.00220	0.00690	0.00019
		Difference	-3.57%	-6.61%	-3.75%	30.61%	-16.48%	-11.68%
		21 knots	1009321.8	60543.8	1069865.6	0.00267	0.00513	0.00015
		Difference	3.33%	9.23%	3.64%	35.43%	-18.06%	-12.88%
	Optimum Model at 21 knots	15 knots	500195.4	30150.8	530346.2	0.00195	0.00763	0.00020
		Difference	-1.14%	-3.28%	-1.26%	15.67%	-7.53%	-5.00%
		21 knots	949862.4	57494.3	1007356.7	0.00221	0.00589	0.00017
		Difference	-2.76%	3.73%	-2.41%	12.16%	-5.96%	-0.82%

Table 7.5. Comparison of resistance and seakeeping performances of all optimum designs

As per Table 7.5, both optimum designs at 21 knots, either in steady water or in wave, have the reduction of total resistance of the ship although the other two designs increase the total resistance. Moreover, surge motion is more stabilized than the other two and heave and pitch motion performances are just a bit lower in the designs optimized at 21 knots. Among these two designs, the best design resulted from optimizing at 21 knots in incident waves can perform more according to the resistance values and therefore, this design is chosen as the optimum design from all the optimization processes.

The selected optimized model has the reduction of 1.26% of total resistance in waves and 1.14% of calm water resistance compared to the base model while running at 15 knots. Nevertheless, at the speed of 21 knots, it shows better performance by decreasing the total resistance to 2.41% and the calm water resistance to 2.76%. Althought the response in surge motion is a bit higher than the original model, it can stabilize more in heave and pitch motion. The wave pattern generated by this optimum design is illustrated in Fig. 7.5, comparing the wave occurance by the base model.

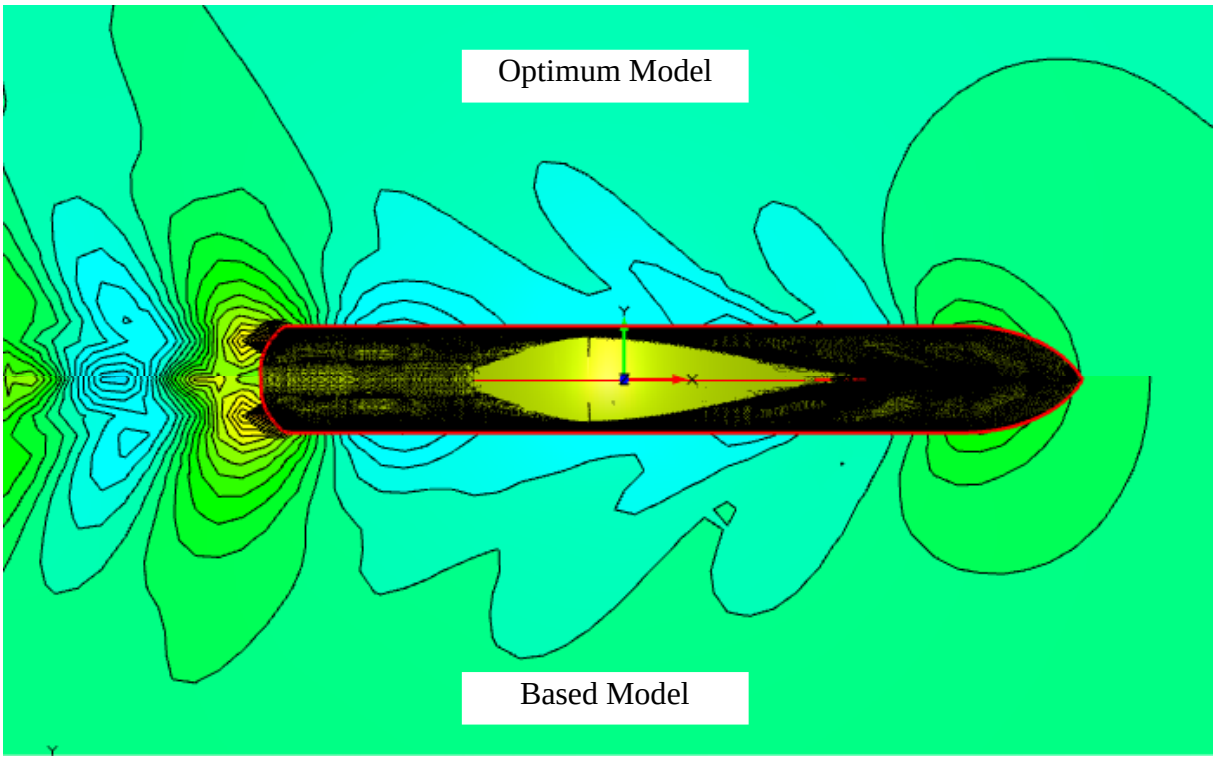

Figure 7.5. Comparison of wave patterns of optimized model and based model

In Fig. 7.6, it can be seen that the selected best design has the sharper and thinner bulbous bow region in the lower part to make the more flexible flow pattern and to reduce the resistance in water. The bow tip is also lower than the based design as well although the flare angle of the fore body is not much different from the original hull. After running the simulation at different speeds with the optimal hull form, the total resistance in the chosen wave is consistantly lower than that of original design as shown in Fig. 7.7. Therefore, it can be concluded that the optimum design chosen has the good performance in reducing the resistance in calm water and in wave as well to estimate the power consumption of the ship in earlier design stage.

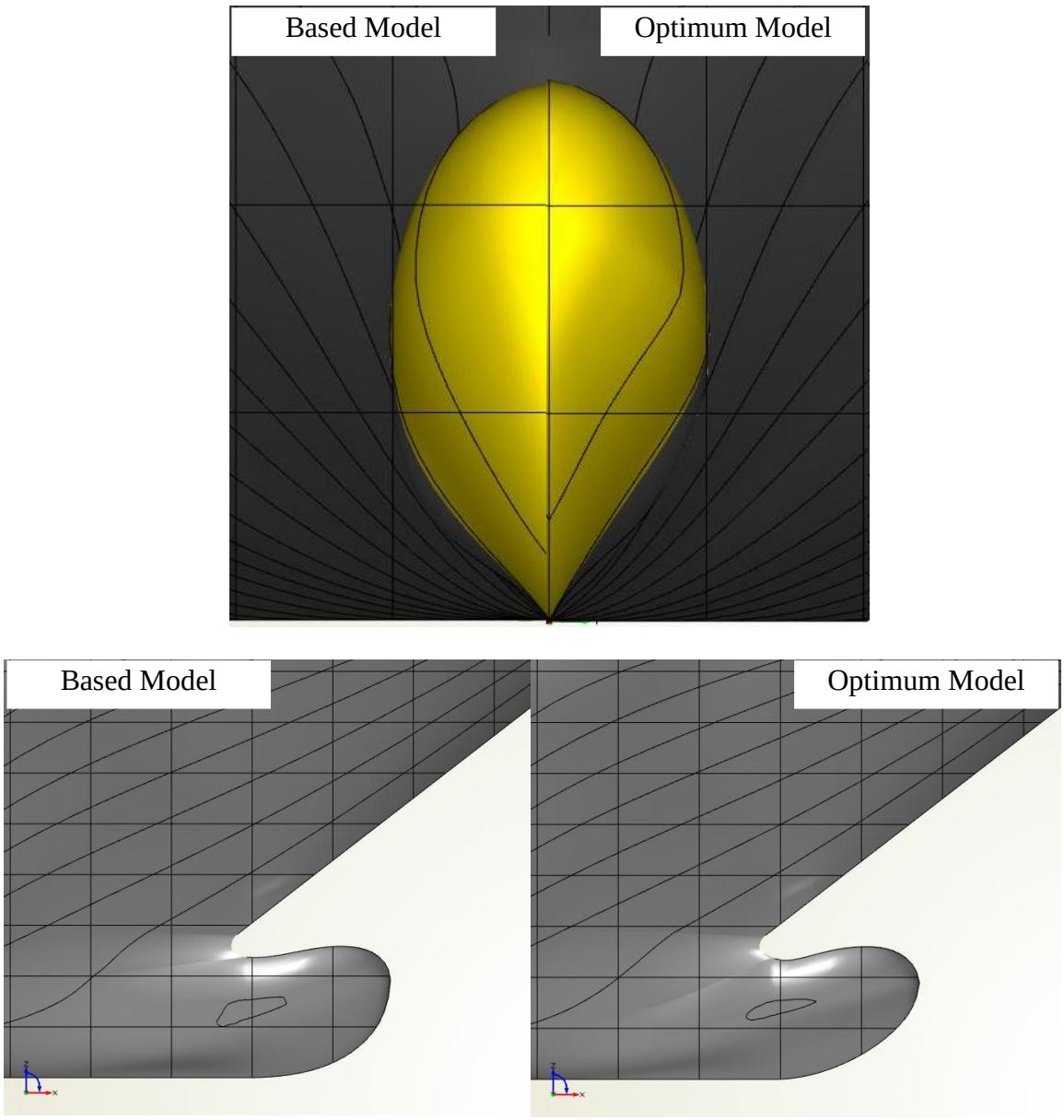

Figure 7.6. Comparison of geometry of optimized model and based model

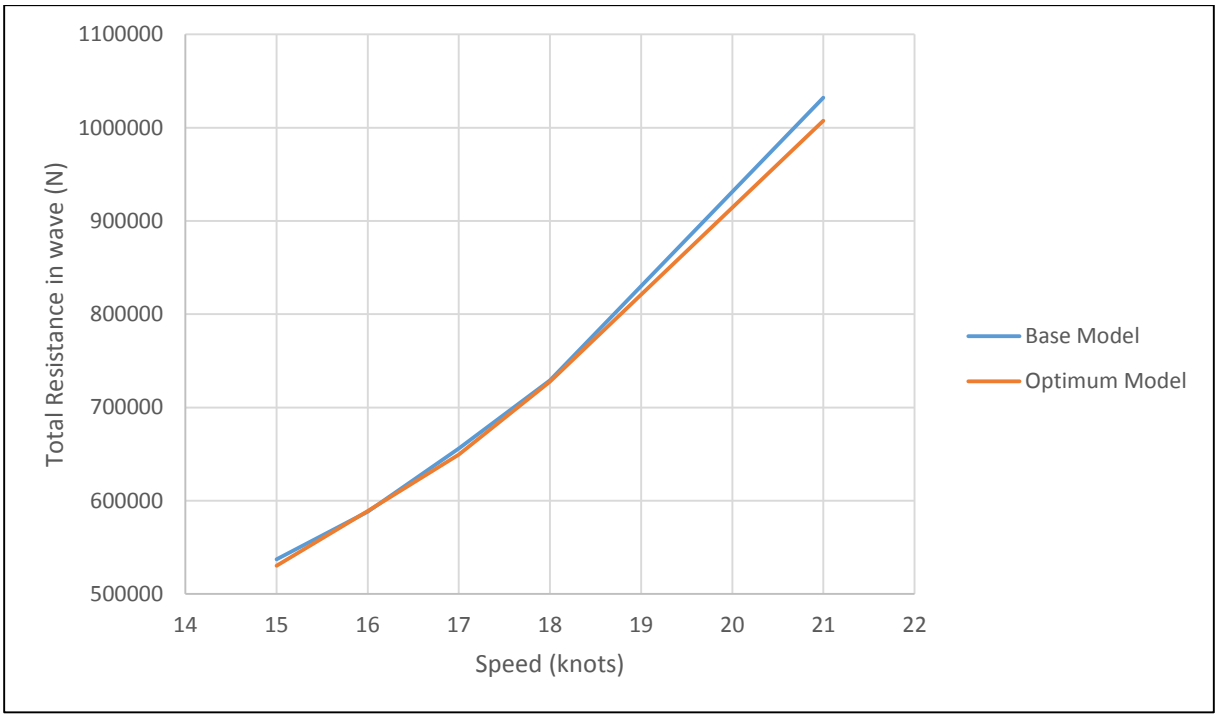

Figure 7.7. Comparison of performances of optimized model and based model at different speeds

8. SUMMARY OF WORK SCOPES

Conventionally, the ship hull form is optimized in calm water condition without care consideration of actual operating conditions in sea states in order to reduce the required power consumption of the ship, in the other way to minimize the resistance occurred by the hull while moving in the water. In spite of using sea margin to compensate the resistance created by waves, it cannot be said as a best approach to estimate the accurate power needed by the ship. In a tentative to solve this problem, the optimization processes of the hull form in calm water condition, including in seaways as well are performed. Moreover, the introduction of new solver, GL Rankine to the optimization process in sea states is also carried out.

In this thesis, two approaches of optimizing the hull form in sea states are presented. Firstly, the closed review for modifying the parametric geometrical model of the cruise liner is performed and the most effective design parameters related to changing most for the hull form geometry are created. The thorough study of each design parameter on the shape of the model is continued in order to know how they behave on the resistance of the ship. The coupling of the CFD solver to the optimization algorithms in the framework of CAESES/FFW is carried out for getting the automatic process of optimizing. In order to receive the global optimum value of the calm water resistance, the study of DOE in the design space is done first, followed by the single objective optimization for different speeds with Tsearch algorithm after selecting the best design from DOE. The different optimum designs for two speeds are then checked and compared for their performances in added wave resistance and motions in seaways.

The second applied approach is that after getting the parametric model and selecting the most effective design parameters, the CFD solver is coupled with the CASES framework to get the direct calculation of added wave resistance in the chosen sea state, including the calm water resistance as well. Then, the DOE in design space is studied for both speeds, followed by single objective optimization in order to get the optimum designs with the lowest resistance of the ship, including calm water resistance and added wave resistance. This approach is the direct optimization of hull form in the sea states.

Besides, for calculating the most reliable and accurate results from the CFD solver, GL Rankine, the thorough understanding and testing of this CFD code is performed, followed by validation of its results with the experimental data from HSVA towing tank.

9. CONCLUSIONS AND RECOMMENDATIONS

9.1. Conclusions

Several conclusions can be done on regarding the optimization techniques used in this thesis and the analysis of CFD code in order to get the reliable results of the simulations. First of all, application of the GL Rankine code in the optimization task is the quite challenge for the author because it took 80% of the time performing for this project while only 20% of the rest time can be used for studying the optimizing process and leads to incomplete process in optimization. It is the newly developed CFD code for using in-house in DNV-GL and not widely used in ship industries yet.

Although it saves a lot of times in simulating the necessary results by taking around one hour for each simulation, steady flow computation or seakeeping analysis, numerous improvements for setting up the input script file have to be done for getting the stable, accurate and convergent results. The interpretation of the output result is the easy-going process and it gives the straight-forward results for computations like wave resistance, friction resistance, total calm water resistance, trim and sinkage, hydrodynamic forces and RAOs of each motion in seakeeping analysis. Nevertheless, handling of input data require a very good knowledge. For example, in this work scope, it is necessary to adjust the panel grid sizes, the initial wave height positions in forward and aft of the ship, wave damping factor and relaxation factor to get the convergence. Those parameters are very sensitive and can lead to unstable and unreasonable output results for the simulation of the design variants generating from the optimizing algorithms. It can also effect on the study of the design parameters because the trends of the influence of parameters on the resistance show wiggling shape, instead of stable and steady trend as shown in Appendix A5.

Moreover, while penalization those ship hull forms with lower skeg on the aft, there are some big or small holes on the aft surface of the ship as illustrated in Fig. 9.1 and it is resulted a very high value of resistance although the simulation run completely without stopping automatically. Therefore, in this project, the skeg of the ship has to be removed in modeling the parametric hull form, in spite of including the skeg in original model. (Shigunov, personal communication) Another issue is that if the input STL geometry has a coarser grid that the triangulation of the panel mesh generated from GL Rankine, there are some ill-shaped in the penalization as in Fig. 9.2 (Brehm, personal communication), but the solver is quite robust and still run the simulation

and getting the result without showing any error. The input setting in this thesis still needs numerous improvement for getting the accurate and stable results.

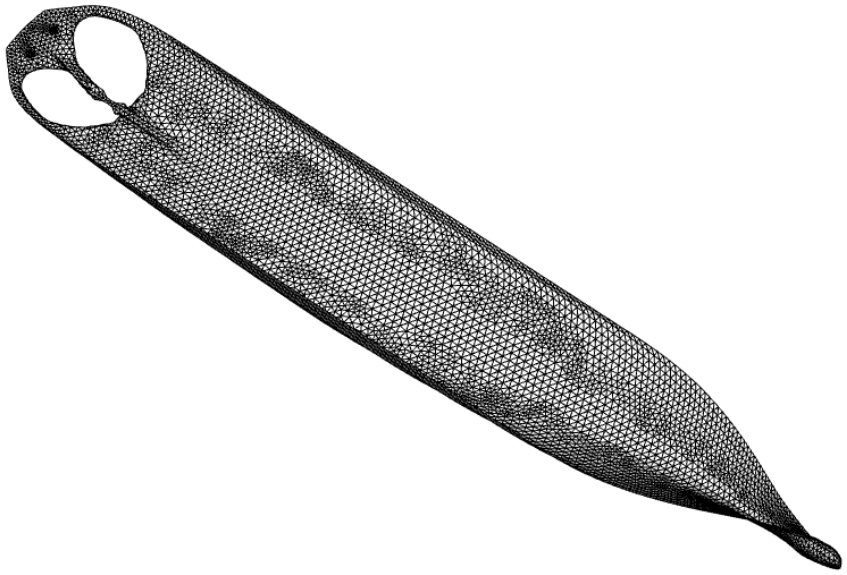

Figure 9.1. Penalization with hole on the aft

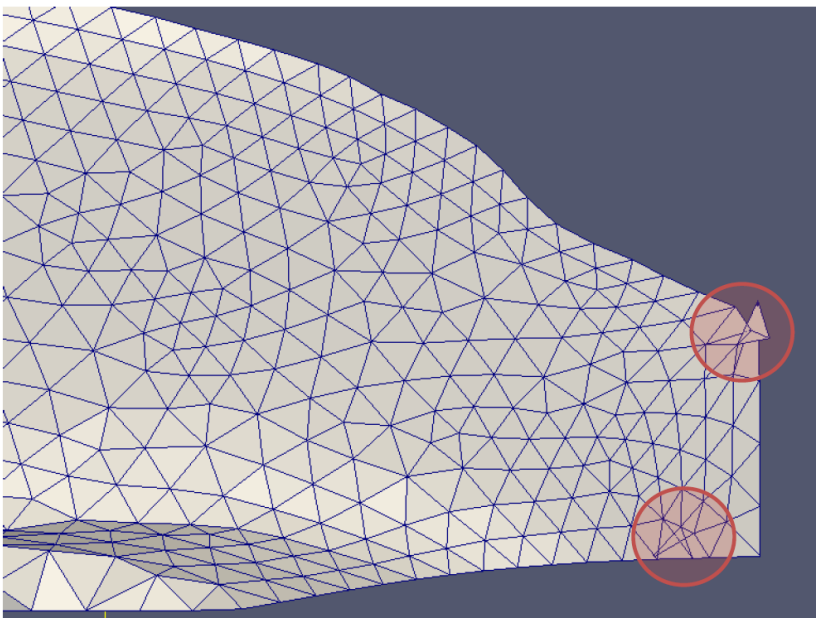

Figure 9.2. Penalization with “ill” shape (Brehm, personal communication)

Regarding for the optimization process, it can be said that the single objective optimization with Tsearch is not quite straight forward because the optimums selected in this case are occurred in the middle of the process and the algorithm did not go back to the minimum value at the end of the optimization, instead still getting the fluctuation and stopping at the higher value. This phenomenon is very obvious for the single objective optimization in calm water condition at 21

knots. As seen in Fig. 6.7, the design variants generated from Tsearch even have the higher results in resistance than the best design selected from DOE search and only one optimum design has the lower value. Moreover, there are several designs (25 designs in this case) which have the numerical calculation errors. In conclusion, for achieving the good and feasible behavior in the optimization, the approaches in this work still require numerous improvements and also for the CFD solver set-up that should modify for auto-selection of input parameters and stable penalization with more reliable result data.

9.2. Recommendations

It can be said that the optimization approaches in this work scope are not the complete task for the early design stage. Due to the time constraint, the author can only do the DOE search and single objective optimizations for both steady flow computation and seakeeping analysis. It should be done furthermore for single objective optimizations with weighted functions for both speeds or multi-objective optimization to get the mutual and feasible design for both speeds. Although the stability aspects and displacement restriction are considered as constraints in this thesis, there are some other constraints can be added according to the requirements of the designers of the ship. For optimization in sea states, the author just selected the added wave resistance for only one wave scenario as the objective of the optimization although it can still be chosen other results such as the motions in some specific conditions or other forces that can affect the seakeeping behaviors of the ship as it is important to maximize the comfort and pleasure for the passengers onboard for the cruise liner. The optimization method relevant to each case study is varied and the proper selection of the approach is required in order to get the good result.

The simulation by GL Rankine is dependent on the input geometry into the set-up file like; it needs 20,000 to 50,000 triangles in the geometry with STL format. For penalization of the model, it should be nice to follow the standard recommendation of the code developer such as 1% of LPP of ship for panel size in middle section and 0.7% for that in forward or aft section. It is wise to keep the default value for wave damping factor and relaxation parameter in the set-up (only needed to change if the solver cannot get the convergent solution) and adjust the initial wave height position in the forward and aft region carefully.

Although the optimization approaches in this thesis are not the complete solution for achieving the optimum design for the early design stage, it represents the first step toward the optimization

of ship hull forms in moderate sea state in future and it is hopeful to implement further for automatic hydrodynamic optimization which is user friendly, straight forward, getting the most reliable and stable solution.

REFERENCES

[1] Gregory J. Grigoropoulos and Dimitris S. Chalkias, 2009. Hull-form optimization in calm and rough water. *Computer-Aided Design*, 42 (2010), 977-984.

[2] Hyunyul Kim, 2009. *Multi-Objective Optimization for Ship Hull Form Design*. Thesis (PhD). George Mason University.

[3] Iacopo Biliotti, Stefano Brizzolara, Michele Viviani, Giuliano Vernengo, Danilo Ruscelli, Mauro Galliussi, Domenico Guadalupi and Andrea Manfredini, 2011. Automatic Parametric Hull Form Optimization of Fast Naval Vessels. *American Society of Naval Engineers*. September, 294-301.

[4] Justus Heimann, 2005. *CFD Based Optimization of the Wave-Making Characteristics of Ship Hulls*. Thesis (PhD). Technical University Berlin.

[5] H. Bagheri, H. Ghassemi and A. Dehghanian, 2014. Optimizing the Seakeeping Performance of Ship Hull Forms Using Genetic Algorithm. *TRANSNAV*, 8 (1), 49-57.

[6] Scott Percival, Dane Hendrix, Francis Noblesse, 2001. Hydrodynamic optimization of ship hull forms. *Applied Ocean Research*, 23 (2001), 337-355.

[7] Sebastian Walter, 2014. Betriebsdaten des Kreuzfahrtschiffsentwurfs. *PerSee – OptiSee Projekttreffen*, AP 4.1.

[8] C. Abt, S.D. Bade, L. Birk and S. Harries, 2001. Parametric Hull Form Design – A Step Towards One Week Ship Design. *8th International Symposium on Practical Design of Ships and Other Floating Structures*, PRADS 2001.

[9] Harries S, 1998. *Parametric Design and Hydrodynamic Optimization of Ship Hull Forms*. Thesis (PhD), Technical University Berlin.

[10] Zhang Ping, Zhu De-xiang and Leng Wen-hao, 2008. Parametric Approach to Design of Hull Forms. *ScienceDirect Journal of Hydrodynamics*, 20(6), 804-810.

[11] J. J. Maisonneuve, S. Harries, J. Marzi, H. C. Raven, U. Viviani and H. Piippo. Towards Optimal Design of Ship Hull Shapes. *EC funded Project FANTASTIC*, G3RD-CT 2000-00096.

[12] P. Ferrant, 2013. Seakeeping Lectures 1&2, *ECN – EMSHIP 2013/2014*, Page 19.

[13] Heinrich Söding, Alexander von Graefe, Ould el Moctar and Vladimir Shigunov, 2012. Rankine Source Method for Seakeeping Predictions. *Proceedings of the ASME 2012 31st International Conference on Ocean, Offshore and Arctic Engineering*, OMAE2012-83450.

[14] Yong Phyo Hong and Petri Valanto, 2014. *PerSee - Experimental Investigation on the Added Resistance of a Cruise Ship Model in Regular Head, Oblique, Beam and Following Wave Volume 1*. Final Experimental Report, S 686/14. Hamburgische Schiffbau-Versuchsanstalt GmbH (HSVA).

[15] S. Harries and M. Brenner, 2014. Simulation-driven Design. *Optimization Course by Friendship-Systems in Ecole Centrale Nantes*, Slide 72.

[16] Helio Bailly Guimaraes, 2014. *Robust Design Optimization for Operational Profile*. Thesis (Master). University of Rostock.

[17] *PerSee* [online]. Friendship Systems. Available from: https://www.caeses.com/about-us/r_a_d/persee/ [Accessed 4 January 2015].

[18] *PerSee* [online]. Universität Duisburg-Essen. Available from: https://www.uni-due.de/persee/index_en.shtml [Accessed 4 January 2015].

APPENDIX

A1. Lines Plan of the Cruise Liner

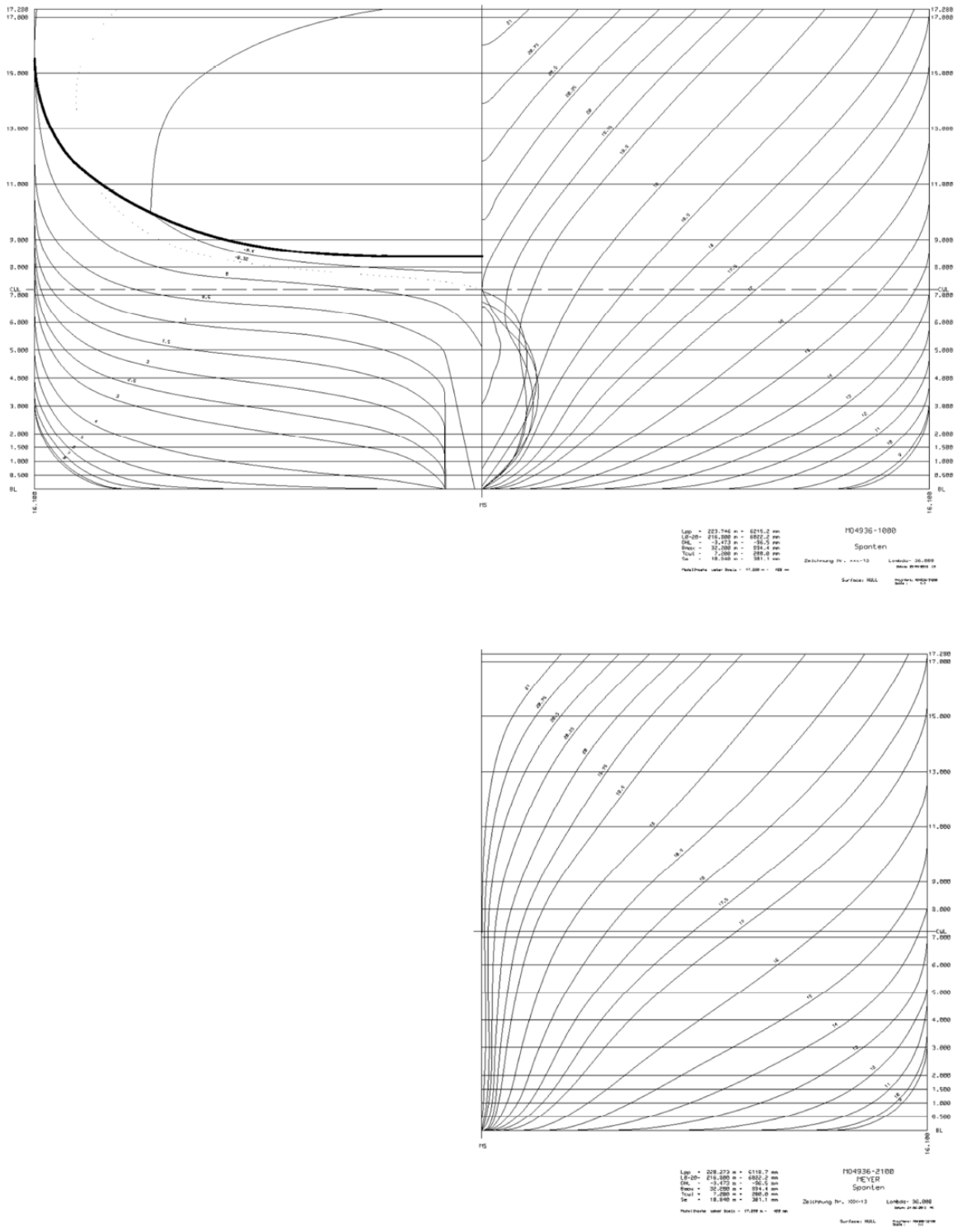

Figure A1.1. Body Plan

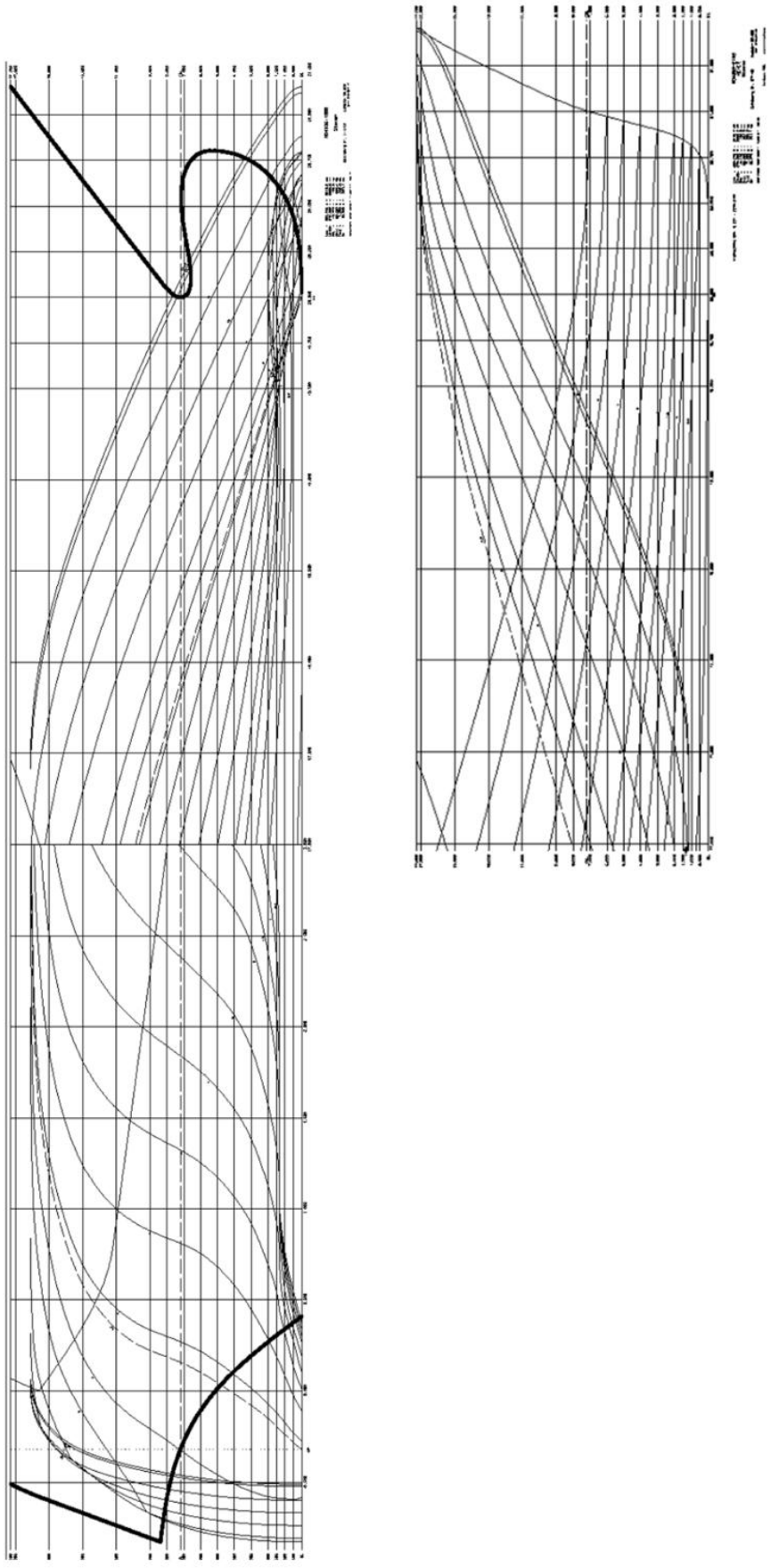

Figure A1.2. Sheer Plan

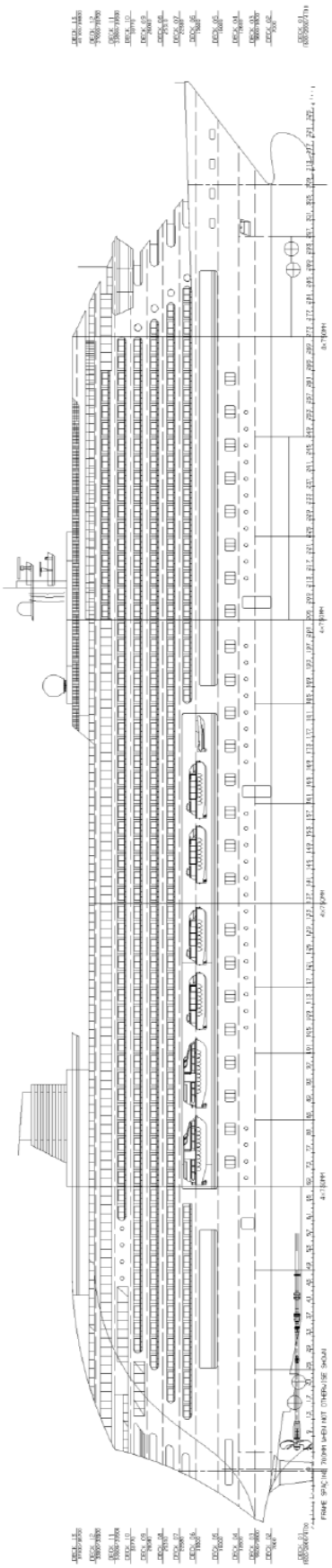

Figure A1.3. General Arrangement Plan

A2. Study on each Design Parameter

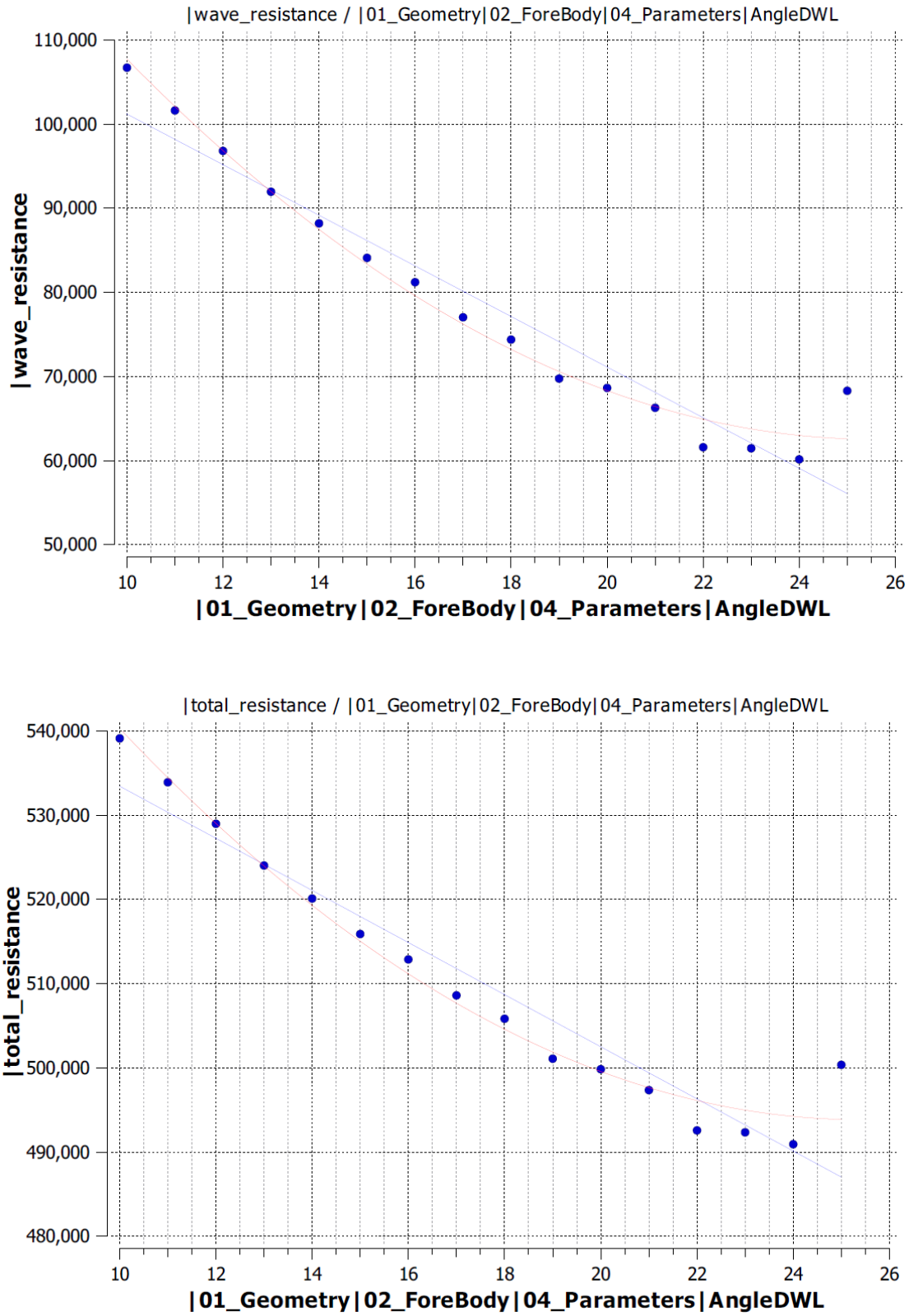

Figure A2.1. Influence of parameter “AngleDWL” on ship resistances

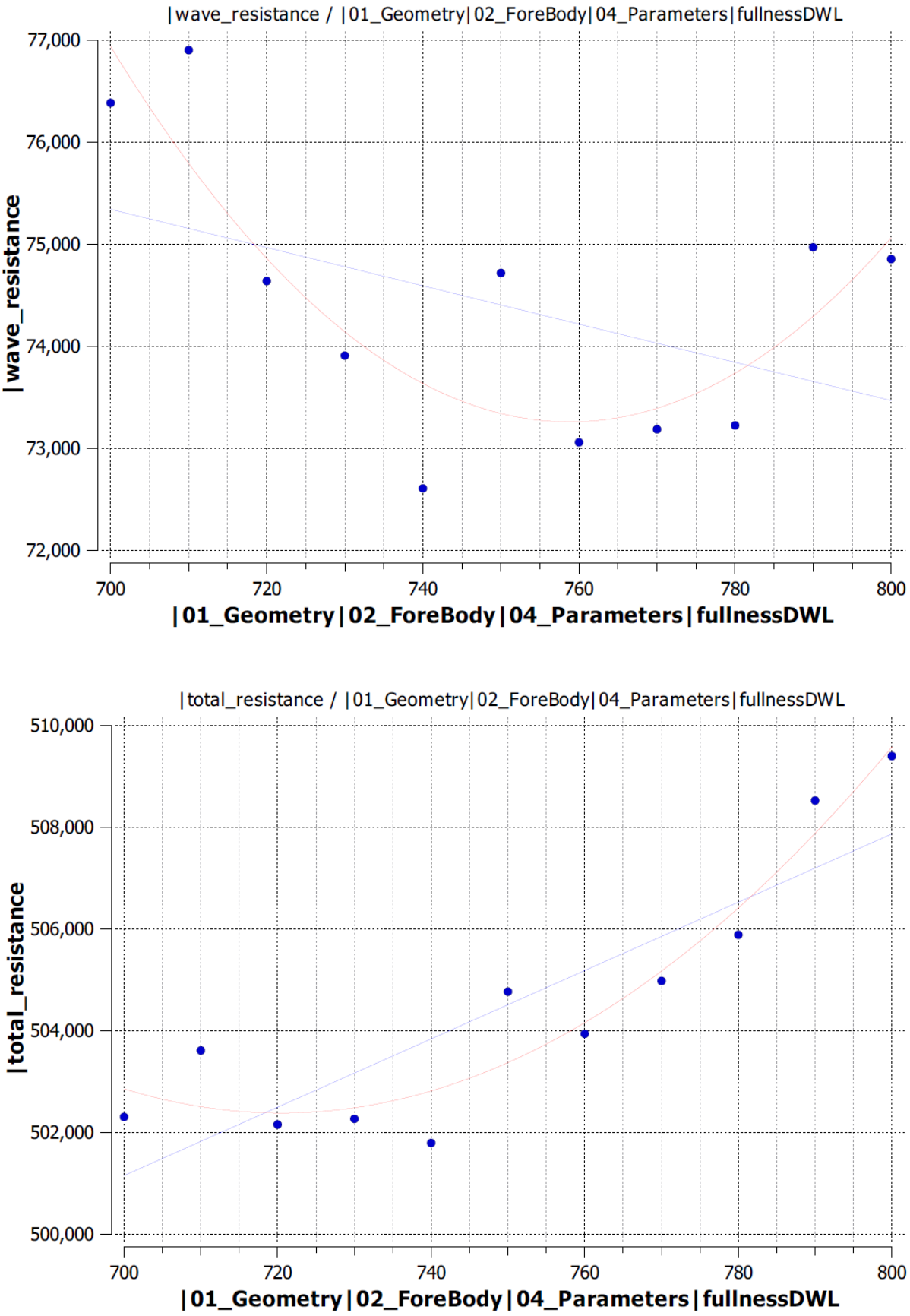

Figure A2.2. Influence of parameter “fullnessDWL” on ship resistances

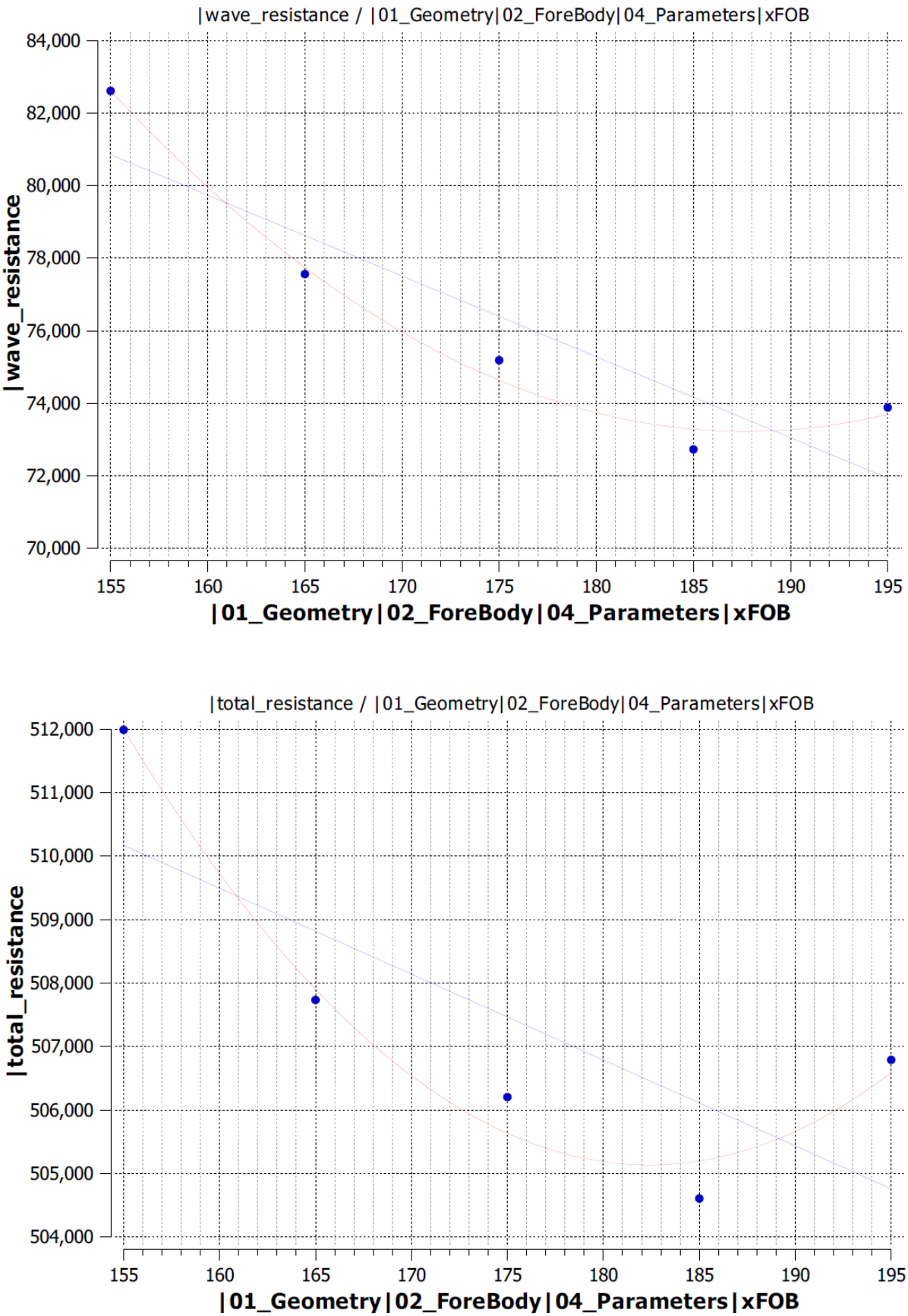

Figure A2.3. Influence of parameter “xFOB” on ship resistances

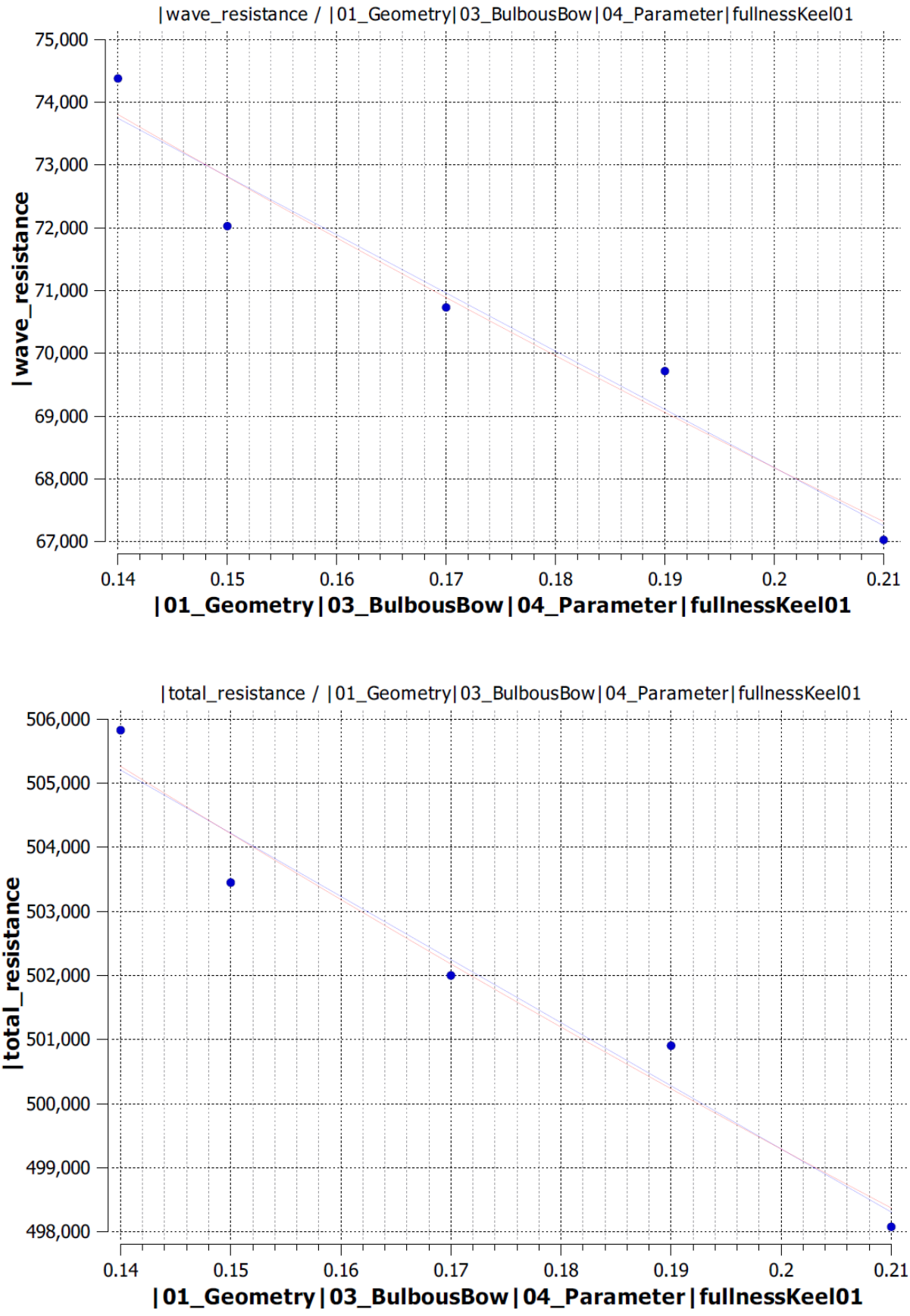

Figure A2.4. Influence of parameter “fullnessKeel01” on ship resistances

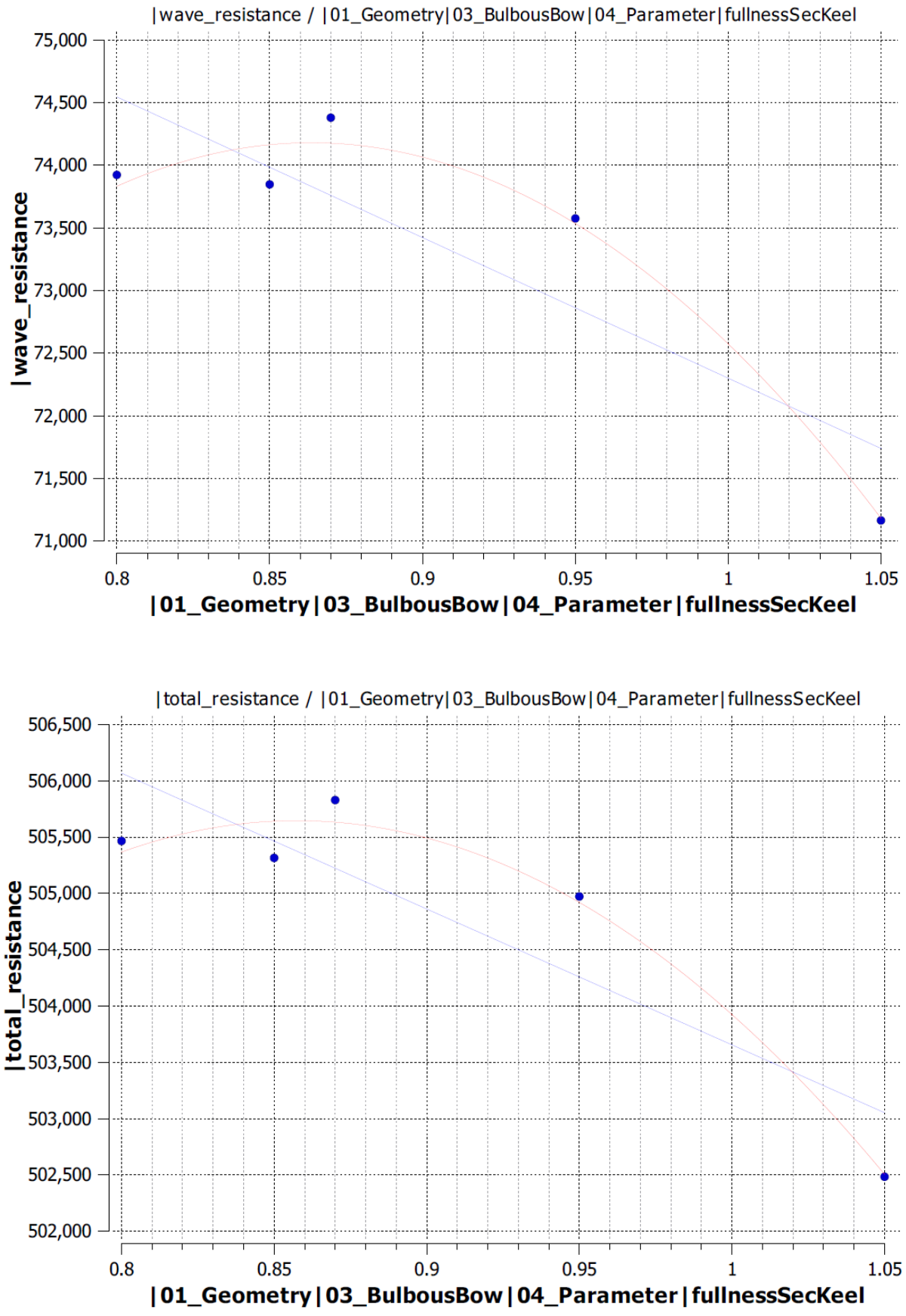

Figure A2.5. Influence of parameter “fullnessSecKeel” on ship resistances

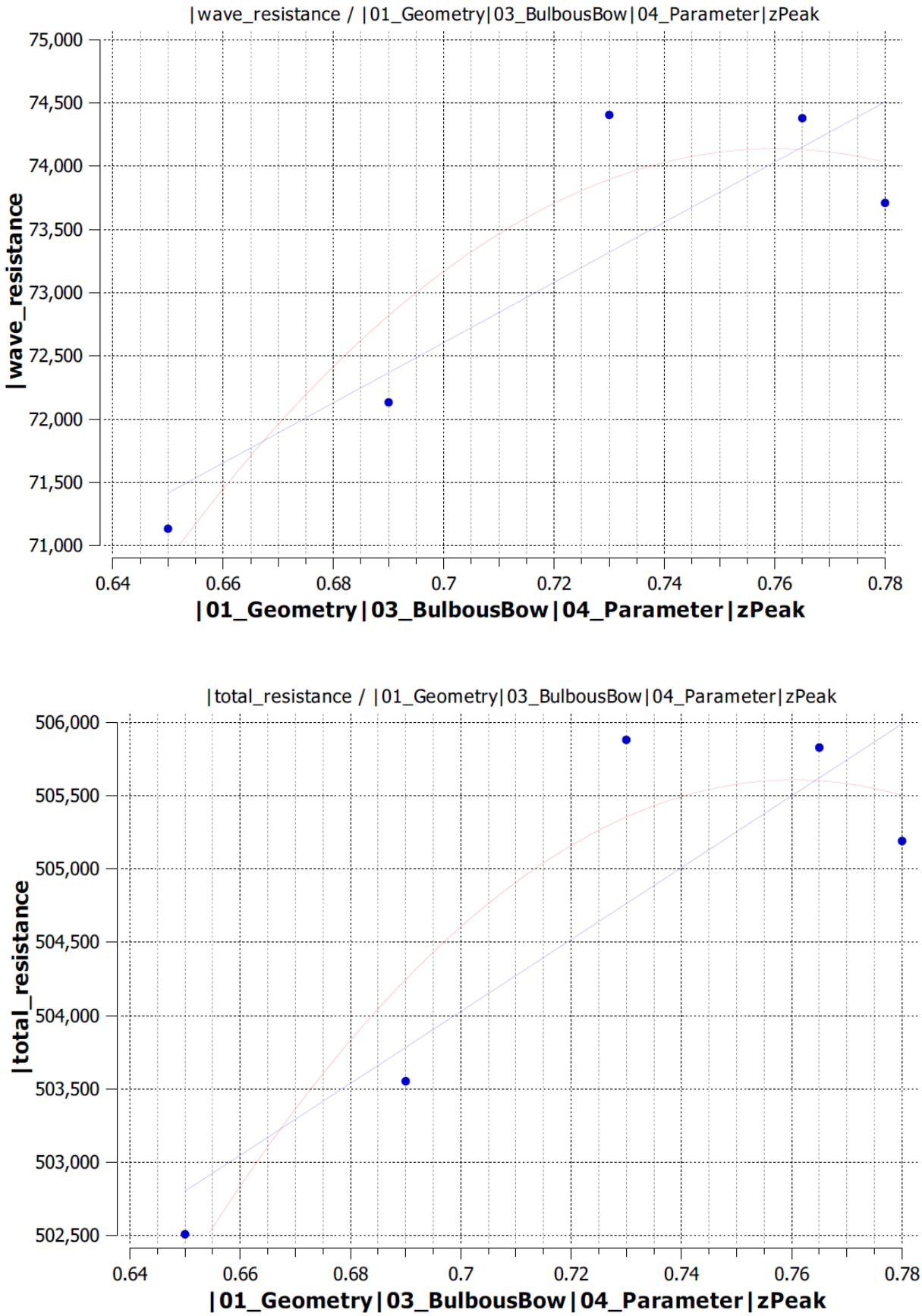

Figure A2.6. Influence of parameter “zPeak” on ship resistances

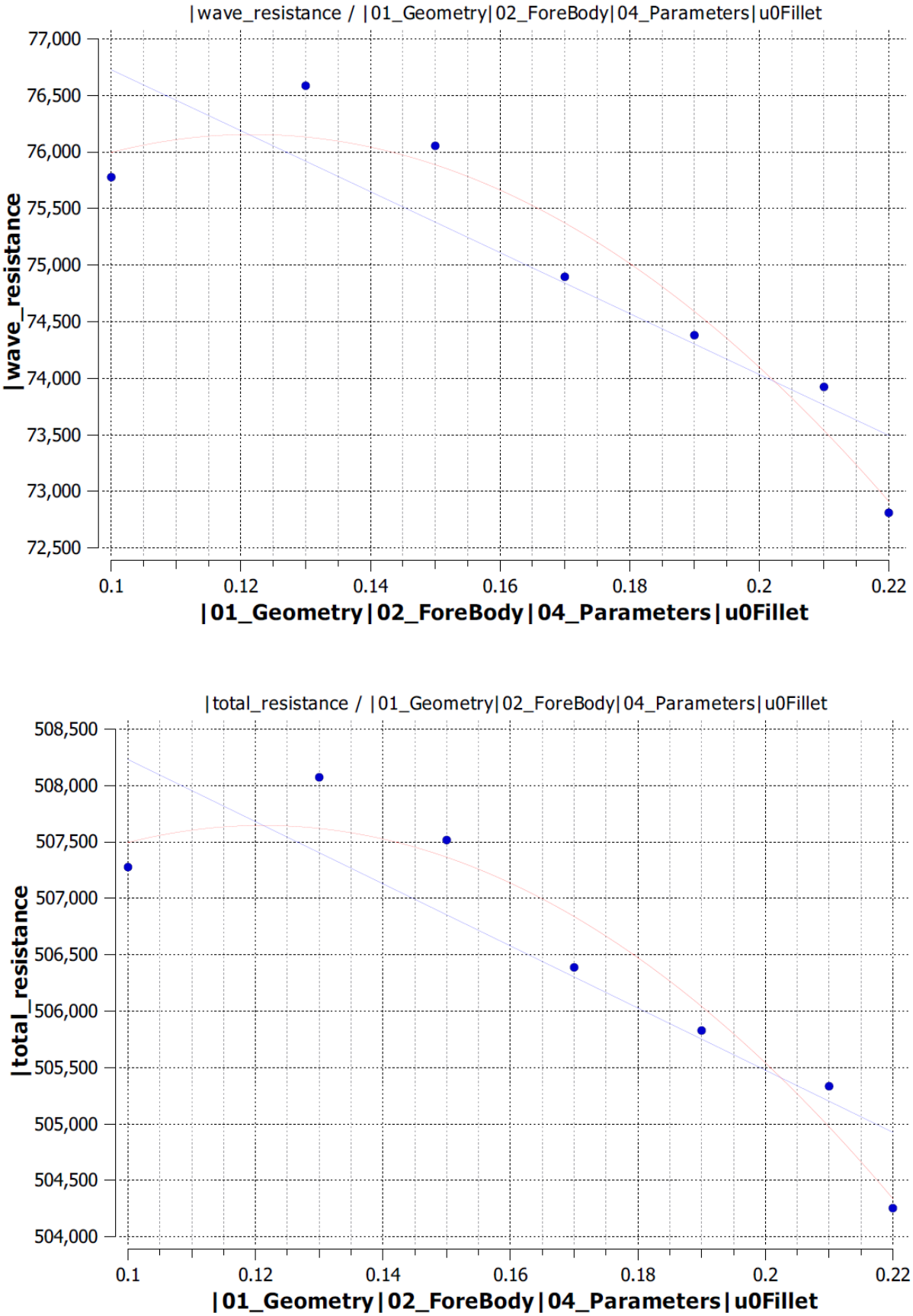

Figure A2.7. Influence of parameter “u0Fillet” on ship resistances

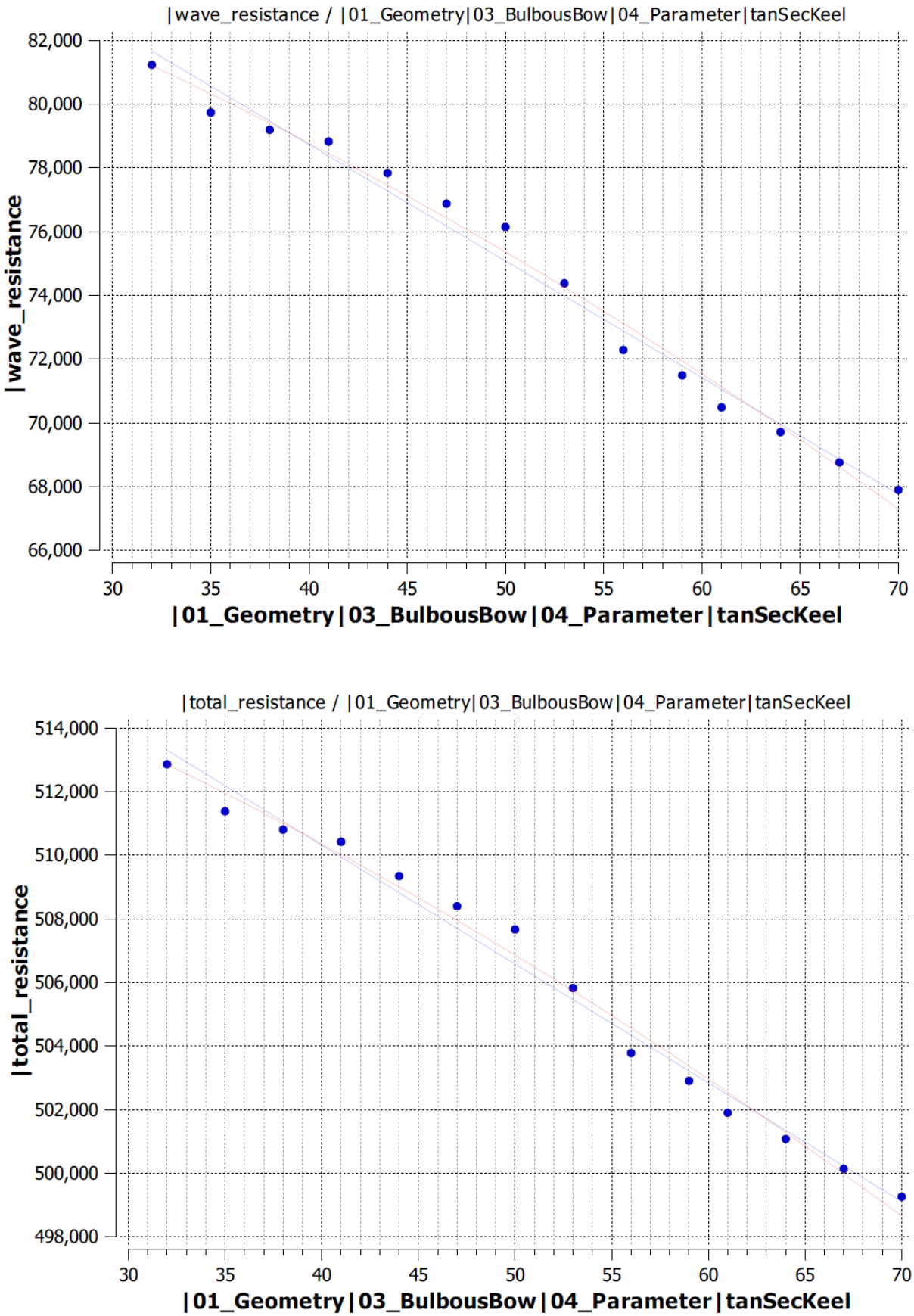

Figure A2.8. Influence of parameter “tanSecKeel” on ship resistances

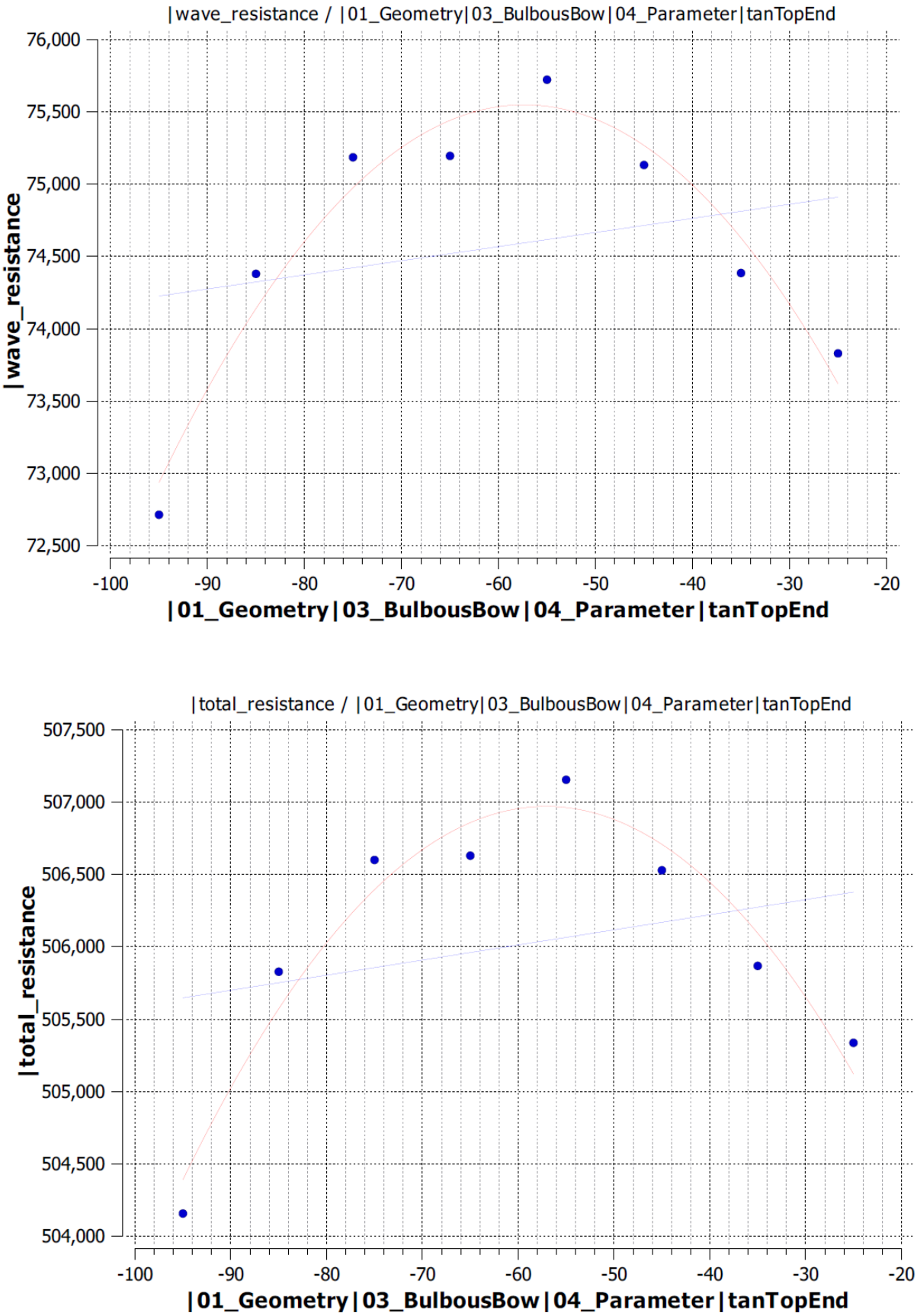

Figure A2.9. Influence of parameter “tanTopEnd” on ship resistances

A3. Set-up Input XML file for GL Rankine Solver

A3.1. Sample XML file for Steady Flow Computation

```
<?xml version="1.0" encoding="UTF-8" ?>
<GLRankine xmlns:xsi="http://www.w3.org/2001/XMLSchema-instance"
schemaVersion="1.0"
xsi:noNamespaceSchemaLocation="RankineConfig.xsd">
<Project version="1.0">
<Configuration>
<ProjectInfo>
     <Generator>
          <Name value="Manually created" />
          <Version value="1.0" />
     </Generator>
     <CreationTime timeStamp="2011-03-14T14:45:00.00Z" />
     <CreatedBy name="alvg" />
     <ProjectName value="Steady Flow Computation" />
</ProjectInfo>

<Computations>
     <Preprocessing>
     <Bodies>
          <Body>
               <BodyDefinition name="CruiseMeyer" sym="1">
                    <BodyParts>
                         <BodyPart name="left">
                              <Surface>
                                   <ReadFromFile
fileName="CruiseMeyer.stl" type="stl" />
                                   <ClipSurface nx="0" ny="1"
nz="0" d="0" />
                                   <Transformations>
                                        <Translation dx="0"
dy="0" dz="-7.2" />
                                        <Translation dx="-
100.97273292" dy="0" dz="0" />
                                   </Transformations>
                                   <LimitPlane nx="0" ny="1"
nz="0" d="0" />
                                   <WriteToFile type="vtk"
fileName="surface.vtk" />
                              </Surface>
                              <BodyPanelGeneration>
                                   <double name="lAft"
value="1.050" />
                                   <double name="lMid"
value="1.575" />
                                   <double name="lBow"
value="1.050" />
                                   <double name="zAft"
value="1.518" />
```

```
                                        <double name="zBow"
value="1.300" />
                                </BodyPanelGeneration>
                           </BodyPart>
                      </BodyParts>
                <WriteToFile type="vtk" fileName="panels.vtk" />
                </BodyDefinition>
           </Body>
     </Bodies>

     <FreeSurface>
           <SetDefaultParameterFor u0="7.7167" />
           <FreeSurfaceDefinition>
                <RectangularFreeSurface />
                <WriteToFile type="vtk" fileName="fs.vtk" />
           </FreeSurfaceDefinition>
     </FreeSurface>

     </Preprocessing>

     <HydroStatics> <!-- HdyroStatics can be omitted if not needed -
->
           <Parameter>
                <double name="rho" value="1025.0" />
           </Parameter>
           <Output>
                <ResultFile>hydrostatics.shr2</ResultFile>
           </Output>
</HydroStatics>

     <NonlinearSteadySimulation>
           <Data>
                <BodyData bodyName="CruiseMeyer">
                     <double name="cogZ" value="8.03847286" />
                </BodyData>
           </Data>
           <Parameter>
                <double name="u0" value="7.7167" />
                <double name="rho" value="1025" />
                <double name="g" value="9.81" />
                <double name="relax0" value="0.3" />
                <double name="relax" value="0.33125" />
                <double name="wdp" value="0.016563" />
           </Parameter>
           <Output>
                <ResultFile>dump.shr2</ResultFile>
                <LogFile>log.out</LogFile>
                <VTKDirectory>data</VTKDirectory>
           </Output>
     </NonlinearSteadySimulation>
</Computations>
</Configuration>
</Project>
</GLRankine>
```

A3.2. Sample XML file for Seakeeping Computation

```
<?xml version="1.0" encoding="UTF-8" ?>
<GLRankine xmlns:xsi="http://www.w3.org/2001/XMLSchema-instance"
schemaVersion="1.0"
xsi:noNamespaceSchemaLocation="RankineConfig.xsd">
<Project version="1.0">
<Configuration>
     <ProjectInfo>
          <Generator>
               <Name value="Manually created" />
               <Version value="1.0" />
          </Generator>
          <CreationTime timeStamp="2011-03-14T16:00:00.00Z" />
          <CreatedBy name="alvg" />
          <ProjectName value="seakeeping computation-GLR Source" />
     </ProjectInfo>
<Computations>
          <SeakeepingLinear>
          <Input>
               <StationarySolution>dump.shr2</StationarySolution>
          </Input>
     <Data>
          <BodyData bodyName="CruiseMeyer">
               <double name="GM" value="2.754" />
               <double name="rollDamp" value="0.0" />
               <double name="r_xx" value="14.47" />
               <double name="r_yy" value="58.07" />
               <double name="r_zz" value="58.07" />
               <boolean name="addRudderForces" value="true" />
          </BodyData>
          <WaveData>
               <Waves omega="1.306" muList="180" />
               <Waves omega="1.249" muList="180" />
               <Waves omega="1.130" muList="180" />
               <Waves omega="0.997" muList="180" />
               <Waves omega="0.843" muList="180" />
               <Waves omega="0.754" muList="180" />
               <Waves omega="0.653" muList="180" />
               <Waves omega="0.596" muList="180" />
               <Waves omega="0.559" muList="180" />
               <Waves omega="0.533" muList="180" />
               <Waves omega="0.506" muList="180" />
               <Waves omega="0.477" muList="180" />
               <Waves omega="0.446" muList="180" />
               <Waves omega="0.394" muList="180" />
               <Waves omega="0.331" muList="180" />
          </WaveData>
     </Data>
     <!-- use only standard parameter -->
     <FreeSurfaceGeneration>
          <DefaultGeneration />
          <WriteToFile type="vtk" fileName="fs.vtk" />
     </FreeSurfaceGeneration>
```

```
      <Parameter>
            <boolean name="outputAbsPhase" value="false" />
            <unsignedInt name="maxNumUnknowns" value="30000" />
      </Parameter>
      <Output>
            <ResultFile>seakeeping.shr2</ResultFile>
            <LogFile>seakeepinglog.out</LogFile>
      </Output>
      </SeakeepingLinear>
</Computations>
</Configuration>
</Project>
</GLRankine>
```

A4. Distribution of Design Variables by SOBOL in Design Space

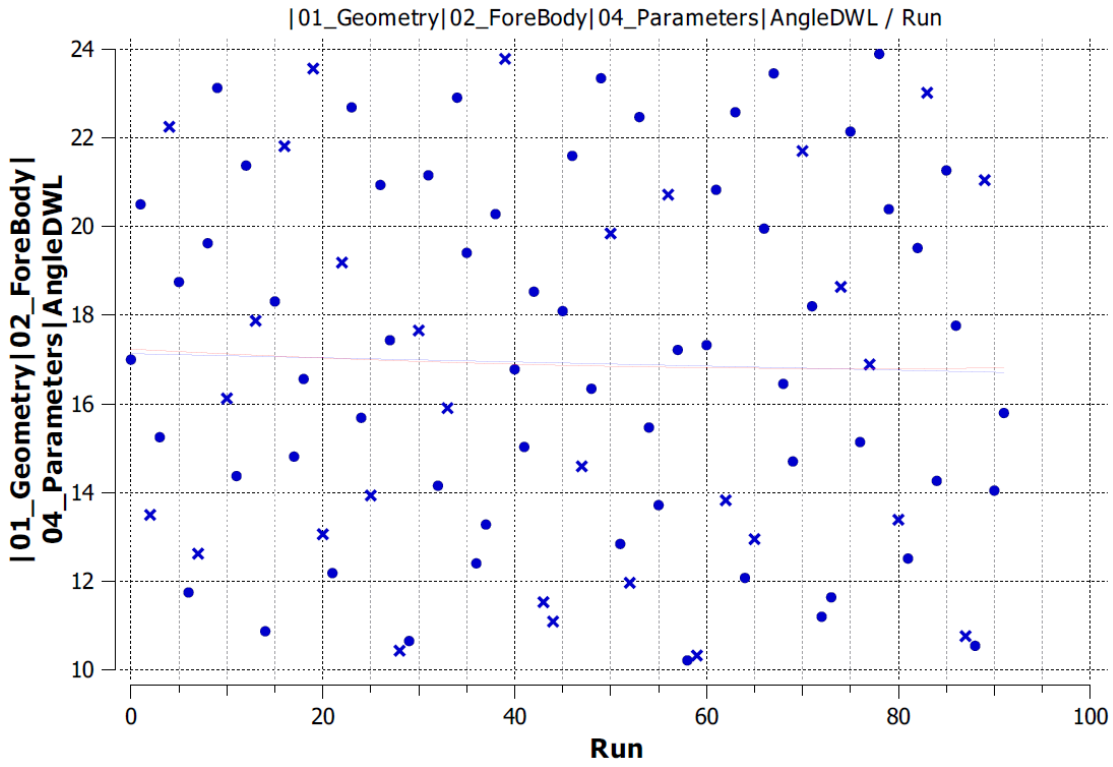

Figure A4.1. Distribution of the values of parameter “AngleDWL”

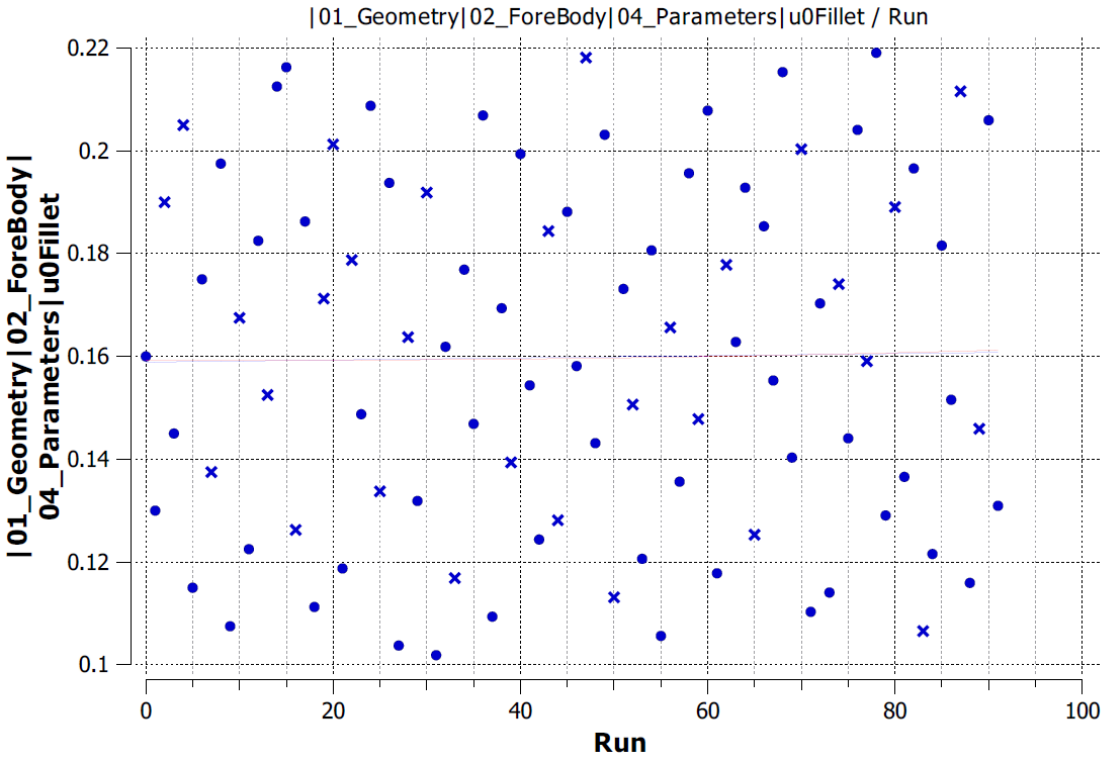

Figure A4.2. Distribution of the values of parameter “u0Fillet”

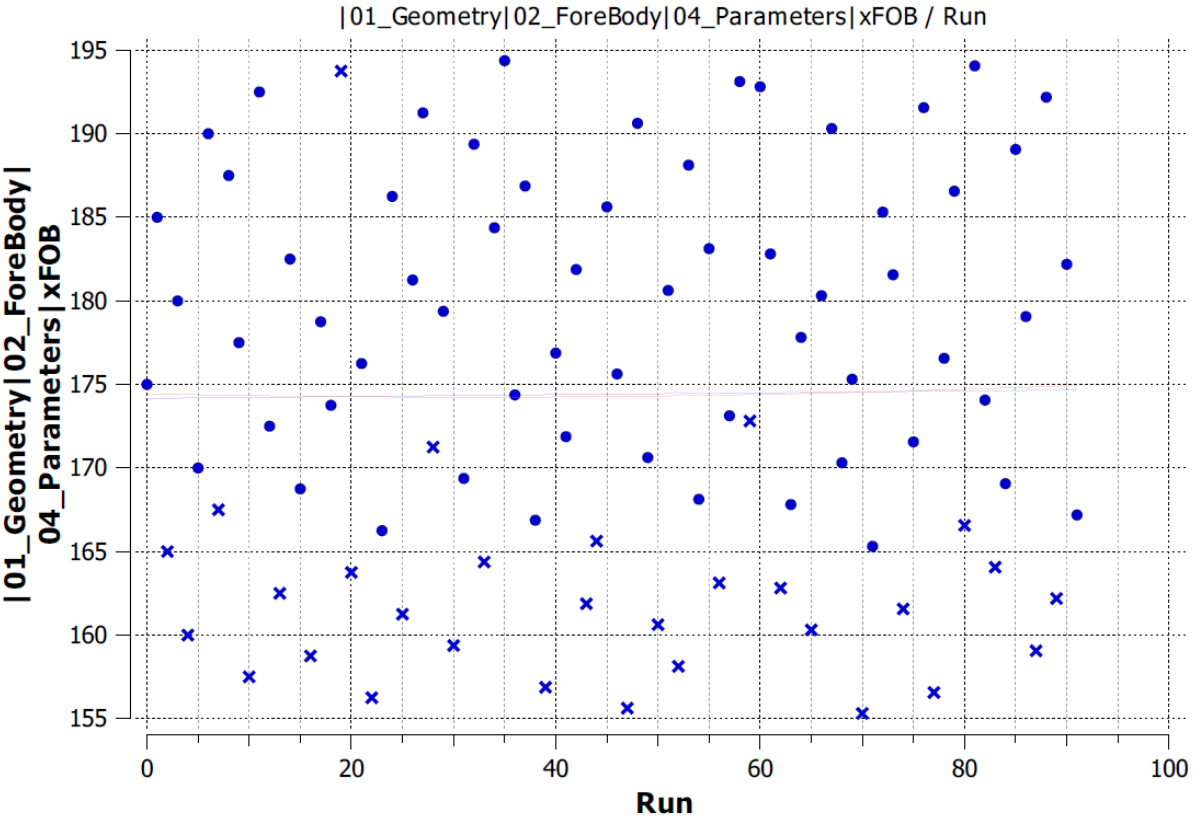

Figure A4.3. Distribution of the values of parameter “xFOB”

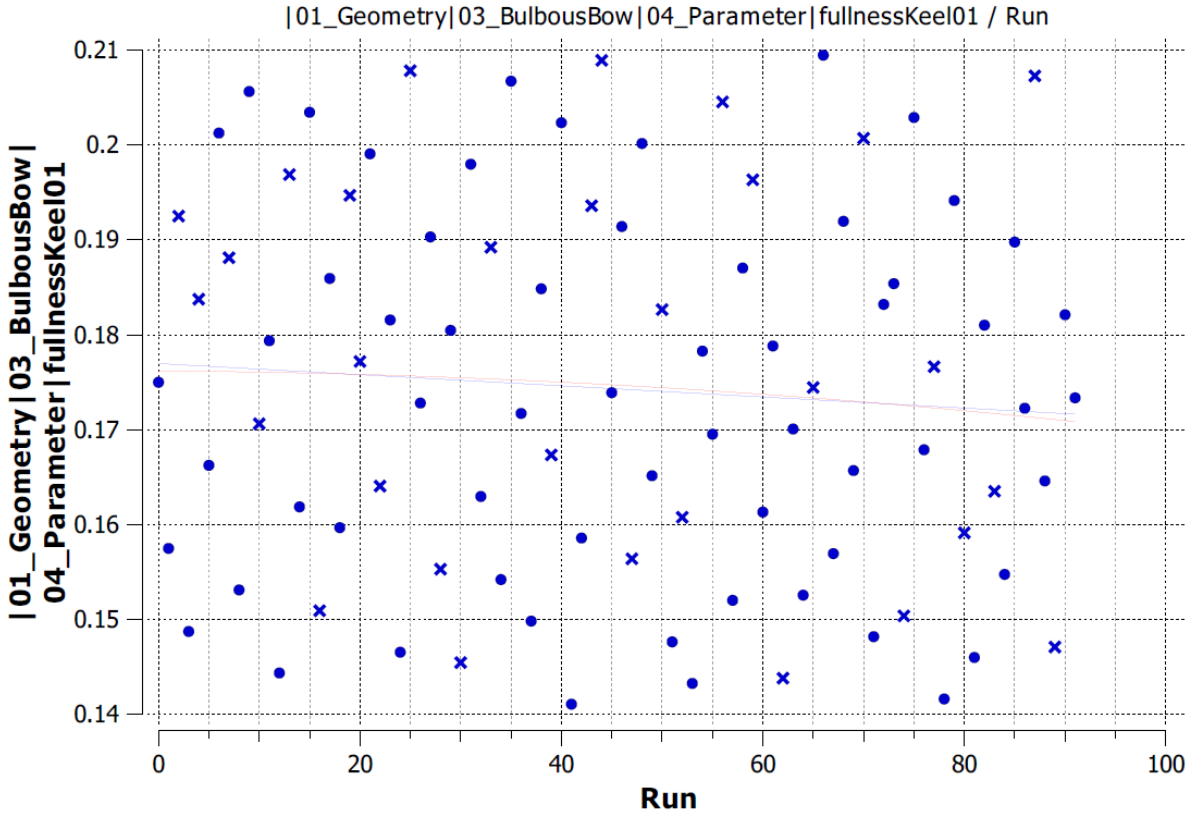

Figure A4.4. Distribution of the values of parameter “fullnessKeel01”

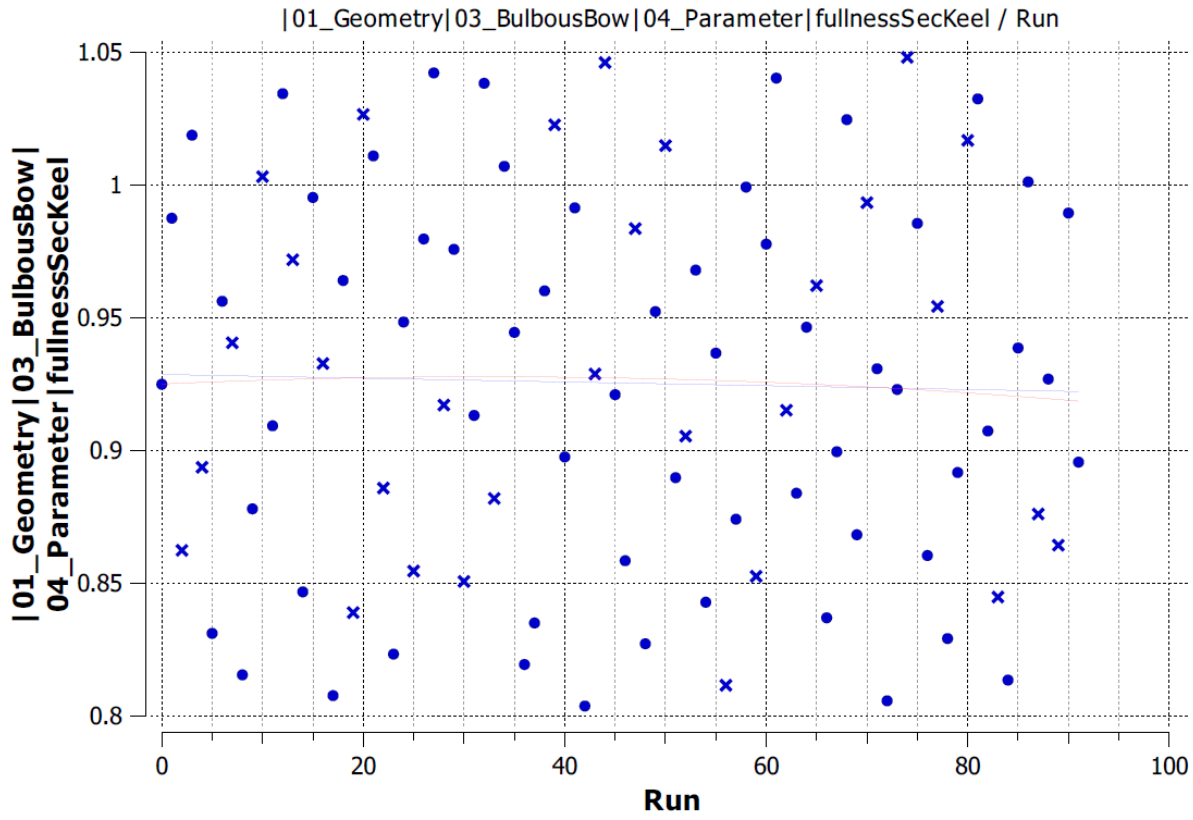

Figure A4.5. Distribution of the values of parameter “fullnessSecKeel”

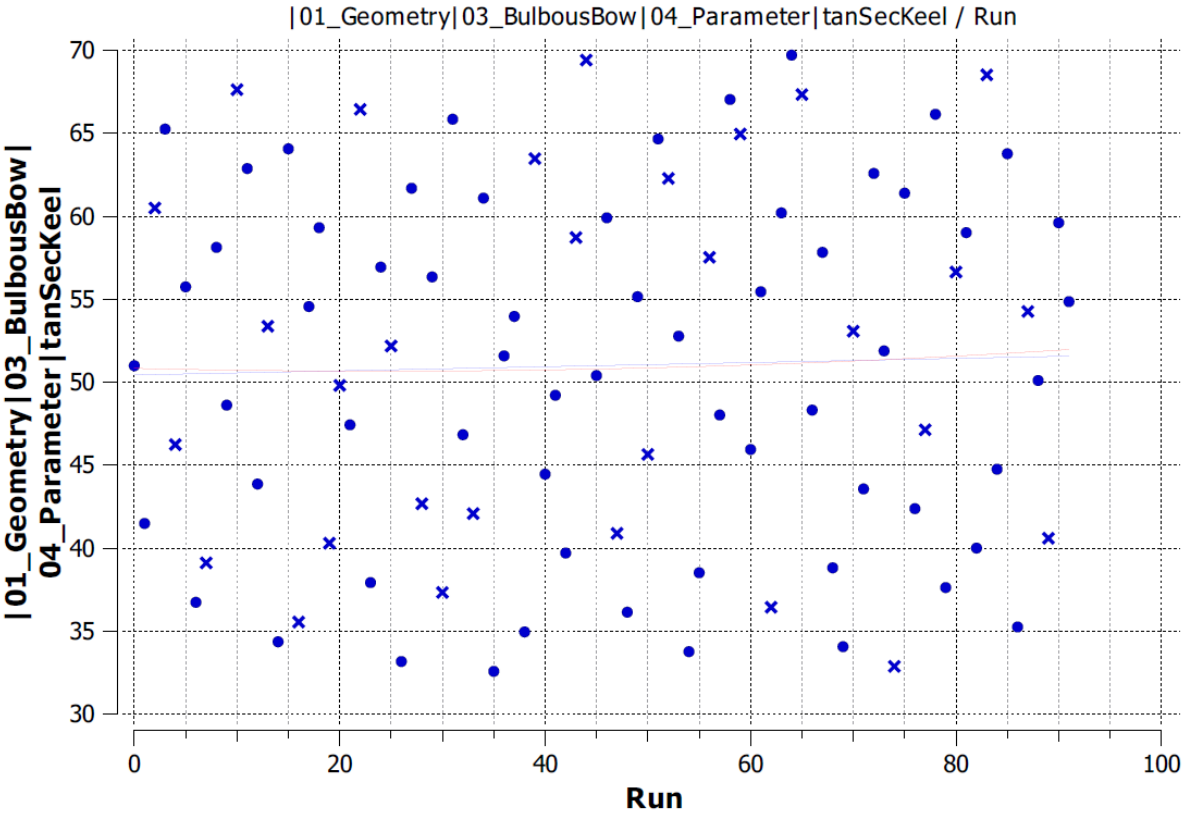

Figure A4.6. Distribution of the values of parameter “tanSecKeel”

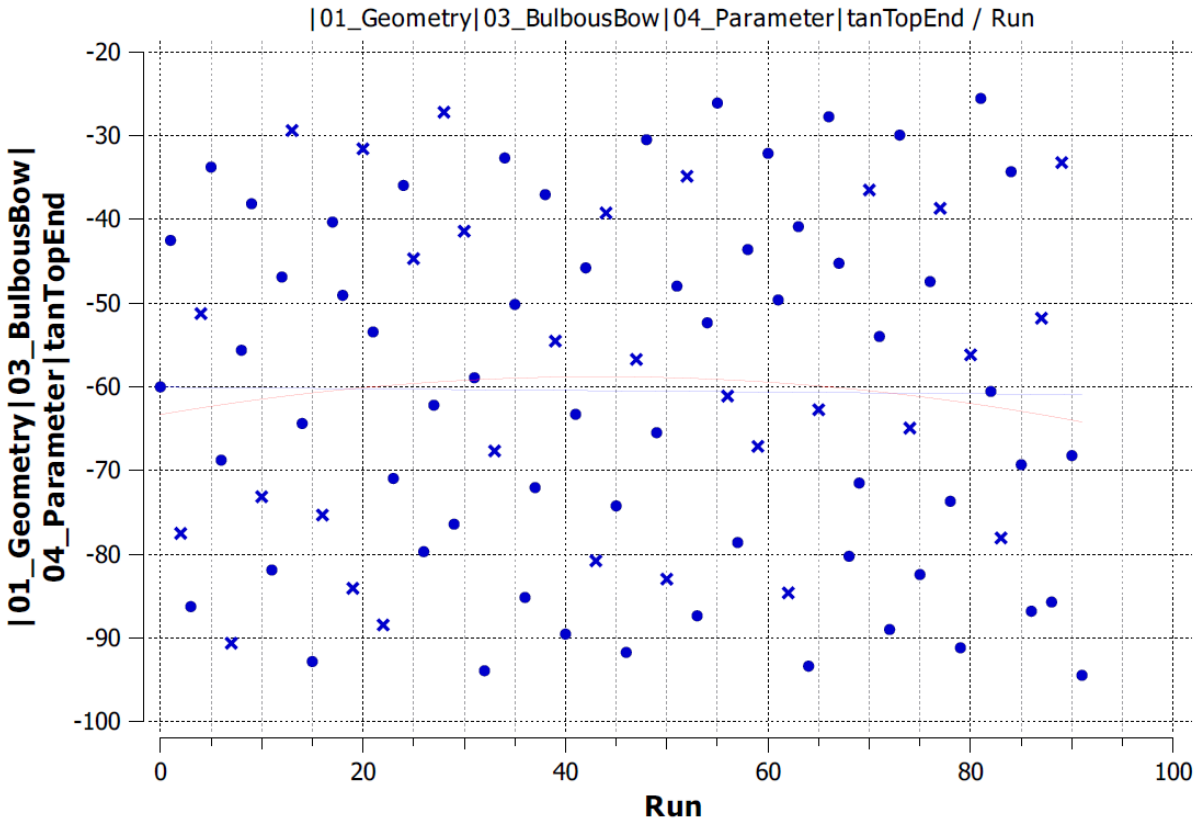

Figure A4.7. Distribution of the values of parameter “tanTopEnd”

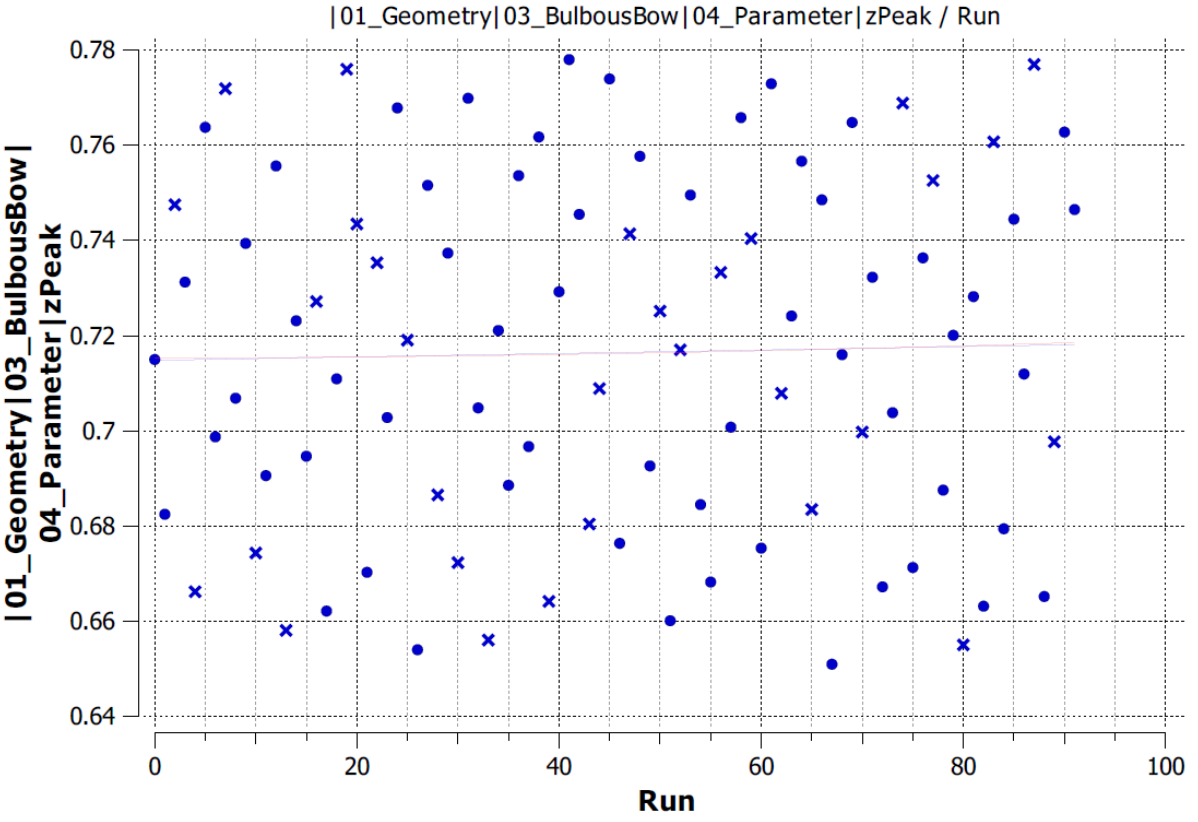

Figure A4.8. Distribution of the values of parameter “zPeak”

A5. Performance of Design Parameter with Irregular Trend

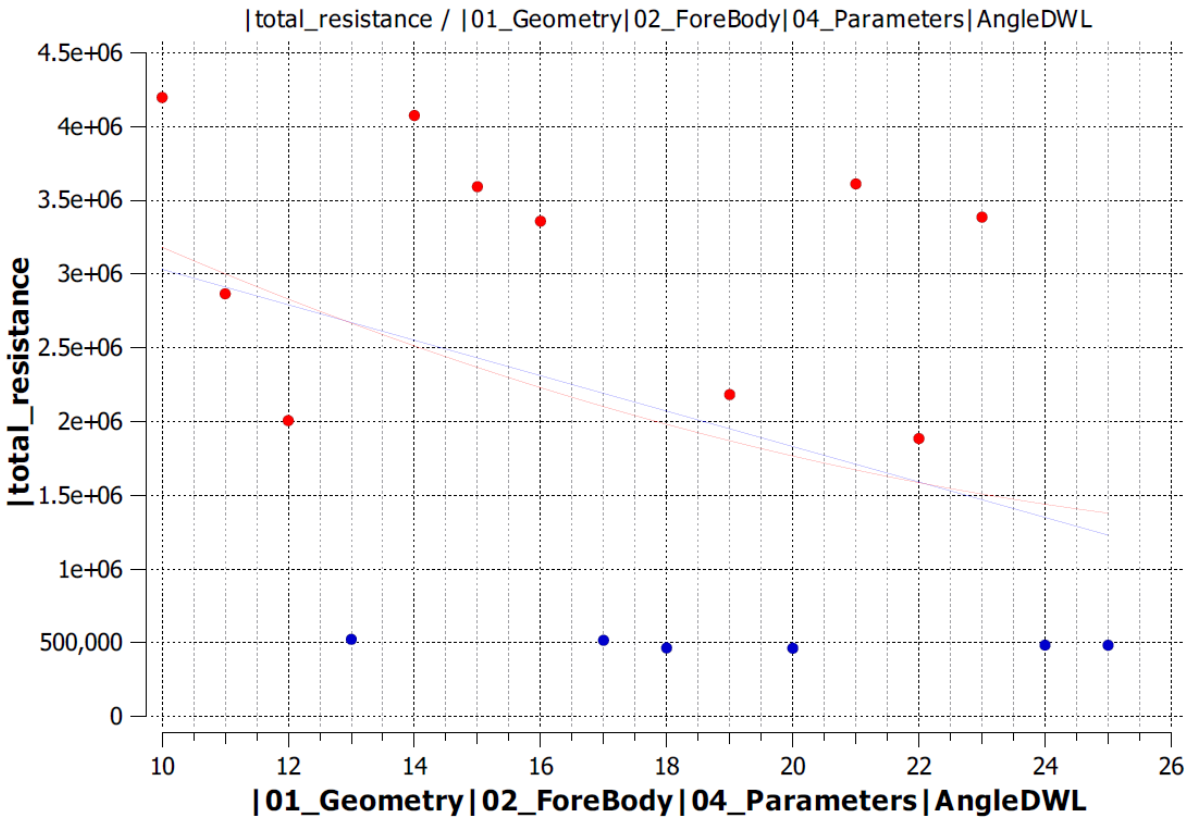

Figure A5.1. Wiggling of performance of design parameter on the resistance